HIGHWAY RESEARCH RECORD

Number 5

Continuously-Reinforced Concrete Pavement

4 Reports

Presented at the
42nd ANNUAL MEETING
January 7-11, 1963

HIGHWAY RESEARCH BOARD
of the
Division of Engineering and Industrial Research
National Academy of Sciences—
National Research Council
Washington, D. C.
1963

Department of Design

T. E. Shelburne, Chairman
Director of Research
Virginia Department of Highways, Charlottesville

COMMITTEE ON RIGID PAVEMENT DESIGN

William Van Breemen, Chairman
Research Engineer, Engineering Research,
New Jersey State Highway Department, Trenton

Harry D. Cashell, Secretary
Chief, Concrete and Concrete Pavement Branch
Physical Research Division, U. S. Bureau of Public Roads

Henry Aaron, Chief Engineer, Reinforced Concrete Pavement Division, Wire Reinforcement Institute, Washington, D. C.
Robert F. Baker, Director, Office of Research and Development, U. S. Bureau of Public Roads, Washington, D. C.
Phillip P. Brown, Consultant, Soils, Mechanics and Paving, Bureau of Yards and Docks, Department of the Navy, Washington, D. C.
Paul F. Carlton, Chief, Research Branch, Ohio River Division Laboratories, Cincinnati
W. E. Chastain, Sr., Assistant Engineer of Research and Planning, Research Branch, Illinois Division of Highways, Springfield
E. A. Finney, Director, Research Laboratory Division, Michigan State Highway Department, Lansing
W. S. Housel, University of Michigan, Ann Arbor
F. N. Hveem, Materials and Research Engineer, California Division of Highways, Sacramento
W. H. Jacobs, Executive Secretary, Rail Steel Bar Association, Chicago, Illinois
C. D. Jensen, Director, Bureau of Materials, Pennsylvania Department of Highways, Harrisburg
Wallace J. Liddle, Chief Materials Engineer, Materials Testing Laboratory, Utah State Department of Highways, Salt Lake City
Ernest T. Perkins, Executive Director, East Hudson Parkway Authority, Pleasantville, N. Y.
Thomas B. Pringle, Chief, Civil Engineering Branch, Engineering Division Military Construction, Office of Chief of Engineers, Department of the Army, Washington, D. C.
Gordon K. Ray, Manager, Paving Bureau, Portland Cement Association, Chicago, Illinois
James P. Sale, Assistant Chief, Special Engineering Branch, Research and Development, Military Science Division, Department of the Army, Office, Chief of Engineers, Washington, D. C.
F. H. Scrivner, Pavement Research Engineer, Texas Transportation Institute, A & M College of Texas, College Station
M. D. Shelby, Research Engineer, Texas Highway Department, Austin
W. T. Spencer, Soils Engineer, Materials and Tests, Indiana State Highway Commission, Indianapolis
Otto A. Strassenmeyer, Associate Highway Engineer—Research and Development, Connecticut State Highway Department, Wethersfield
K. B. Woods, Head, School of Civil Engineering and Director, Joint Highway Research Project, Purdue University, Lafayette, Indiana

Contents

Determining and Evaluating Stresses of an In-Service Continuously-Reinforced Concrete Pavement

M. D. SHELBY and B. F. McCULLOUGH, respectively, Research Engineer and Design Engineer, Research Section, Highway Design Division, Texas Highway Department

The determination of an optimum percentage of longitudinal steel in a continuously-reinforced concrete pavement, for a given region, is a pressing problem facing highway engineers. To arrive at a satisfactory solution, in-place performance tests are required to check theoretical formulas used to design these pavements. In Walker County, Texas, an area of moderate climate, the Texas Highway Department constructed an experimental continuous pavement to compare the relative performance of 0.5 and 0.6 percent longitudinal steel (yield stress of 50,000 psi). This comparison was made on the basis of performance under traffic, the transverse crack spacing, the transverse crack width, and stresses in the concrete and steel due to the wheel loads as well as those due to the environmental conditions of the area.

To date, both steel percentages (0.5 and 0.6 percent) have performed satisfactorily on this project. Other factors (such as cement type, time of placement, concrete properties, and the average crack spacing) were found to influence steel and concrete stresses more than the steel percentage as long as slab continuity is maintained. The magnitude of effect for each of these factors is presented in the report. In addition, an empirical equation based on a statistical analysis of the data collected during this experiment is presented. This equation shows the interrelation of each of the influencing factors and the magnitude of effect on steel stress during the early stages of the pavement life.

• THIS PAPER is a part of a continuing study by the Texas Highway Department pertaining to the development and testing of continuously-reinforced concrete pavement in Texas. A part of the previous work conducted by the Texas Highway Department in this field was presented earlier in a Highway Research Board publication (1).

The study contained in this report pertains to an experimental continuously-reinforced concrete pavement consisting of 11.3 mi of new location on Interstate Highway 45 (Project I 45-2 (3) 102) in Walker County, Texas. The project begins at the Walker-Montgomery County Line and traverses a rural area to a point approximately 2 miles south of Huntsville, Texas. Figure 1 shows the location and general layout of the project. The highway is a divided type of facility consisting of two lanes in each direction. A typical section of the pavement structure on the project is shown in Figure 2. Beginning at the surface and moving downward, the pavement consists of a uniform 8-in. slab 24 ft wide which was placed monolithically. An open-graded sandstone material was used as the subbase layer, and the top 6 in. of the natural sand-clay soil was treated with 3 percent lime (by weight) to form a stabilized layer and act as a moisture barrier to minimize moisture variations in the lower clay strata.

The ADT count on this section of roadway was approximately 5,300 vehicles per day

Paper sponsored by Committee on Rigid Pavement Design.

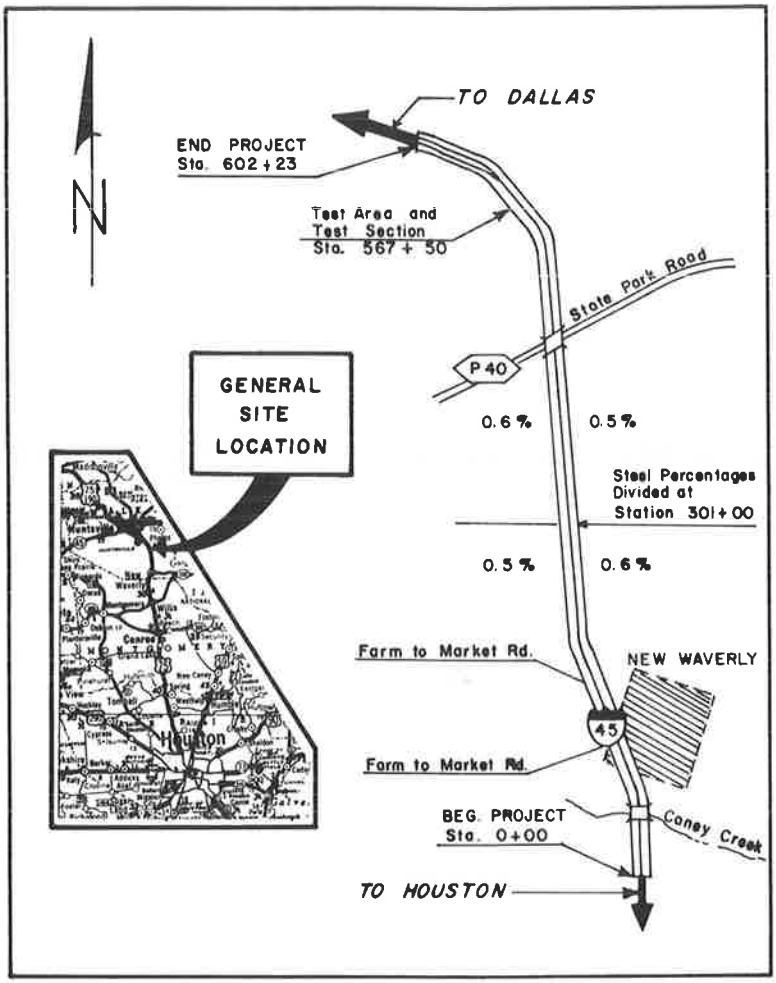

Figure 1. Location and layout of Walker Co. project.

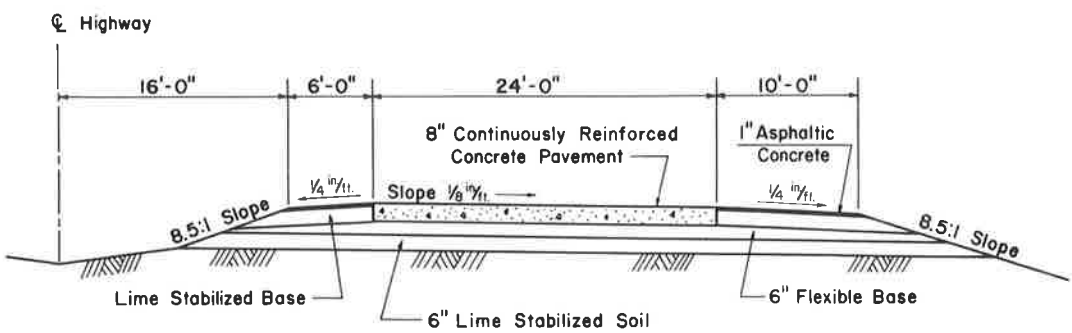

Figure 2. Typical half-section for Walker Co. project.

in 1960. A large percentage of this traffic consists of trucks, because this highway serves as the main artery between the Houston and the Dallas metropolitan areas. Therefore, numerous axle loads of excessive magnitude are experienced each day on this section. An analysis of loadometer data and traffic counts by the new AASHO method revealed the roadway had a traffic factor of 760 equivalent applications of an 18,000-lb axle load per day in 1960 (2).

Huntsville is located in the southeastern part of the State which is an area of moderate rainfall and temperature. The winters are generally mild, broken by intermittent cold spells. The average yearly rainfall for the area is 45 in., and the average monthly temperature ranges from 51 F in January to 84 F in August.

Design

An attempt was made in the design of the continuously-reinforced concrete pavement on this project to arrive at a balanced stress condition between the steel and the concrete; this concept has been pointed out in recent technical papers (3). Therefore, the plans and specifications called for several unique design features to incorporate and investigate these concepts. One feature was the use of two different percentages of longitudinal steel in the concrete pavement to obtain comparative service. Another feature is the use of a controlled flexural strength specification for the concrete.

Steel. —The plans called for one-half of the pavement to have 0.5 percent longitudinal steel and the other half to have 0.6 percent longitudinal steel for the purpose of making an analytical evaluation of the effect of steel percentage on performance. To eliminate the possibility of the unequal traffic flow on the two roadways affecting the comparison, each directional roadway was divided equally between the two steel percentages. The north end of the northbound roadway and the south end of the southbound roadway contained 0.5 percent longitudinal steel, and the opposite ends of each of these roadways contained 0.6 percent longitudinal steel (Fig. 1).

The longitudinal steel for the 0.5 percent design consisted of No. 5 round bars at 7½-in. centers, and No. 5 round bars at 6½-in. centers for the 0.6 percent design. The longitudinal bars for both designs were located at middepth of slab. Although the designs are referred to as the 0.5 percent or 0.6 percent design, the actual percentages are 0.52 percent and 0.59 percent. The specifications required the use of a hard-grade steel or the equivalent thereof for the longitudinal reinforcing steel, whereas intermediate-grade steel was permissible for transverse bars. The transverse steel throughout the project consisted of No. 4 round bars at spacings of 24 in. center to center.

Concrete. —To prevent the design of concrete mixes that tended to produce excessive concrete strengths, a maximum flexural strength was specified in addition to the normal minimum. The specification called for the concrete to be designed with the intention of producing a flexural strength within a range of 550 to 675 psi at 7 days. The optimum design flexural strength was specified as 600 psi at 7 days.

A minimum cement factor of 4 sacks per cubic yard was allowed on this project. This represents a 20 percent reduction from the normal minimum of 5 sacks per cubic yard generally prescribed. As an aid to strength control and for durability purposes, the use of 2 to 5 percent entrained air was mandatory on this project.

DEFINITIONS

Slab. —The portion of a continuously-reinforced concrete pavement placed during one consecutive period of paving operations, such as a day. The length of the slab would be measured between consecutive transverse construction joints.

Slab Segment. —The portion of a slab between any two consecutive transverse cracks in the pavement.

Test Section. —A slab or part of a slab used to determine crack pattern development.

Study Section. —The portion of a slab used to investigate the variation of a crack pattern due to other variables.

Test Area. —The area within a slab where strain and/or movement measurements are conducted.

Average Crack Spacing. —The average length of the slab segments within a designated test section.

Cycle. —Any 24-hr period of time in the life of a pavement during which measurements of movement, strain, etc., are performed. The cycles are numbered consecutively with the first cycle starting with the initial placement of concrete.

Plugs. —Gage plugs installed in concrete to provide reference points from which to measure minute movements between any two adjacent plugs:

a. Opening. —distance between any two adjacent plugs increasing.
b. Closing. —distance between any two adjacent plugs decreasing.

SCOPE OF EXPERIMENT

Choice of Site

After a study of the project plans and a survey of the project, a location near the north end of the project was selected as the most feasible test area from the standpoint of reducing the extraneous variables to a minimum. The test area was located on a tangent section with a relatively flat grade to eliminate any possible effect of curvature or slope on the results. During the initial considerations, it was decided that the two roadways should not be placed over a week apart and should be placed during the summer months to minimize differential weather conditions. The first condition required the site to be near a location where the paving train would switch roadways and reverse directions. The site selected was to be placed in the month of August, a time period that would present relatively uniform weather conditions during the early life and progressively more severe conditions during the first year.

TABLE 1

RESUME OF VARIABLES MEASURED

Variable	Method of Measurement	Remarks
1. Steel strain	SR-4 electrical strain gages, type A-4, paper back	Placed on selected steel bars to measure transverse and longitudinal distribution of steel strains; hourly reading for observation period
2. Concrete strain	Berry strain gage with 20-in. gage length	Brass plugs placed in concrete surface at 20 in. center to center; hourly readings for observation period
3. Crack width	Microscope with graduated eyepiece, 20 power	Hourly readings made at a selected location over a crack during the observation period
4. Slab temperature	Stainless steel temperature bulbs connected to a Honeywell recording thermometer	Bulbs placed in the slabs to determine temperature gradient and obtain mid-depth temperature; continuous readings during observation period
5. Crack pattern development	Adjacent test sections in both roadways (each about 2,000 ft long)	Periodic observations made for crack pattern development
6. Crack pattern variation	Study sections 400 to 500 ft long throughout project	Periodic observations of crack pattern
7. Concrete properties	Lab tests and field tests	Strength tests: flexural, tensile, compression, shrinkage, elasticity, and air entrainment
8. Steel strain due to wheel load	Same as 1	Static and dynamic tests; static test consists of placing wheel load at crack and at various points away from crack

Nature of Experiment

The field experiment was planned with the objective of determining and evaluating variations in (a) strains in concrete and steel, (b) crack patterns, and (c) crack widths due to variations in longitudinal steel percentages and climatic conditions. The ultimate goal of the experiment was the correlation and determination of the interrelation between these variables. In addition, a secondary study was initiated to study the temperature gradient of the concrete pavement during climatic cycles. Table 1 gives a resumé of the tests performed, instrumentation, and the reading procedures used during the experiment. As a follow-up to the previous table, Table 2 outlines the boundary conditions and parameters related to each measured variable. In essence, these two tables give the method of measurement and the dependent and independent variables used to attain the objectives and goals of the experiment.

Analysis of Variables

Figure 3 shows the general layout of the steel and concrete strain test area. To simplify the installation of testing equipment, the instrumentation was placed in the median. All leads were brought to a storage box in the median through rubber and metal conduits placed 6 in. beneath the subbase surface. All pavement instrumentation was placed in the inside lane on both roadways. Figures 4 and 5 show a more detailed layout of the instrumentation used in each of the two roadways to appraise the first three dependent variables in Table 1; i.e., steel strain, concrete strain, and crack width.

The steel strains were measured by the use of waterproofed SR-4 electrical strain gages. (Appendix A gives a detailed description of the waterproofing procedure.) Figures 4 and 5 show the number and relative position of the gages. These gages were positioned so that longitudinal strain distribution along the bar and transverse strain distribution at a crack could be determined. Bar C, using gages 1 through 7, was installed for determining longitudinal strain distribution. The distance of 10 ft between gages 1 and 6 was believed a sufficient distance to allow another transverse crack to form; hence, the steel strain distribution between cracks could be determined. The gages at the preformed crack (6, 9, and 11 in Fig. 4) on bars A, B, and C allow the transverse strain distribution at a crack to be determined. The gages on bars A and B located away from the crack give a check on the initial longitudinal strain distribution away from the crack. Strain readings were made by using a variable resistance in a Kelvin double-bridge circuit. The variable resistance has a sensitivity of 1 micro-in. of strain, and a range from 1 to 15,000 micro-in. To alleviate errors induced by contact resistance in the switching panel and temperature effects on lead wires, dual leads were used in the wiring. The circuit for the bridge is shown in Figure 6. The con-

TABLE 2

VARIABLES, BOUNDARY CONDITIONS, AND PARAMETERS

Parameters and Boundary Conditions	Outline of Experiment		
	Variable Measured (Dependent Factors)	Boundary Conditions[a] (Fixed Factors)	Parameters[a] (Changeable Factors)
1. Weather conditions during placement of slab	1. Steel strain	1-6, 12a	7-11, 12b, 13, 14
2. Weather cycles; i.e., winter, summer, rainfall, etc.	2. Concrete strain	1-6, 12a	7-11, 12b, 14
3. Slab thickness	3. Crack width	1-6, 12a	7-11
4. Subgrade, subbase, construction control, etc.	4. Slab temperature gradient	1, 3-7, 12b	2, 8, 9, 10b, 12a
5. Concrete pavement curing procedure	5. Crack pattern development	1-8	9, 14
6. Steel type	6. Variation in crack pattern	3-7	1, 8, 9, 14
7. Cement type	7. Steel strain due to wheel loads	1-11	12b
8. Concrete properties			
9. Age			
10. Temperature: (a) slab, (b) air			
11. Average crack spacing of slabs			
12. Positions of measurement in slab: (a) vertical, (b) horizontal (trans. or long.)			
13. Axle load			
14. Steel percentage			
15. Concrete strains			

[a]Numbers refer to numerical sequence of parameters and boundary conditions listed.

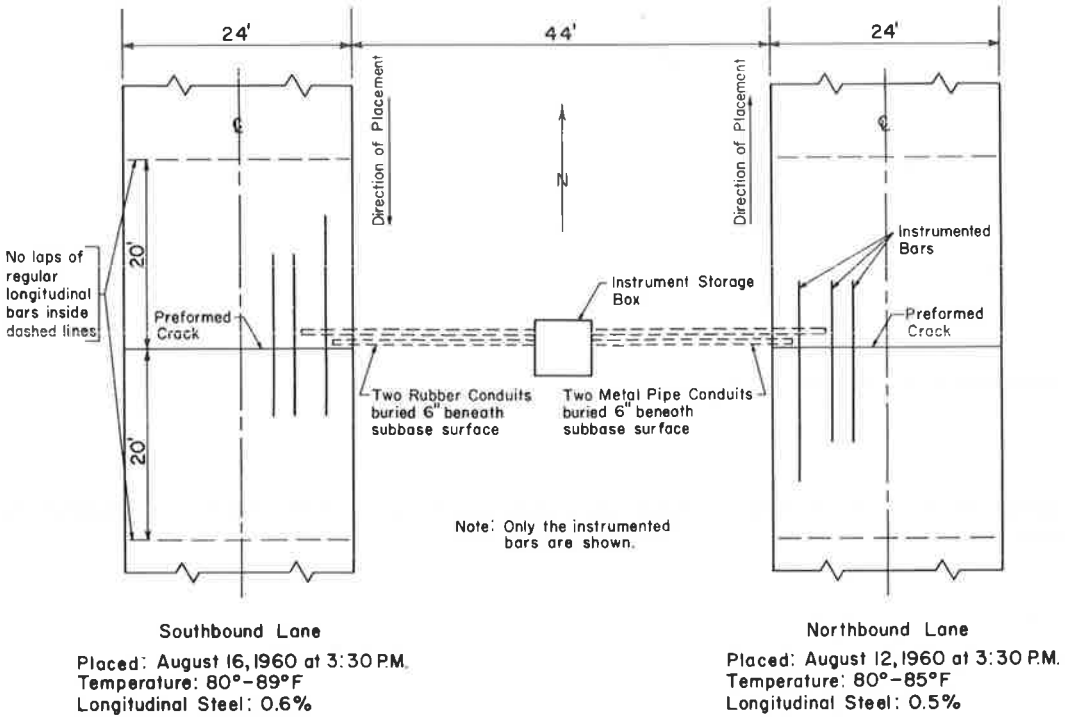

Figure 3. General layout of Walker Co. test area at station 567 + 50.

struction and calibration of the bridge has been reported by Gersch and Moore (4). For the purpose of detecting "zero drift" due to instrument leads and variable battery voltage, a special reading procedure was used. A reading was taken on each gage in the series, then the position of the active and temperature gage in the circuit was reversed. This procedure gave a resistance reading greater and a resistance reading less than the zero resistance for each gage; hence, any movement of the zero reading could be detected.

The second variable, concrete strains, was measured on brass gage plugs placed in the surface of the concrete at 20-in. centers by the use of a Berry strain gage. Figures 4 and 5 show the layout of the gage plugs. The gage used is capable of detecting movements as small as 0.0002 in. which gives a strain sensitivity of 10 micro-in. over a 20-in. gage length.

The third dependent variable, width of the crack at the surface, was determined by the use of a 20 power microscope. The microscope's eyepiece had a built in scale graduated in increments 0.001 in. with a range of 0.0 to 0.1 in. The microscope was positioned in the identical spot each time a reading was taken in order to obtain comparable data.

The instrumentation for studying the temperature, the fourth dependent variable, was arranged with the goal of obtaining middepth temperatures for stress considerations, and determining temperature distribution through the slab. The latter study was made only in the northbound roadway. Stainless steel temperature bulbs were placed in the slab, and connected to a Honeywell continuous recording thermometer placed in the median.

The fifth dependent variable, crack pattern development, was evaluated by the use of a slab for each percentage of steel. These two slabs, hereafter referred to as test sections, are approximately 2,500 ft long. Each of the instrumentation sites, or test areas, is located within these test sections. The sixth dependent variable, variation in crack pattern, was studied by selecting eight short sections of roadway to encompass

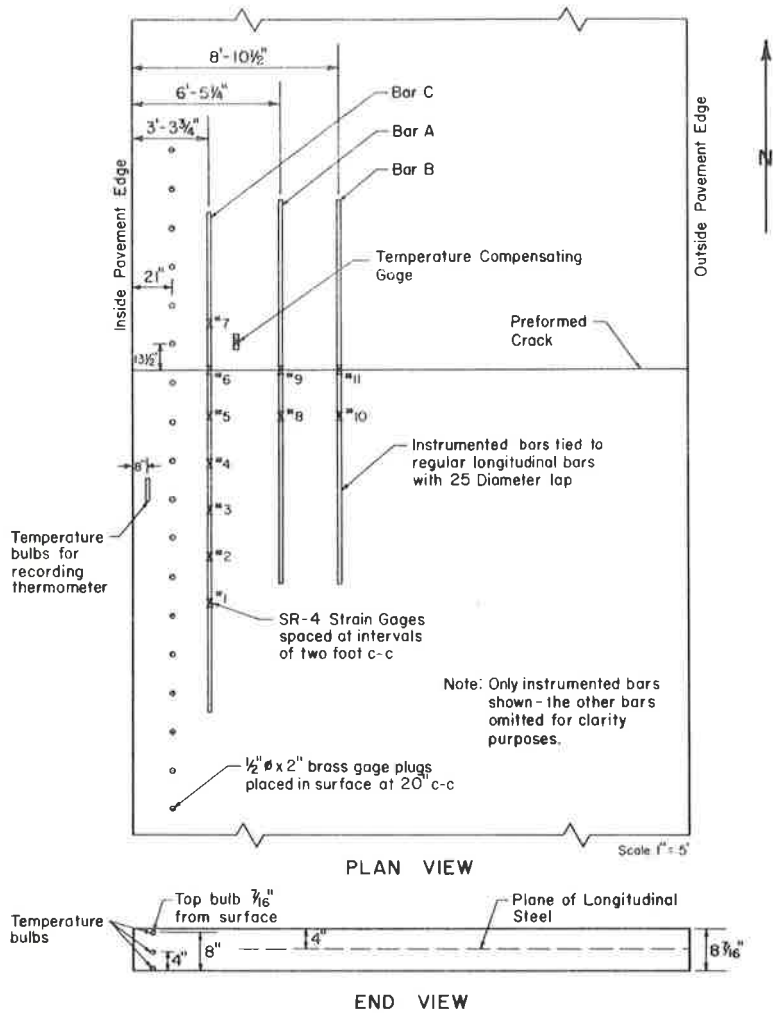

Figure 4. Detailed layout of instrumentation for pavement with 0.5 percent longitudinal steel (NBL), Walker Co.

TABLE 3

PERTINENT DATA CONCERNING WHEEL LOAD TESTS

Loads:
1. Gross, 20,880 lb.
2. Rear axle, 15,570 lb.
3. Front axle, 5,310 lb.
4. Rear wheels, 7,785 lb.
5. Front wheels, 2,655 lb.

Tires:
1. Dual.
2. Total contact area for duals, 138 sq in.
3. Contact pressure, 56.8 psi.
4. Size, 9 x 22.5 x 10 ply.

Time = Sept. 16, 1960, 8:00 to 9:30 AM.
Test procedure, northbound lanes (0.5 percent steel):
1. Static load over crack with readings on every gage.
2. Static load at various positions away from crack with readings taken on gage at crack.
3. Dynamic strains taken for gage at the crack for creep speed and 15 mph.

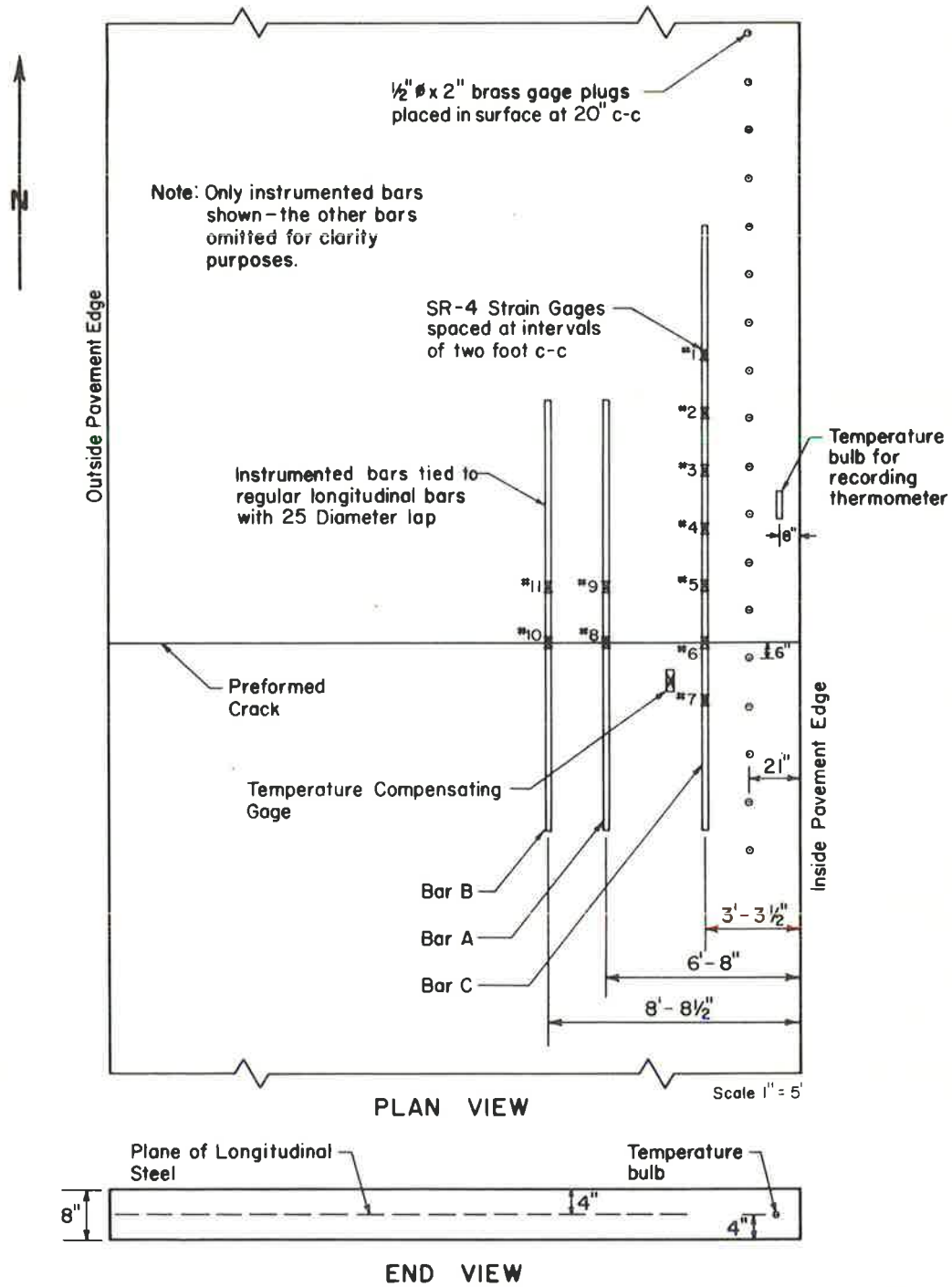

Figure 5. Detailed layout of instrumentation for pavement with 0.6 percent longitudinal steel (SBL), Walker Co.

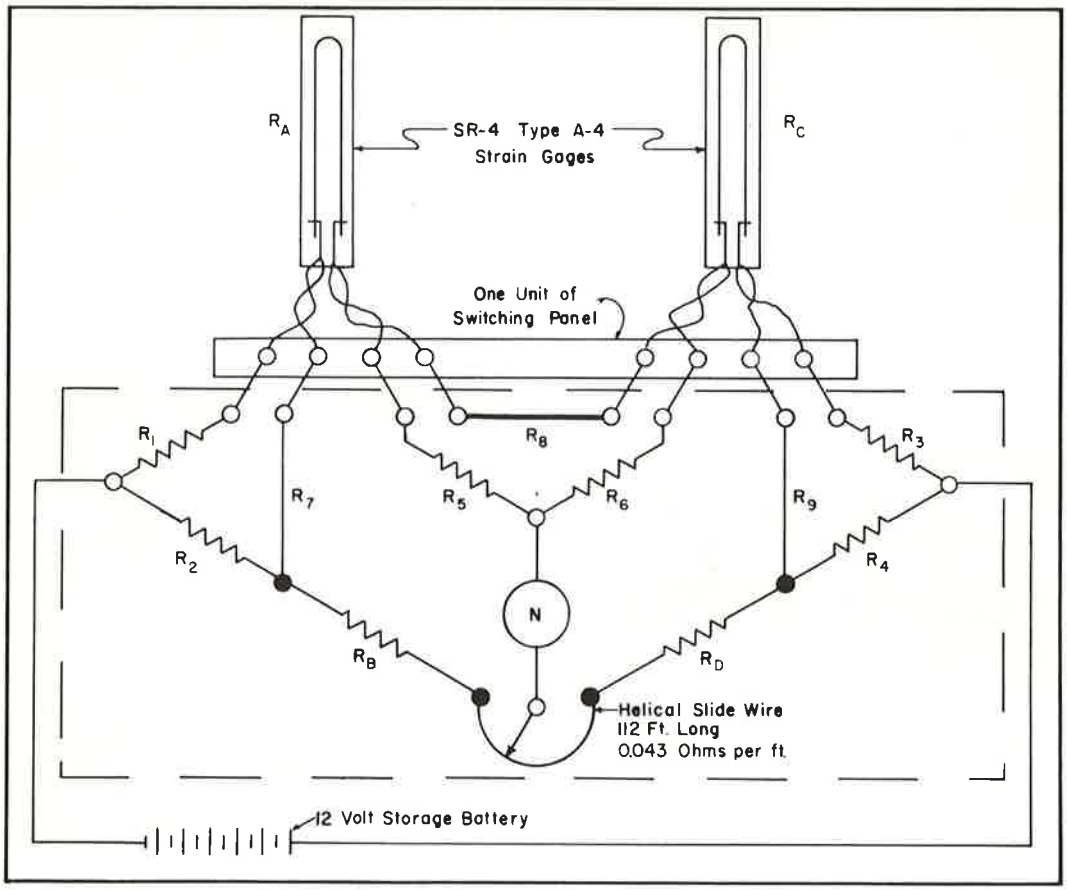

Figure 6. Bridge circuit used for measuring steel strains.

as many parameters as possible. These short sections hereafter referred to as "study sections" are 500 to 600 ft long.

The seventh variable, steel strain variation due to wheel loads, was evaluated through the use of a loaded truck and the strain gage installation. The load tests consisted of two phases: (a) static loading and (b) dynamic loading. Data concerning the test are given in Table 3.

Due to the contractor's supply problems, another variable entered the test during the construction operations. A type III cement (high-early strength) was used in the NBL, whereas a type I cement (normal) was used in the SBL. Therefore, the stresses in the two roadways could not be compared initially without taking this factor into consideration.

FIELD INSTALLATION AND READING PROCEDURES

General Construction Procedures

The experiment was organized in such a manner that the installation of the instrumentation could be done with no interruption of the normal paving operations. The steel bars used for instrumentation were obtained from the contractor's stockpile and instrumented before construction; therefore, the test site is as representative of the general construction practices used throughout the project as possible.

The concrete was placed in accordance with Item 320, "Concrete Pavement," of the

Texas Highway Department Standard Specifications (1951). The pavement was placed uniformly—full width (24 ft) and full depth. The bar mats were assembled and tied on the subbase immediately in front of the paving train. Bar chairs placed at approximately 3-ft centers on alternating transverse bars were used to hold the bar mats at the desired elevation. Waterproof paper curing of the concrete pavement was required for a period of three days after placement. The paving train consisted of a mechanical concrete spreader, a 34E dual-drum mixer, transverse screeds, longitudinal float, hand finishing with straightedges, followed by a belting for a nonskid surface. Figures 7 to 9 show general construction procedures on the project. Due to the hardness of the

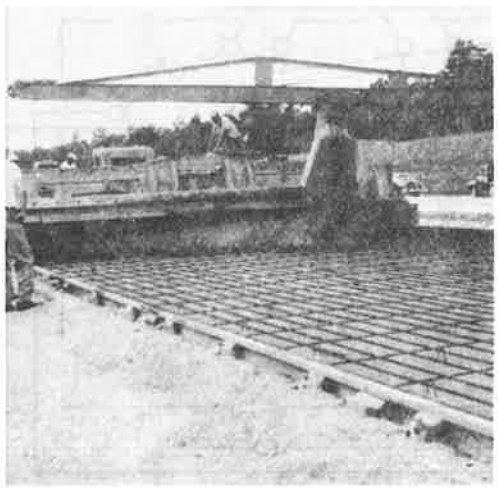

Figure 7. Concrete spreader and mixer boom.

Figure 8. Straightedging crew.

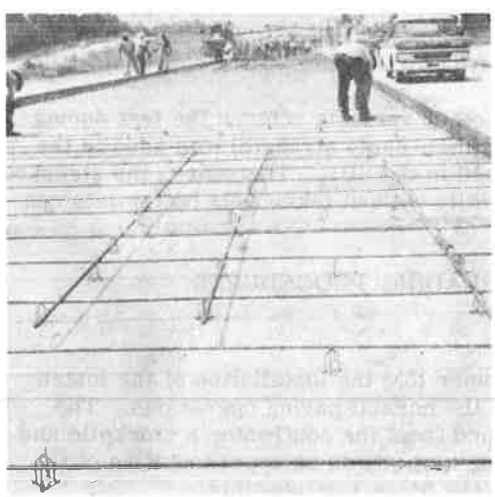

Figure 9. Placement of reinforcing steel.

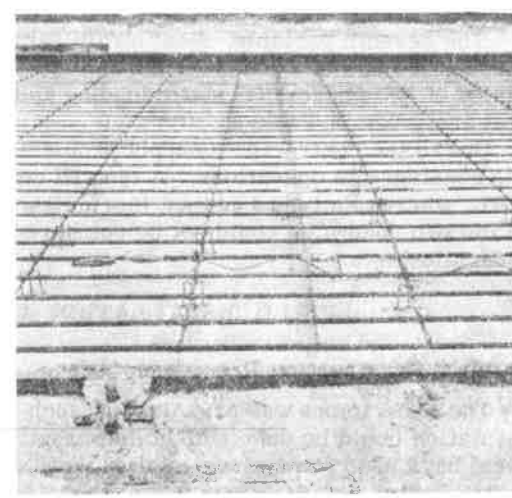

Figure 10. Strain gages and metal angles for preforming cracks.

coarse aggregate, the contractor elected to form the longitudinal joint during the normal paving operations.

Field Installation

Due to the nature of the contractor's operations, the majority of the instrument installation for each test area had to be made on the day of concrete placement. The conduits containing the wire leads for the instrumentation were buried before placing the forms; and the steel was positioned and the leads pulled through the conduit after the passage of the subgrade planer. After the instrumented bars were placed in the mat and tied, the resistance and resistance to ground of each gage were checked. Each strain gage on the steel bars, as well as the temperature bulbs, were covered with concrete by hand before the concrete spreader passed. For the purpose of controlling the formation of a transverse crack, a 2- by 2-in. galvanized metal angle was nailed to the subbase for the full pavement width (Fig. 10). The gage plugs used for measuring concrete movement were installed in the surface of the pavement immediately after the passage of the longitudinal finishing float.

A comparison of conditions during the placing operations reveals that both test areas were placed at the same time of day (3:30 PM) and at approximately equal air temperatures. This condition was felt to be a necessity if the data from the two test areas were to be compared. The curing paper was layed on both test areas at approximately 6:00 PM on the respective days of placement.

Procedure for Field Readings

Preliminary investigations had indicated that if the steel and concrete strain measurements were to be of any value, a number of readings would be required for the gages during each cycle (5). The strain had been found to be in a constant state of change; therefore, the significance of an isolated reading would be difficult to interpret. In this study, an attempt was made to acquire a set of strain readings at least every 2 hr, and in no case did the number of readings drop to less than six strain readings per 24-hr period. Several sets of strain readings were taken near the time of sunrise and during the midafternoon (between 3:00 and 6:00 PM) because these two periods represented the periods of maximum and minimum strain in a cycle. Intermediate points between the maximum and minimum values served the purpose of revealing the characteristics of the change.

In an effort to obtain an orderly arrangement for studying the data, consecutive numbers were given to each cycle during which strain measurements were taken. The first cycle after placement of the test site in the northbound lanes—the first to be placed—was designated as cycle 1. Because the southbound roadway was not placed until four days later, the initial readings were not taken in the southbound roadway until the fifth cycle. Both concrete strain and steel strain readings were taken in the northbound roadway for the first eight days of the pavement life, and hence the first three days in the southbound roadway. After these initial cycles, the concrete strain measurements were discontinued and only measurements of the steel strains were made. These subsequent measurements amounted to seven additional cycles for each roadway. It might be noted that the steel strain readings were taken over a wide spread of weather conditions which allow the results of the experiment to be applied over a wide set of conditions.

METHOD OF ANALYSIS

Background information pertaining to an explanation of the method used in analyzing the data obtained during this experiment is given in Table 2. Each variable in the table was studied for the standpoint of observing the effect of each parameter on the dependent variable. For example, each of the measured parameters that could possibly affect the magnitude of steel strain (such as temperature, cement type, average crack spacing, with age) was investigated separately. This was accomplished by investigating the effect of temperature while holding the other parameters constant as far as possible.

Then an attempt was made to combine the effect of these parameters on the dependent variable.

Statistical Analysis

A statistical approach was used in analyzing much of the data because numerous readings were taken during the course of the experiment. The degree of interrelationship between any two factors was determined by regression analysis techniques. The type of analysis was ideal for using an electronic computer because this equipment results in a much greater speed of calculation and enables a much broader scope of study.

A linear regression analysis was generally found as the type most adaptable to the data, which tended to confirm preliminary suppositions. The linear regression analysis results simply in a line describing the average relationship between two variables under consideration that is derived by the method of "least squares." The first order equation (linear) used was

$$Y = a + b\,x \tag{1}$$

in which

Y = dependent or "predicted" variable;
x = independent or "predicting" variable; and
a, b = correlation constants.

In addition to determining the regression equation, the coefficient of determination d was also calculated for each equation to serve as a guide in the reliability of the analysis. This coefficient simply gives a measure of the explained variation of the dependent variable due to the effect of a variation in the independent variable (6). For example, a coefficient of determination of 0.91 for a steel-strain slab temperature regression analysis simply means that, for the data analyzed, 91 percent of the change in steel strain can be attributed to changes in the slab temperature. Naturally, the higher the coefficient, the better the correlation. Values of 0.90 and greater indicate there is an excellent degree of correlation between the two variables. The coefficient of determination is obtained by squaring the coefficient of correlation.

CRACK PATTERN OBSERVATIONS

Earlier in the report it was pointed out that a slab consisting of a complete day's placement of concrete for each percentage of steel was selected for the purpose of observing the crack pattern development and comparing the performance of the two steel percentages. In addition to these two test sections, eight study sections were selected for the purpose of analyzing the wide variation in average crack spacing found over the project.

Test Sections

The two test sections were used to evaluate the effect of age and steel percentage on the development of the crack pattern (Table 2). In this section, the study is made from the standpoint of the average crack spacing of the slab. The average crack spacing is obtained by simply dividing the length of the slab under consideration by the number of cracks within the slab. Periodic surveys of the test sections were taken on the basis of counting the number of cracks within each station. Table 2 enumerates the boundary conditions involved on these test sections.

Data pertaining to the average crack spacing were difficult to attain during the first ten days because paper curing was used during the construction operations. The paper remained on the pavement surface from 3 to 10 days depending on the rate of paving. Therefore, data for the test section during the early ages were collected by simply pulling back the paper in localized areas and recording the number of cracks. This operation was performed between sundown and sunrise to avoid any possible effect on

the curing. The average crack spacing for the slab during this early period was obtained by extrapolating the values found for the short sections.

Effect of Age.—Figure 11 shows the effect of age on the average crack spacing for both of the test sections during the first year. The average crack spacing shown on the figure is based on the entire slab length. As has been shown by other studies, the crack spacing decreases with age, but the degree of change is striking (7).

The decrease in average crack spacing from 10 to 200 days is 67 percent for the northbound roadway (0.5 percent) and 57 percent for the southbound roadway (0.6 percent). This exceeds the total percentage change experienced in other States during the first five years (7). The spacing decreased rapidly during the early age, and reached a leveling out point at about 125 days. Indications are that this pavement has attained its final crack spacing. In essence, these pavements have attained a desired crack spacing during the first year of life.

Percent Steel.—Figure 11 can also be used to compare the effect of steel percentage on the average crack spacing of a slab. As would be expected, there is an inverse relation between the average crack spacing and the percent of longitudinal steel, but the relation is changing with time. At 10 days, there is an average crack spacing differential of 4.6 ft between test sections, which is a 70 percent difference in terms of the spacing for the 0.6 percent section. At 200 days, the difference is 0.7 ft or 25 percent in terms of the spacing for the 0.6 percent section.

It is apparent on these test sections that age is tending to nullify the effect of the two different percentages of longitudinal steel. With all other things equal (flexural strength, curing conditions, etc.), this observation would probably hold true on other sections as long as there is a sufficient percentage of steel to satisfy the design conditions. Al-

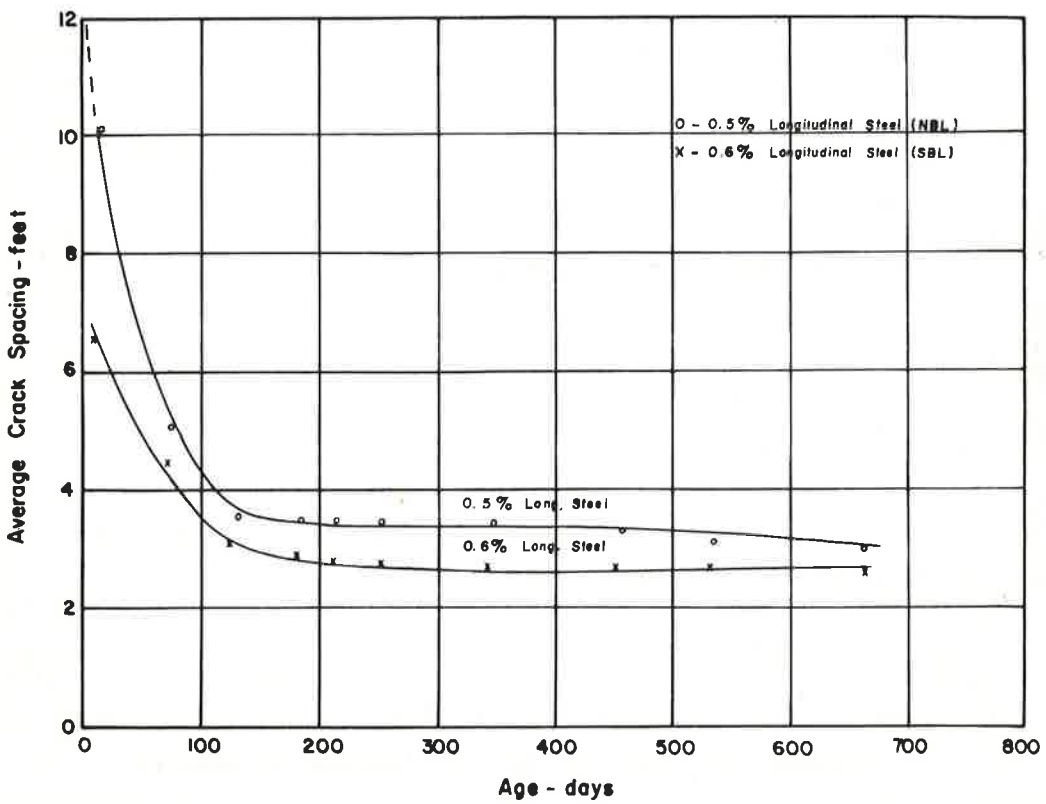

Figure 11. Relationship between age and average crack spacing on test sections.

though there is still a 25 percent difference in crack spacing for a 0.1 percent change in longitudinal steel, the relative magnitude of the difference is small. In addition to the fact that age is nullifying the effect of steel percentage, the crack spacing on both sections is well below what was considered as an optimum design maximum of 6 to 8 ft.

Distribution of Crack Spacing.—A study of the average crack spacing within each station (100-ft sections) indicated there was a uniform variation in the magnitude of the average crack spacing with distance along the slab. The average crack spacing increased in the direction of concrete placement for a given day's placement. This observation held true for both steel percentages. Figure 12 shows the average crack spacing at intervals of 100 ft along the southbound slab (0.6 percent) at 10 days and 345 days. In comparing the two lines, age appears to be nullifying the effect of location on the average crack spacing.

At 10 days, the average crack spacing within a slab increased at a rate of 0.096 ft per station in the direction of placement, whereas the rate had reduced to 0.036 ft per station at 345 days. The top line—the relation at age of 10 days—shows a wide differential at a distance of 1,700 ft from the start of the pour. The crack spacing at this point becomes much wider in relation to those experienced in the first 1,700 ft. One explanation for this could be the delay in paving operations experienced at this location. In addition to distance, the time of placement based on construction records is presented in the figure along with the approximate time the concrete attained its final set. The time of final concrete set was taken at 6 hr after placement, based on other investigations of Texas cements (8).

An examination of the temperature-time records revealed that this delay caused the final set of the concrete to occur at a time when the drop in the air temperature had

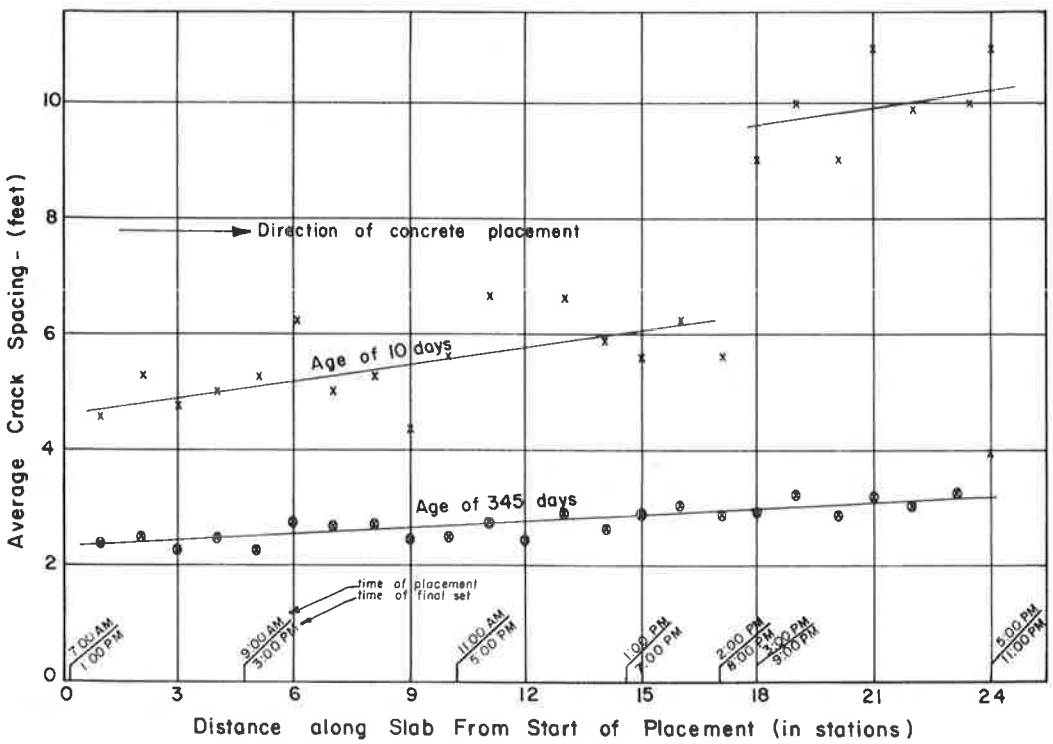

Figure 12. Effect of relative position within slab on average crack spacing, SBL (0.6 percent).

started to level off. Hence, the latter part of the slab experienced very little thermal reduction from its setting temperature during the first night. Therefore, the concrete in this section had a longer period to build up strength before the thermal reduction in the next cycle was experienced. This resulted in fewer cracks in this section of slab during the initial cycles. A number of cycles occurred before this unbalanced condition was stabilized. Uniformity of distribution was present at an age of 345 days.

Study Sections

In an effort to determine the reason for the wide variation in crack spacing in the project, eight "study sections" were selected at various locations. Each of the "study sections" had the following boundary conditions: (a) 500 to 600 ft long, (b) placed before midafternoon, and (c) located on level sections or relatively slight grades. In addition, the terminals of all study sections were located 100 ft or more from the nearest transverse construction joint to eliminate the effect of any possible end action. The locations were selected so that the range of flexural strengths within a study section did not exceed 40 psi.

When analyzing the data, it became apparent that an insufficient number of study sections had been selected. In essence, an attempt was made to evaluate the effect of four variables (age, average flexural strength, percent steel, and curing temperature) on the average crack spacing with only eight study sections. Generally it was not possible to hold three of the variables constant and vary the fourth due to this lack of data.

Curing Temperature.—The curing temperature selected for this analysis was the maximum air temperature recorded by the U. S. Weather Bureau on the day of placement. Figure 13 shows an inverse relation between the average crack spacing and the

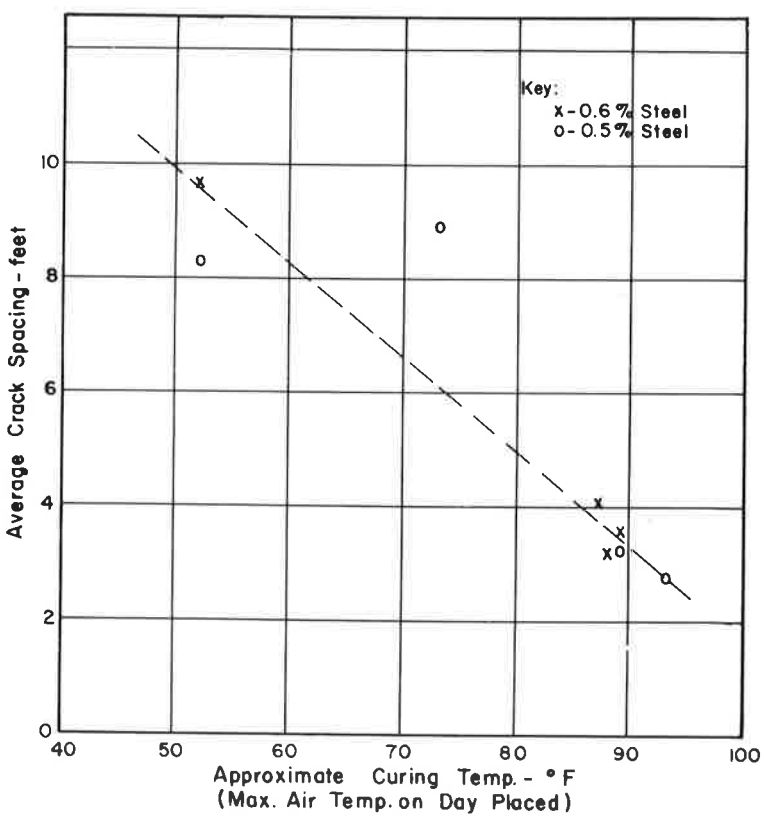

Figure 13. Average crack spacing vs approximate curing temperature for study sections.

curing temperature. This observation agrees with the results of other investigations. The curing temperature has a pronounced effect on the crack spacing in that a reduction of 40^0 in the maximum curing temperature results in an increase of 4.5 ft in the average crack spacing.

Percent Steel.—Each of the factors referred to thus far contains both the 0.5 percent and the 0.6 percent longitudinal steel study sections. It is apparent from all these studies that the differences between the other variables are more significant in influencing the crack pattern than the 0.1 percent difference in longitudinal steel present in the project.

STRESSES IN REINFORCEMENT

To analyze the stresses in the longitudinal steel, data were collected in the form of strain. These strain measurements were made at hourly intervals during the first eight days and three days after placement in the northbound (0.5 percent) and southbound (0.6 percent) roadways. After these initial measurements, hourly strain measurements were recorded through a 24-hr period at periodic intervals during the first year of life.

The strain measurements were converted to stress on the basis of the procedure in Appendix B. The steel stresses were then studied from the standpoint of cement type, cyclic behavior, and distribution along the longitudinal bars.

Effect of Cement Type

A study of the strain vs time plots for the gages located at the transverse control cracks on both pavements showed that the northbound roadway had a much higher strain immediately after the crack occurred than the southbound roadway. A comparison of the strain variation was made by computing the ratio of steel strains at the transverse cracks in each of the roadways:

$$R = \frac{\text{Increase in steel strain in NBL at failure}}{\text{Increase in steel strain in SBL at failure}} = 4.3 \qquad (2)$$

In other words, the longitudinal steel of the northbound roadway (0.5 percent) had approximately four times as much stress at the crack after the concrete failed in tension (crack formed) as the southbound roadway (0.6 percent). Identical weather conditions during the early life precludes this as a possibility for the high ratio, and reasoning would not credit the magnitude of the ratio solely to the small difference in the longitudinal steel percentage. This reasoning leads to the possibility that the major part of this difference is due to the two types of cement used. Because type III cement (high-early strength) was used in the northbound roadway, whereas type I cement (normal) was used in the southbound roadway, it might be tentatively surmised that the use of type III cement with continuously-reinforced concrete pavement can produce undesirable results.

Figure 14 shows the effect of cement type on steel stresses during the early curing period. The dashed portion of each of the relations is the change in the steel stress conditions at the time of pavement cracking. The change in stress magnitude in both cases is noteworthy. On cracking, the stress in the steel goes from approximately 500 to 4,500 psi with type I cement, a difference of 4,000 psi. With the type III cement, the stress in the steel goes from 2,000 to 20,000 psi, a difference of 18,000 psi. The cracking in concrete with a type III cement is of an explosive nature.

As background for an explanation of the extreme differential in stress levels, the following observations should be made from Figure 14. First, the failure in type I occurs at approximately 14 hr, whereas the failure in type III does not occur until 33 hr, which is in the second 24-hr cycle. For an understanding of the forces involved in a continuous pavement before and after cracking, the simplified free-body diagrams (Fig. 15) show that periods of concrete contraction are the ones of major concern with this type of pavement.

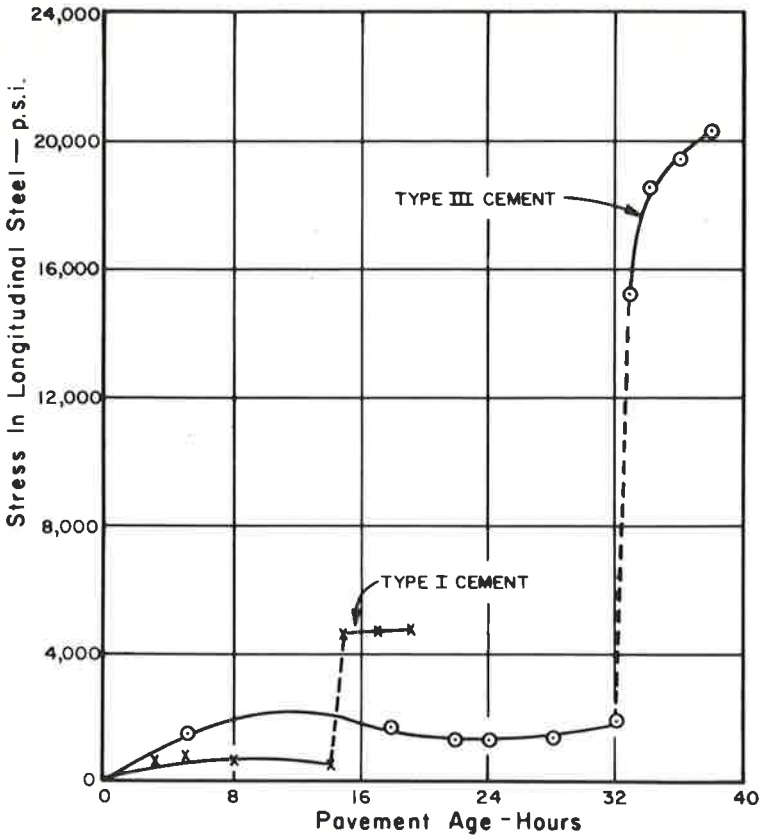

Figure 14. Effect of cement type on steel stress.

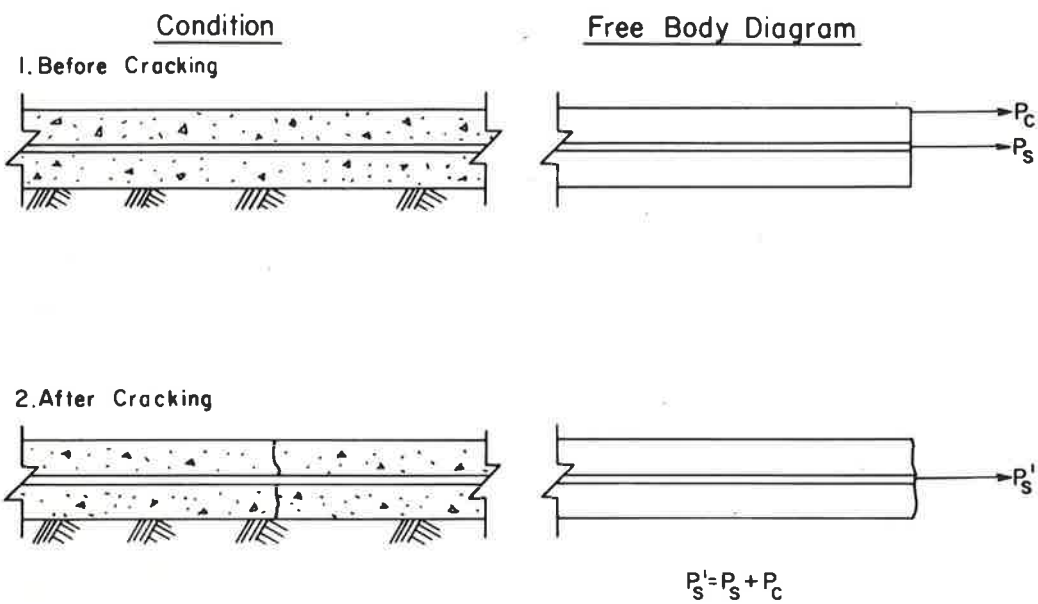

Figure 15. Force conditions before and after concrete cracking.

The left side of Figure 15 shows the conditions before cracking (top) and after cracking (bottom). On the right, the free body or force diagram for each of these conditions (neglecting the effect of subbase friction) is shown. In the force diagram for the period before cracking, the forces developed in the pavement by volumetric changes are carried by the concrete and the steel. After the crack occurs, the concrete cannot carry tensile forces; therefore, the steel must carry the total force developed. Hence, the tensile stress in the steel will always be greater at a crack than in the interior of a slab.

Now with the concept of the steel carrying the total force at a crack (Fig. 14), and the observation from Figure 15 that the concrete cracked at 14 hr with type I cement and at 33 hr with type III cement, an explanation of the observed differential stress levels is apparent. The basic difference between type I and type III cement is that type III attains its strength much more rapidly than type I, especially during the first 72 hr.

At the time of fracture, the type I cement had attained a strength of only 40 psi and the type III had attained a strength of 220 psi (9). This means that approximately 2, 500 lb of force were dropped into each steel bar when the type I cement was used, whereas up to 11, 000 lb of force were dropped into each bar with the type III; hence, the reason for the difference in steel-stress levels for the two cement types after cracking.

Cyclic Nature of Stresses

The stresses in each of the operating gages located at the preformed cracks in each roadway were of a cyclic nature. The stress-time plots in Appendix C show the variation of stress with time experienced at each of the gages. The stresses generally ranged between a maximum and a minimum during each 24-hr period that were not constant but varied with time. Also, the lesser steel percentage had a smaller minimum strain in addition to the logical higher maximum strain. The data presented in the stress-time relations were accumulated under a wide variety of weather conditions, such as air temperature extremes ranging from 25 to 95 F, summer and winter seasons, dry to humid atmospheric conditions, sunny and cloudy days. Therefore, any relations derived would encompass a variety of weather conditions.

With these general observations in mind, an investigation was conducted to determine the factors influencing each cycle. Then, the possible factors affecting the variation in maximum and minimum stress between cycles were investigated.

A comparison of the stress-time relation reveals the maximum stress generally occurs during the period of minimum temperature and vice versa. This agrees with the observation of an inverse relation between steel stress and temperature made in the past during other investigations (10). Figure 16 compares the typical fluctuation in steel stress and temperature during a daily cycle. As would be expected, the data show under normal atmospheric conditions the maximum strain for the cycle is experienced just before the sun rises, and the minimum strain experienced during mid-afternoon. Because air temperature measurements and slab temperature measurements at various depths were taken for each of the cycles, the question becomes which of the temperatures most accurately reflect the changes in steel stresses. After selecting the most appropriate temperature, this temperature could be used in all the other analyses.

Comparing Strain-Temperature Correlations at Various Depths. —In the northbound roadway, a constant record of the slab temperature near the top, near the bottom, and at the middepth of the slab was kept along with strain measurements (Fig. 4). In an attempt to determine which temperature offered the best correlation, a linear regression equation predicting steel strain in terms of temperature at the various depths was calculated for the first eight cycles. In addition, the average of the three temperatures (top, middepth, and bottom) was used to predict the steel strain.

Table 4 gives the coefficient of determination for the strain-temperature relations at different slab depths for gages 6 and 11 in the northbound roadway. These two gages were selected because they were located at the preformed crack, and furthermore, showed the greatest variations in strain. The table shows the best correlation is obtained by using the average of three temperatures. This observation also tends to veri-

fy conclusions arrived at during other investigations (10). The middepth also gives excellent correlation and in actuality there is very little difference in the degree of correlation between the middepth temperature and the average of the three temperatures.

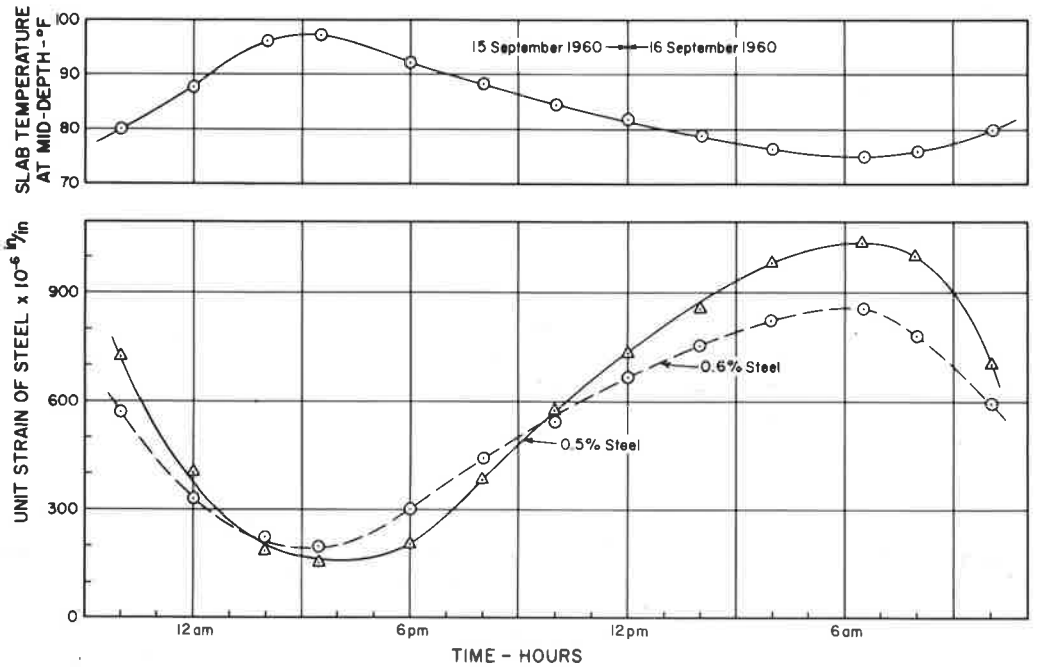

Figure 16. Relationship between steel strain and slab temperature at middepth during typical cycle.

TABLE 4

COMPARING CORRELATION OF SLAB TEMPERATURE AT VARIOUS DEPTHS WITH STEEL STRAIN[a]

Cycle No.	Coefficient of Determination							
	Gage 6[b]				Gage 11[b]			
	Mid-depth Temp.	Top Temp.	Bottom Temp.	Avg. Temp.	Mid-depth Temp.	Top Temp.	Bottom Temp.	Avg. Temp.
1	0.283	0.137	0.483	-	0.041	0.049	0.005	-
2	0.695	0.776	0.362	-	0.417	0.594	0.138	-
3	0.935	0.498	0.511	0.920	0.838	0.756	0.183	0.902
4	0.957	0.945	0.849	0.980	0.878	0.959	0.782	0.938
5	0.918	0.881	0.744	0.973	0.832	0.898	0.635	0.914
6	0.991	0.784	0.725	0.983	0.974	0.812	0.674	0.980
7	0.900	0.913	0.564	0.987	0.992	0.751	0.780	0.978
8	0.996	0.902	0.865	0.994	0.987	0.920	0.840	0.996

[a] Data from linear regression analysis comparing slab temperature at various depths with longitudinal steel strain.

[b] Gages 6 and 11 located at preformed crack in NBL.

The reason for this observation is evident after a study of the slab temperature-time relationships. Generally, the slab temperature at the top of the pavement attains its minimum and maximum magnitude for a cycle approximately 2 hr before the temperature at middepth, whereas the converse is true for the bottom temperature. Hence, the average temperature nullifies this time lag and gives the best correlation. The temperature at the middepth also gives excellent correlation because it is approximately the same as the average temperature.

Effect of Temperature on Steel Stress. —Because the average slab temperature gives the best correlation, it was used to study the effect of temperature on steel stress in each of the cycles for each of the roadways. As reported in the preceding section, a linear equation was used to predict the steel stress at a crack in terms of the average slab temperature. Using the format of Eq. 1, the stress-temperature equation is defined as

$$S_S = S_0 - K_S T_a \quad (3)$$

in which

S_S = stress in longitudinal steel for any given temperature T_a (psi);
S_0 = stress in longitudinal steel at 0 F (psi);
K_S = rate of change in longitudinal steel stresses due to temperature change (psi/^{0}F); and
T_a = average temperature of slab (^{0}F).

Table 5 gives the values of the constants S_0 and K_S for each of the cycles during which steel strain measurements were taken. Values of these constants are given for gages at the transverse cracks in both the northbound (0.5 percent) and the southbound (0.6 percent) roadways. However, these constants only apply to the cycle under consideration. The reason for the omission of values for the southbound roadway during the first several cycles is that this roadway was not placed till five days after the northbound roadway. Figure 17, which shows the relation between stress and temperature for a typical cycle, can be referred to for an illustration of the meaning of these constants. The value of S_0 is obtained by simply projecting the regression line to the intersection of the 0 F temperature line, whereas the value of K_S simply reflects the slope of the regression line.

TABLE 5

VALUES OF REGRESSION CONSTANTS FOR STRESS EQUATIONS FOR GAGES AT TRANSVERSE CRACKS, LINEAR REGRESSION ANALYSIS

Cycle No.	Regression Constant Value									
	NBL Gages				SBL Gages					
	6A		11A		8B		10B		3B[2]	
	S_0[1]	K_S[1]	S_0	K_S	S_0	K_S	S_0	K_S	S_0	K_S
1	11,170	103	-	-	-	-	-	-	-	-
2	13,530	132	-	-	-	-	-	-	-	-
3	131,180	1,315	127,230	1,266	-	-	-	-	-	-
4	159,240	1,629	200,700	2,126	-	-	-	-	-	-
5	125,000	1,239	164,410	1,681	-	-	-	-	-	-
6	143,210	1,480	169,650	1,763	6,510	69	3,170	51	-	-
7	159,950	1,674	187,480	1,959	86,800	889	90,320	945	14,040	147
8	164,990	1,716	202,370	2,153	89,000	892	88,630	903	-	-
9	101,530	1,005	125,960	1,282	73,020	684	73,870	707	59,180	553
10	94,130	941	112,030	1,152	74,580	729	77,080	780	58,890	580
11	99,350	1,065	95,200	1,045	56,820	504	46,520	473	80,650	945
12	71,600	626	61,140	457	49,080	377	53,590	629	-	-
13	73,650	912	75,010	992	48,210	486	37,740	459	36,090	421
14	42,170	386	51,910	584	42,770	410	29,130	330	-	-
15	71,420	892	72,600	967	37,180	299	25,810	292	31,100	312

[1] $S_S = (S_0 - K_S T)$
[2] Crack did not form until 9th cycle.

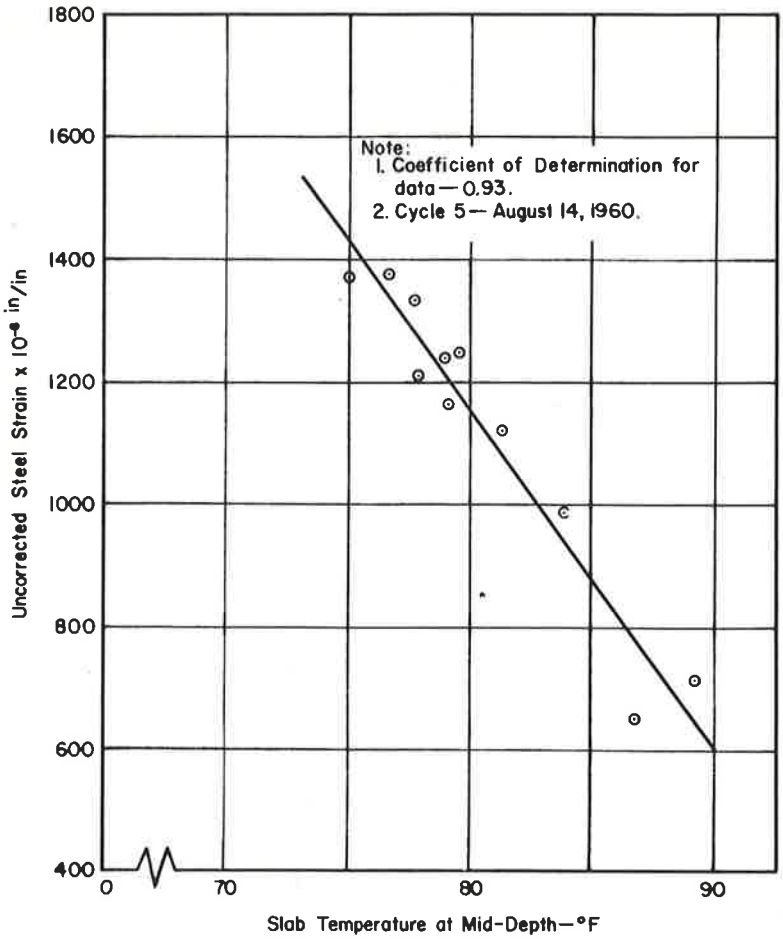

Figure 17. Relationship between steel strain and middepth slab temperature, Walker Co., NBL (0.5 percent).

When the first three cycles after placement are deleted, the coefficient of determination for each regression analysis is generally in excess of 0.90. The majority of the coefficient values fall between 0.95 and 0.99. This is an excellent degree of correlation between the two variables. As pointed out earlier, these values mean that 95 to 99 percent of the change in steel stress within a cycle can be attributed to a change in slab temperature. Therefore, it is concluded that within any given cycle the primary factor affecting the change in steel stress at a transverse crack is the magnitude of the slab temperature.

The low values for the coefficient of determination obtained during the initial cycles after concrete placement can partially be attributed to the fact that the initial transverse crack did not form in the pavement until the middle of the first cycle in the northbound roadway. An additional factor to consider is that the concrete properties (such as tensile strength, modulus of elasticity, and thermal coefficient) experience their most rapid change during the initial 72 hr (9). During these initial cycles, the curing of the concrete plays an important part in determining the stress level of the steel.

It is apparent that from Table 5 the values of the constants are decreasing with each successive cycle. In other words, a specific temperature apparently produces a smaller stress with each succeeding cycle.

Stress Variations Between Cycles. —The effect of age on the average crack spacing was presented previously, and it may be recalled that the average crack spacing decreased with age. Therefore, logically, the average crack spacing was correlated with the values of the linear regression constants S_0 and K_S for each cycle. These constants now become variables dependent on the average crack spacing which in turn becomes the independent variable. Figures 18 and 19 show the relation for this project between K_S and the average crack spacing for 0.5 percent and 0.6 percent longitudinal steel, respectively, and Figures 20 and 21 show the relation between S_0 and the average crack spacing for each steel percentage. The regression constants for each gage at a transverse crack are combined on the appropriate graph for its steel percentage.

The data for gage 3B, which was at an uncontrolled crack, fit the same pattern as those at the controlled crack. Both constants are directly related to the average crack spacing. This simply means the steel stress (for any given temperature condition) will decrease as the average crack spacing decreases. There is scattering of points on the graphs, but again, the data were taken during a wide variety of weather conditions. Using the regression analysis, the equations for each of these relations can be derived in terms of average crack spacing X measured in feet. This analysis results in equations similar to the regression format of Eq. 1.

For 0.5 percent (D = 77 percent):

$$K_S = 391 + 99\,X \tag{4}$$

For 0.6 percent (D = 87 percent):

$$K_S = 194 + 84.7\,X \tag{5}$$

For 0.5 percent (D = 83 percent):

$$S_0 = 32,410 + 9,850\,X \tag{6}$$

For 0.6 percent (D = 87 percent):

$$S_0 = 22,000 + 8,140\,X \tag{7}$$

These equations express the basic relationship experienced during the first year for each steel percentage. The coefficient of determination for the regression equations ranges from 77 to 87 percent. Although these are not excellent correlations, they are fairly good considering the variety of conditions. For the purpose of analysis, these four equations could be compared either from the viewpoint of steel percentage or from the standpoint of each constant.

First, considering the figures and equations from the standpoint of steel percentage, one logical observation becomes apparent. The slope of regression lines for both constants K_S and S_0 is greater for the roadway with 0.5 percent longitudinal steel than the one with 0.6 percent. This observation along with consideration of temperature explains the earlier observation that the 0.5 percent steel had a lower minimum as well as a higher maximum stress than the 0.6 percent steel. The higher rate of change allows a much greater change in stress between the maximum and minimum temperature with a given crack spacing.

Next, in Figures 18 and 19, lines cross the zero ordinates for K_S at values of 390 and 195 psi per $^{\circ}$F for 0.5 and 0.6 percent longitudinal steel, respectively. This of course is in the range of the value of thermal coefficient for steel (around 190 psi per $^{\circ}$F). An analysis of the stress system verifies this observation, because it is obvious that the "tied" steel would build up thermal stresses in proportion to its own thermal coefficient if no concrete were present, which is equivalent to zero crack spacing. This supposition indicates the slab segment, including the concrete, is fluctuating or moving along its length with changes in temperature. Therefore, it may be concluded that the rate of change in thermal stresses at a crack in continuously-reinforced concrete pavement is some function of the steel's thermal coefficient plus the length of the slab segment.

Figures 20 and 21 show that the regressional lines cross the ordinate at values of 32,300 and 22,000 psi for 0.5 and 0.6 percent longitudinal steel, respectively. Further

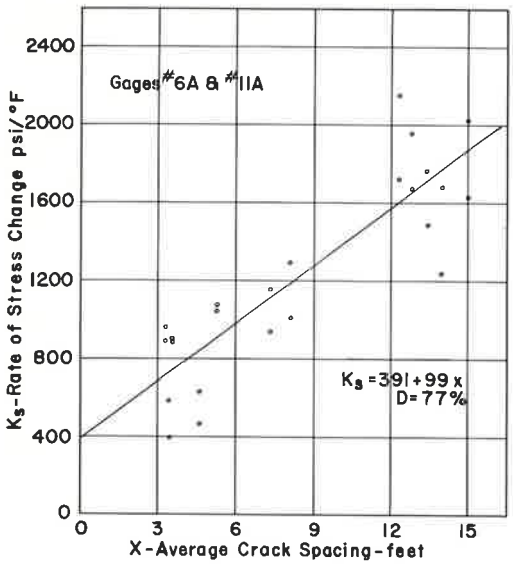

Figure 18. K_S in terms of average crack spacing, 0.5 percent.

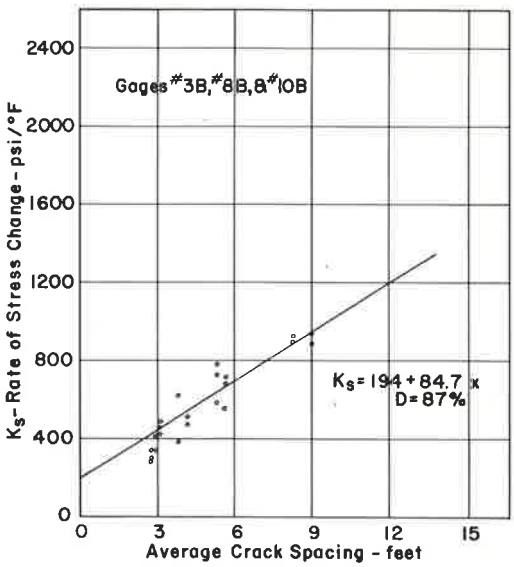

Figure 19. K_S in terms of average crack spacing, 0.6 percent.

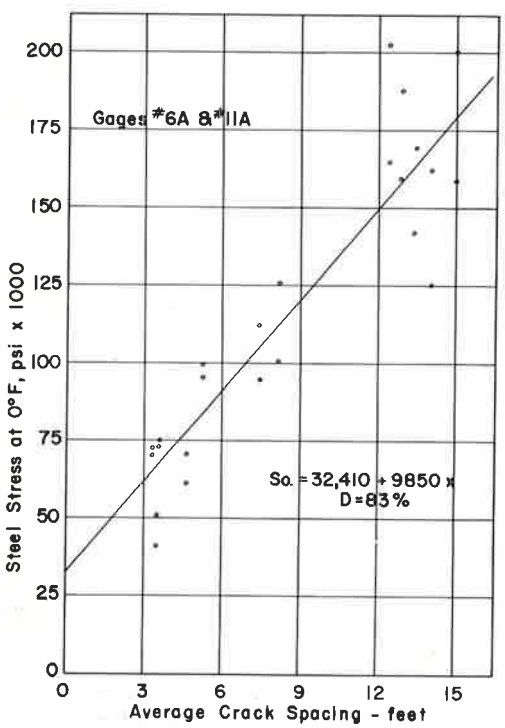

Figure 20. S_o in terms of average crack spacing, 0.5 percent.

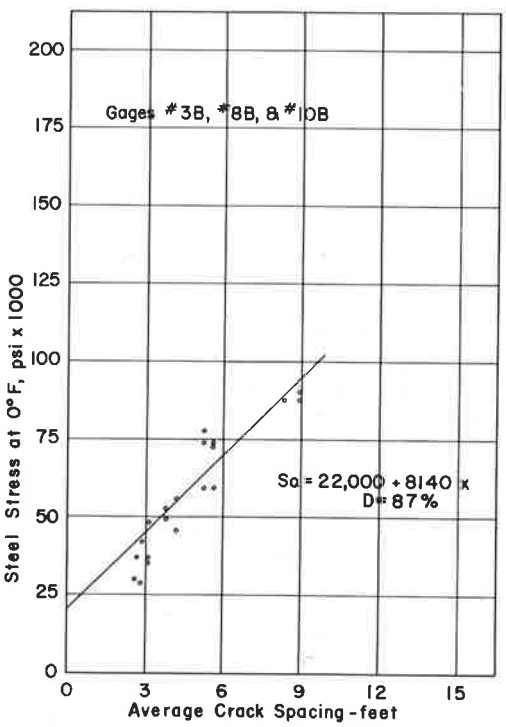

Figure 21. S_o in terms of average crack spacing, 0.6 percent.

the temperature of the concrete at the time of final set was approximately 95 F. By using the relations mentioned previously and considering the setting temperature, the magnitudes of S_0 can be explained. Without the presence of the concrete—zero crack spacing—the restrained steel would develop a stress of approximately 18,000 psi with a temperature drop from 95 to 0 F.

Combination of Slab Temperature and Crack Spacing.—The relations found for stresses within a cycle can be combined with the relations for stress between cycles to predict the stress at any period in the life of the pavement (for a given set of conditions for slab temperature and average crack spacing). Eq. 3 can be combined with the expressions in Eqs. 4 through 7 to arrive at an expression for steel stress at any given slab temperature and crack spacing.

Combining Eqs. 3, 4, and 6 for 0.5 percent relation:

$$S_0 = 32,410 + 9,850\ X - (391 + 99\ X)\ T \quad (8)$$

and combining Eqs. 3, 5, and 7 for 0.6 percent relation:

$$S_S = 22,000 + 8,140\ X - (194 + 84.7\ X)\ T \quad (9)$$

in which a positive number denotes tension, and a negative number denotes compression.

Steel Stress Distribution

This phase of the study primarily considers the longitudinal distribution of stress along the reinforcing steel. As a point of interest, mention is also made of the transverse distribution of stress along a crack on this project. Figures 4 and 5 show the positioning of the strain gages in the pavement.

An examination of the stress magnitudes experienced with the gages located at the transverse cracks indicated the gages nearest the edge of the pavement had slightly greater stresses than those nearer the longitudinal centerline. In contrast, those gages located in the interior of the slab segment did not show any pattern of stress difference in a transverse direction.

Considering the longitudinal distribution, the stresses in the steel were measured at 2-ft intervals over a span of 12 ft. The investigation found, as would be expected, that the maximum steel stress is located at a transverse crack, whereas the interior area between cracks experienced less steel stress. The magnitudes of stress experienced were a function of crack spacing and temperature as previously noted. In this section, the stress distribution is studied from the standpoint of crack spacing and variation within a cycle.

Variation with Crack Spacing.—Figure 22 shows the steel stress distribution in the southbound roadway (0.6 percent) at three different intervals during the pavement's early age. The top of the figure shows the stress distribution immediately before the first crack occurred. The middle and bottom show the distribution after the first and second cracks developed in the test area. The position of the cracks in relation to the gages is shown by the inset at the top of each portion of the figure.

Generally, the ratio of stresses at the cracks are in the order of four times the magnitude of those in the interior. The distribution is very similar to those theoretically proposed by earlier investigations (11). However, both gages 3 and 6 had stresses of a lower order of magnitude than the adjacent gages before cracking occurred. Both were located at points where cracks came into the pavement. A plausible explanation of this observation cannot be given at the present time.

Variation Within a Cycle.—Figure 23 contrasts the longitudinal stress distribution in the southbound roadway at the maximum and minimum temperature in a typical cycle. This figure is typical of the steel stress distribution relations other than the changes in the stress magnitude attributed to changes in temperature. The dashed line represents the steel stress distribution at the minimum temperature experienced in the cycle, and the solid line is for the distribution at the maximum temperature.

The maximum stress is experienced at the crack during the minimum temperature, as would be expected. The stress level along the bar is approximately the same at all locations during the period of maximum temperature. At the interior area between cracks, the stress has its smallest magnitude during the period of minimum temperature. If the stress level of the steel were solely a function of the temperature, then the stress level in the interior area would be greater during the period of minimum temperature.

This points out that a compressive force is applied to the steel by the slab in the slab segment interior, then the slab attempts to contract due to a temperature drop. The compressive force applied to the steel by the contracting slab then cancels out the

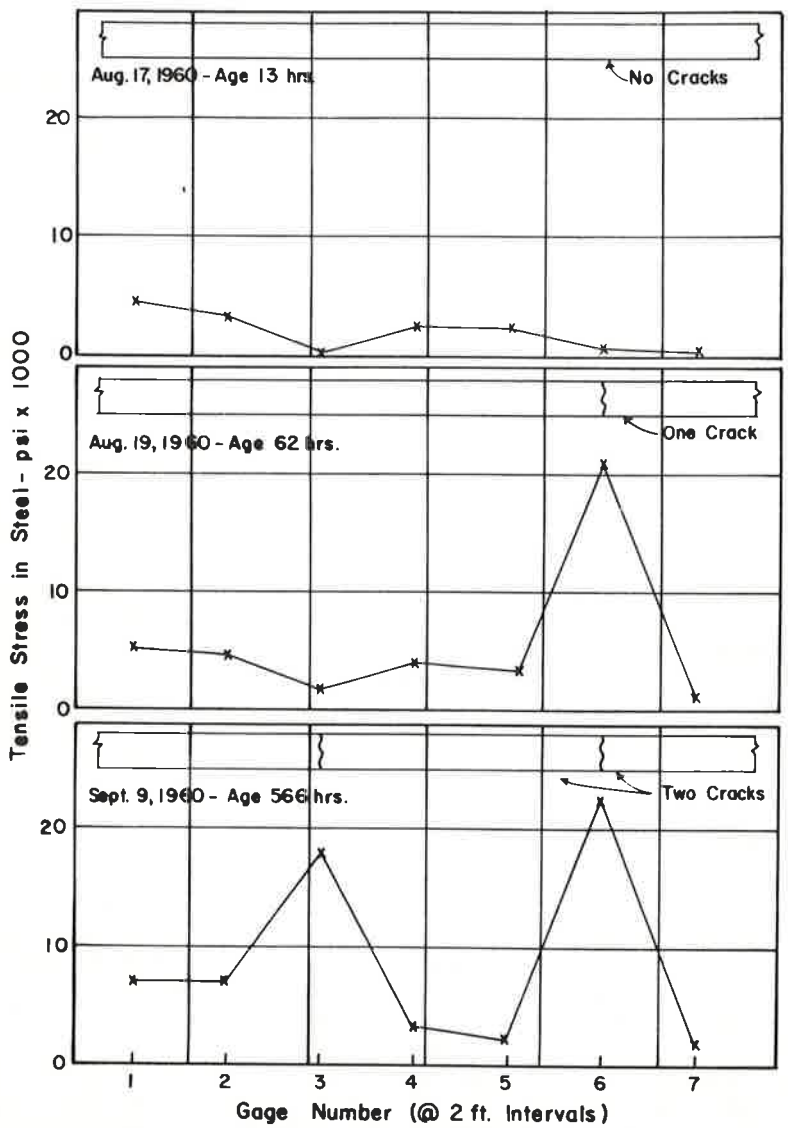

Figure 22. Variation in steel stress distribution with change in crack spacing, 0.6 percent.

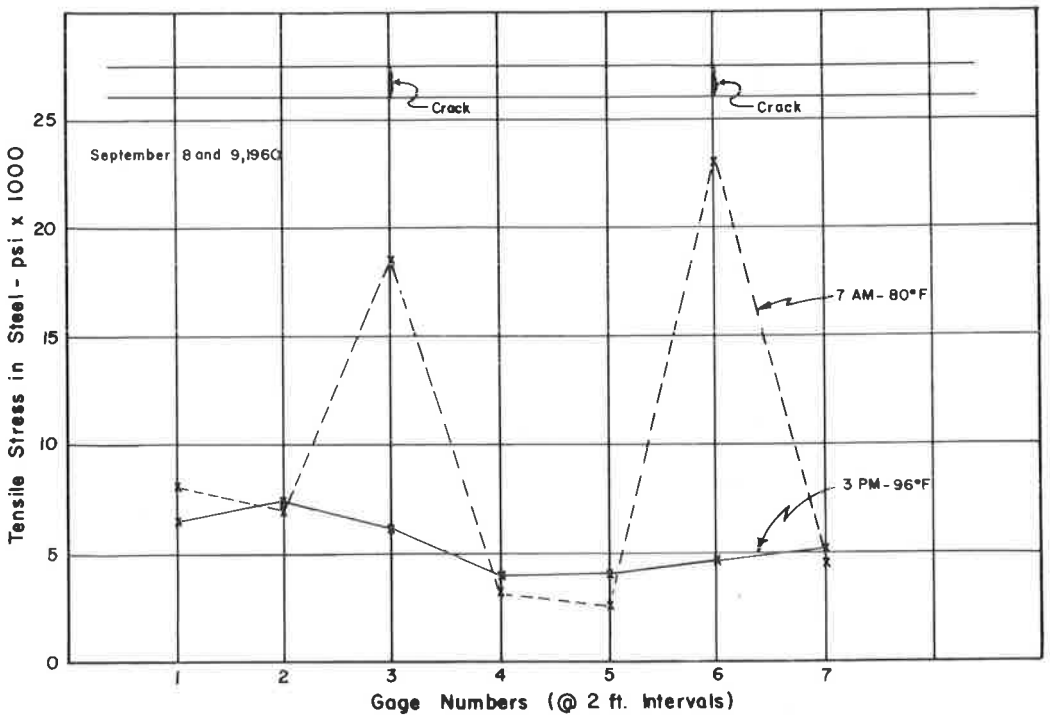

Figure 23. Comparing steel stress distribution between minimum and maximum temperature, 0.6 percent.

additional internal tensile stress that would have developed in the steel as a result of the temperature drop. Hence, a smaller stress is recorded in the slab segment interior during the period of minimum temperature than during a period of maximum temperature.

This study of stress distribution points out that each individual slab segment is a fluctuating body. These segments expand and contract with temperature changes although the center of the slab segment is fixed in relation to the ground. Any opening movement that occurs at a crack must be balanced by a closing movement in the area between cracks. Any study of continuous pavement to develop theoretical stresses should take this fact into consideration. By comparison, a continuous pavement is similar to a jointed pavement except that the movement is severely restricted by the steel.

Wheel Load Test

This phase of the study was an investigation into the effect of a wheel load on the steel stresses in a continuously-reinforced concrete pavement. The study consisted of two different types of wheel loading: static and dynamic. Static load tests consisted of determining the longitudinal distribution of the steel stress with the wheel at the crack, and the variation in steel stress at the crack as the wheel moves away from the crack. The dynamic load test consisted of measuring the steel stress at the crack with a vehicle moving over the crack at varying velocities.

The wheel load used in the test was the left rear wheels of a single-axle dual-wheel dump truck loaded with sand. Table 3 and Figure 24 give pertinent data concerning the test and the vehicle used. An important point in relation to this phase of the test is that the readings were taken in the morning hours when the crack was at or near its maximum opening. Therefore, these tests represent the most critical loading period for the cycle.

Static Load.—Figure 25 shows the longitudinal distribution of stress due to the wheel load being placed directly over the crack. The ordinate is labeled "change in stress due to staic load"; hence, temperature stresses have been deleted from consideration. This figure shows that at a distance of approximately 3 ft from the crack (moving in a direction away from the truck), the steel stress goes from tension to compression. The zero reading at gage 7 when moving toward the front wheels could possibly be due to the influence of the front wheels. The steel stresses at the interior points are minor when compared to the stress at the crack

Figure 24. Vehicle used in wheel load tests.

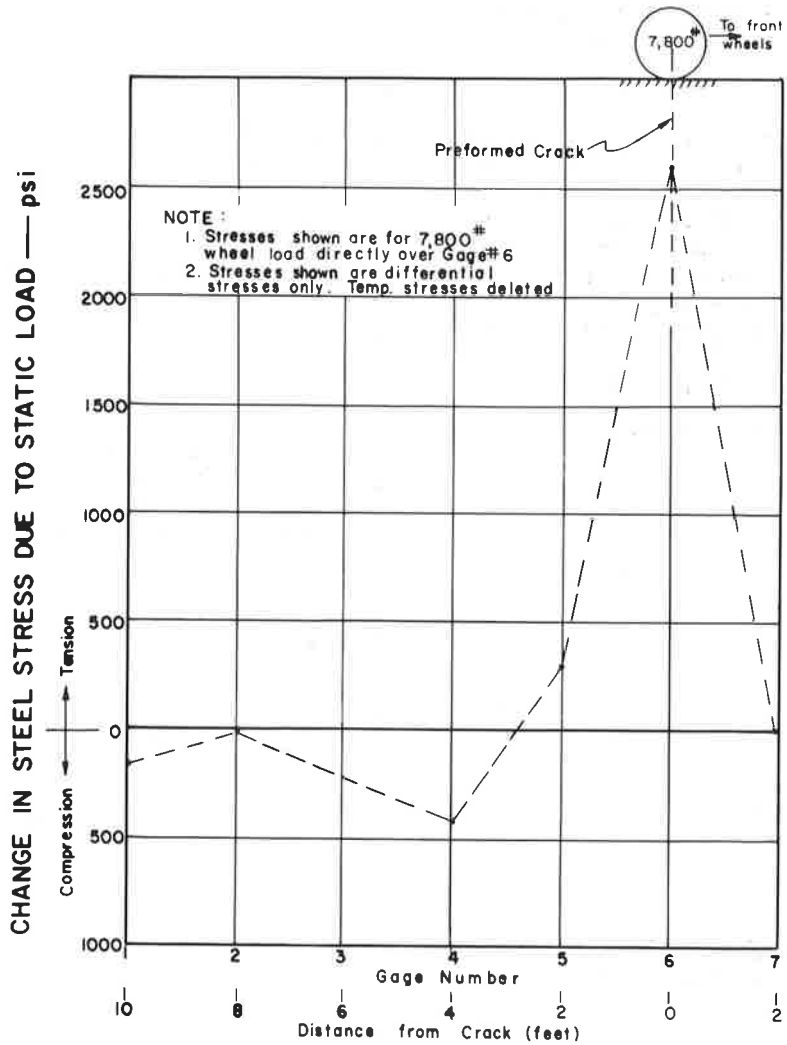

Figure 25. Effect of static load on steel stress distribution, NBL (0.5 percent).

being less than one-sixth of the magnitude. Carrying this logic further, the stress at the crack due to the static wheel load (2,600 psi) appears to be relatively insignificant when the fluctuations of stress due to temperature variations (5,000 to 40,000 psi) are considered. Inasmuch as small stress variations in steel (such as those experienced with the static load) will not fatigue steel within a practical number of applications, it might be concluded that, for this steel ratio, metal fatigue would not occur at the crack for the wheel load applied.

Figure 26 shows the effect of various positions of the wheel load on the magnitude of stress at the crack. The steel stress approaches zero at a distance of approximately 4 ft from the crack. Although the loading conditions are slightly different, the zero stress point is at approximately the same distance found in the previous relation.

Dynamic.—Figure 27 shows that within the limits of the data, the stress obtained at the crack is inversely proportional to the velocity of the wheel load. In other words, the stress at the crack decreases as the velocity increases. At the maximum velocity used (15 mph) the stress experienced is approximately one-eighth the stress experienced with a static load.

These limited tests tend to indicate that external loads (such as truck loads) do not materially affect the steel stress level when considering the total stress due to other factors. This leads to a tentative deduction that fatigue of steel at a crack due to wheel loads is not a factor to be reckoned within a properly designed continuous pavement.

CONCRETE MOVEMENT

For the purpose of analyzing the stresses in the concrete, the data were collected in the form of movement. Movement is used in lieu of strain in this investigation, because any measured movement is not due to strain of the concrete, but to relief from restraint stresses developed due to suppressed volume changes of the concrete. The data measurements were made at hourly intervals during the first eight days and three days after placement in the northbound (0.5 percent) and southbound (0.6 percent) roadways. In the following analysis, the data were studied from the standpoint of cyclic behavior and longitudinal distribution of movement.

Movement at a Transverse Crack

Data pertaining to variations in width of a transverse crack were obtained by two different methods. One method was by the use of the Berry strain gage and the gage plugs across a crack (Figs. 4 and 5). The other method was by use of a microscope

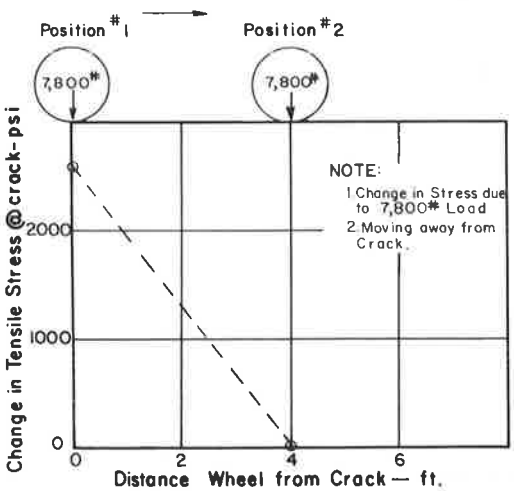

Figure 26. Effect of distance of static load from a crack on steel stress at a crack, NBL (0.5 percent).

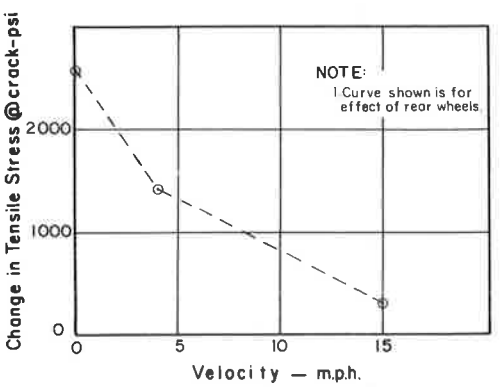

Figure 27. Effect of velocity of load on steel stresses at a crack, NBL (0.5 percent.)

with a graduated eyepiece. The microscope was located along the line of gage plugs and in the identical spot each time a reading was taken, which allowed the duplication of readings.

The first step in this analysis was to determine which slab temperature gave the best correlation with crack width. The linear regression analysis showed that the middepth temperature and the average of the three temperatures gave the best correlation, as was the case with steel stresses and temperature. This observation is rather surprising considering that both methods of measurement were made at or near the surface. It might be tentatively concluded that middepth temperature or the average slab temperature should be used in any crack width studies.

A comparison of the analysis of the data obtained with the two methods of measurement showed almost identical results. The observation applied to the data from both roadways.

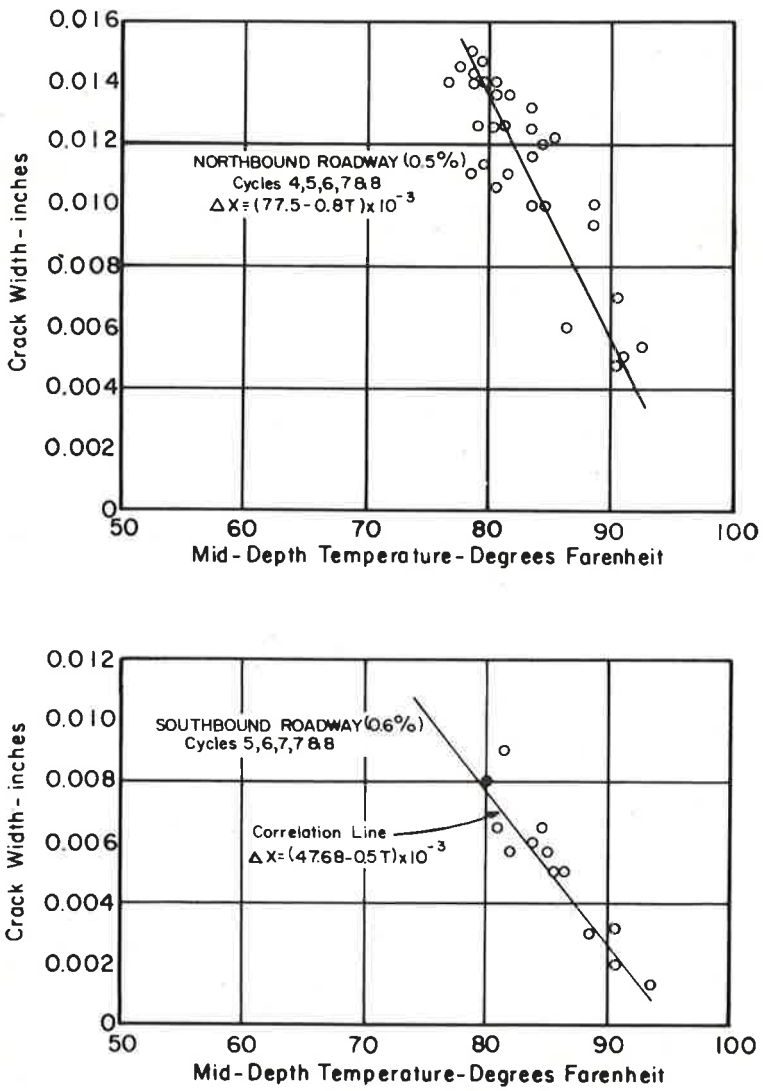

Figure 28. Relationship between crack width and middepth temperature for preformed crack in each roadway.

Figure 28 shows a typical relation between crack width and the slab's middepth temperature for the control crack in each of the roadways. The top part of the figure is for the northbound roadways and the lower portion for the southbound roadway. A regression analysis was made for each crack for which data were available, which includes the natural formed cracks as well as the control crack. The equations for each of the cracks in a given roadway were equal for all practical purposes. (This observation indicates the method of preforming the cracks did not influence the results.) Therefore, the equations were combined into an average equation.

For 0.5 percent:

$$\Delta X = (63.1 - 0.64T)\ 10^{-3} \tag{10}$$

For 0.6 percent:

$$\Delta X = (50.3 - 0.52T)\ 10^{-3} \tag{11}$$

in which

ΔX = crack width (inches);
T = middepth temperature of slab (^{0}F); and pavement age = less than 20 days.

In comparing the data for the two roadways, the equations indicate that a 20 percent increase in steel will result in a 20 percent reduction in crack width. Of course, there are other factors such as cement type that could influence these results. In general, the equations show, as would be expected, that the crack closes as the temperature increases and opens as the temperature decreases. One important point in the considerations of these equations is that the crack widths obtained by the use of the equations are

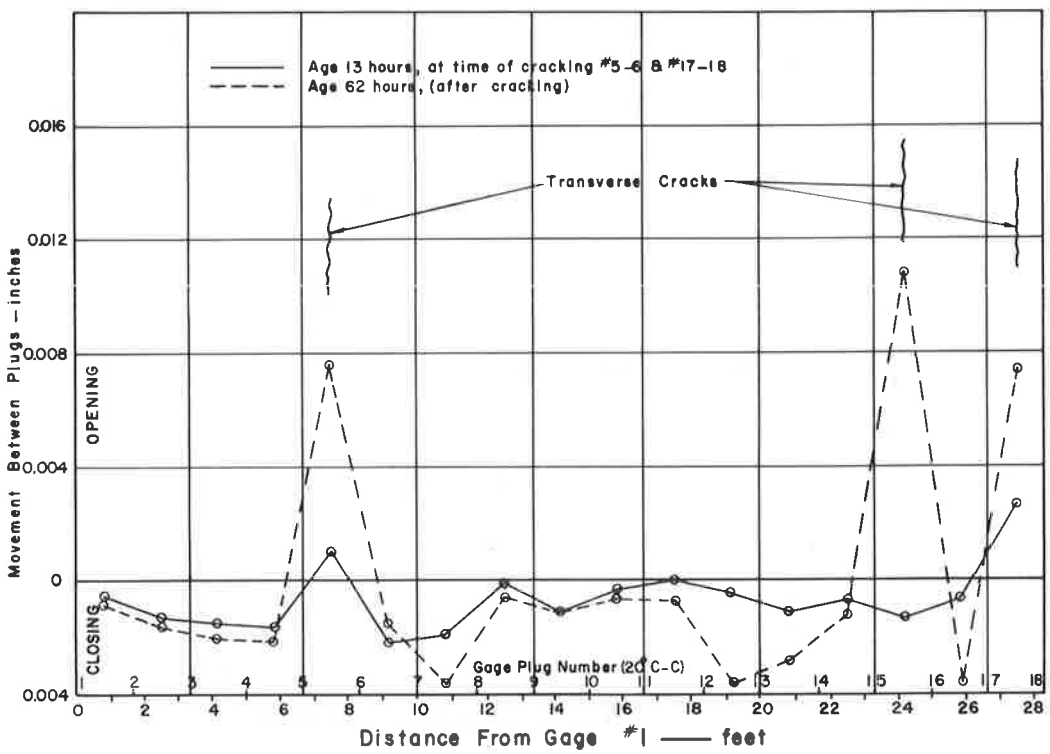

Figure 29. Comparing movement distribution at minimum temperature as new cracks appear in slab, SBL (0.6 percent).

strictly the magnitude at the surface. The crack width near the steel would be less than the magnitudes shown here for any given set of conditions.

Distribution of Movement

To obtain a better understanding of the meaning of movements between gage plugs, these movements should be studied as a unit. This can be accomplished by plotting the movement between each gage plug vs the distance from gage plug 1 to the midpoint between the set of gage plugs for a specified pavement age. In this way, the distribution pattern of movements can be investigated in relation to age, slab cracking, and temperature. Figures 29 and 30 are plots of movement distribution in the southbound roadway at various ages.

Figure 29 compares the movement distribution at minimum middepth temperature as the crack spacing changes. The distributions shown are for pavement ages of 13 and 62 hr which are identical with the periods used for studying steel stress distribution in Figure 21. The solid line is for an age of 13 hr which is the period of initial cracking, and the dashed line represents a period after the cracks have formed (62 hr). From the solid line, it is apparent that excessive opening movement in relation to the other gages is beginning to occur between gages 5 and 6 and gages 17 and 18. The area between gages 5 and 6 is at the point of incipient cracking because the strain for this movement is 50×10^{-6} in. per in. based on a 20-in. gage length (ultimate strain at time, approximately 55×10^{-6} in. per in.). The next set of measurements 40 min later indicated the slab had cracked. The data show the slab had already cracked between gages 17 and 18 at 13 hr. This means an uncontrolled crack (gages 17 and 18) formed before the preformed crack (gages 5 and 6). Although both the steel strains and the concrete movement data indicated the slab had cracked at 13 hr, the cracks did not become visible to the eye until 24 hr later.

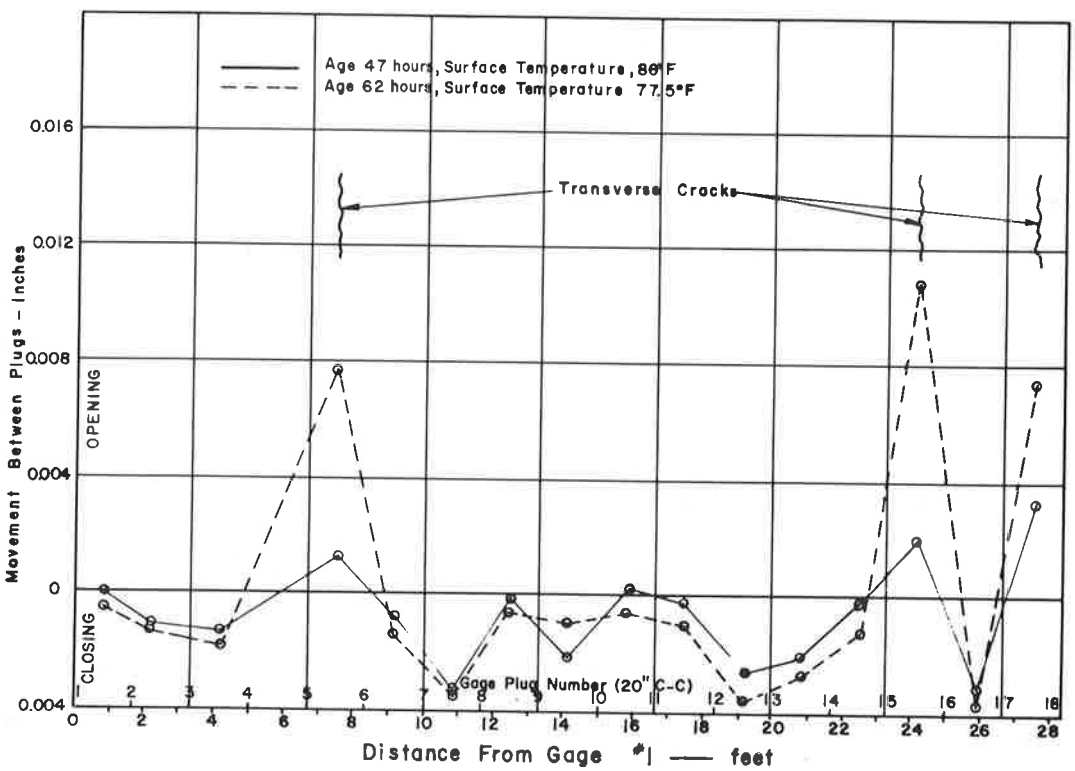

Figure 30. Comparing movement distribution at maximum and minimum temperature, SBL (0.6 percent).

The dashed line is the distribution at 62 hr. At this time, three cracks had developed within the test area. In contrasting the two distributions, as the crack opens up, the increased width at the crack is offset by an increased closure in the area between gage plugs. (The dashed line is below the solid line in the interior of each slab segment.) As would be expected, the algebraic sum of movements in the slab segments is approximately zero.

Comparing the two distributions, it is evident that approximately 60 to 70 in. of the slab segment away from the crack is fluctuating or moving. The areas between gages 7 and 8 and gages 12 and 13 are absorbing the bulk of the movement, whereas the slab segment between gages 8 and 12 is not experiencing movement. This area of no movement indicates that the full restraint stresses due to suppressed volume changes are developed. The next crack in the slab segment developed between gages 9 and 10, which are in the area of full restraint.

Figure 30 was inserted to compare the distribution of movement between adjacent plugs, that occurs during the minimum and maximum temperature within a cycle. As shown previously, cracks close as the temperature is increased. An apparent observation from the data is that the movement at a crack is absorbed over a considerable length of the slab segment. The interior area between cracks experiences more closing movement at the minimum temperature than at the maximum.

ANALYSIS OF RESULTS

A fundamental precept in the design of a continuously-reinforced concrete pavement is the determination of the optimum percentage for the longitudinal steel. Sufficient steel must be provided to hold the cracks tightly closed and to prevent the steel from being overstressed. Because the study of the distribution of stresses in the longitudinal steel presented in this report shows the maximum steel stress to be at the transverse cracks, as analysis would indicate, this area becomes one of the controlling factors in design. In the following sections, an attempt was made to analyze the factors influencing steel stresses and the formation of transverse cracks in the pavement. An understanding of the interrelation of the influencing factors could serve as a background for a rational design approach.

Factors Affecting Steel Stress

The data obtained from this study have indicated the changes in stress in the longitudinal steel were affected by two factors: the temperature and the average crack spacing of the slab. The individual slab segments of the pavement slab are in a constant state of fluctuation in the longitudinal direction. This movement results in an opening and closing of the transverse cracks, which in turn results in an induced stress in the steel.

Temperature.—The magnitude of stress in the steel due to slab temperature is a direct function of the concrete's and the steel's thermal coefficient of expansion and contraction. The steel would naturally develop stresses due to restraint of volumetric changes even if in an isolated condition, but the internal stress of the steel would amount to only a small part of the actual stresses experienced. A temperature drop of 10 F resulted in as much as a 20,000-psi change in steel stress in some instances on this project, whereas the theoretical maximum that would be induced in the restrained steel, if it was in an isolated condition, would be approximately 1,700 psi. This enormous difference in stress levels must be attributed to the limited restraint of the attempted movement of the slab segment at the crack by the longitudinal steel. This attempted movement by the slab segment is a direct function of the thermal coefficient of the concrete. The greater the thermal coefficient, the more the change in stress for a corresponding temperature variation. This explanation points out the desirability of obtaining a concrete with a small thermal coefficient.

Average Crack Spacing.—The stress in the longitudinal steel was found to be a direct function of the average crack spacing. In attempting to explain this observation, it is pointed out that the previous observation concerning the thermal coefficient and the fluctuating movement experienced as the temperature changes is interrelated with the

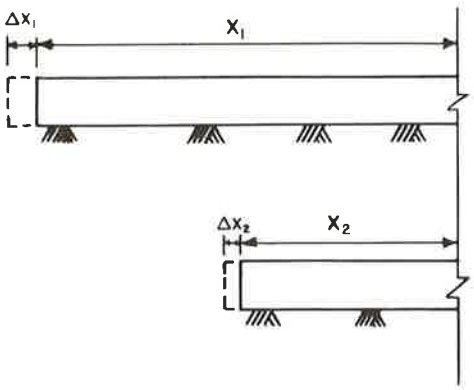

For temperature drop ΔT, movement experienced in two slabs of uniform materials but of different lengths would be

$$\Delta X_1 \sim X_1 K \Delta T$$

$$\Delta X_2 \sim X_2 K \Delta T$$

X_1 and X_2 represent only variance in the two formulas.

Figure 31. Study of slab movement in relation to slab length.

crack spacing. The magnitude of the attempted movement and the actual movement (crack width) is a function of the slab segment length. Figure 31 illustrates this statement. The magnitude of the actual movement that would result from a given temperature change would decrease as the length of the slab segment decreases.

With this postulate in mind, the consequence of the attempted movement of the slab segment in relation to the steel is examined. The data presented earlier concerning concrete movement indicated that the closing movement between cracks equals the opening movement at the crack (crack width) for the case of a temperature drop. This opening movement of the crack is a result of steel strain over a short section of the steel bar. The length of the steel bar experiencing movement at the crack is the distance along the bar that must absorb the opening movement, or in essence this length may be considered as the gage length of the tensile specimen. Because unit strain is simply the elongation (or movement) divided by the gage length, an increase in the attempted movement will result in an increase in strain; i.e., stress. It was shown previously that this attempted movement was a function of slab length; hence, the stress in the steel for a given temperature drop is a direct function of the slab length. Consequently, the stress in the steel for a given temperature drop decreases as the average crack spacing decreases.

The function would not be a linear one as might be tentatively concluded; the area of bond failure (gage lengths) would increase with age. This increase in gage length would also reduce the steel stress in addition to the decreasing average crack spacing.

Combination of Temperature and Crack Spacing.—The postulates previously discussed point out that the stress in the steel is a complex interaction problem that involves slab segment length, thermal coefficient, and temperature change. A temperature drop results in an attempted movement by the slab segment which is resisted by the longitudinal steel.

An increase in the steel stress results in elongation of the steel, which in turn tends to relieve the restraint forces developed in the concrete. Because the force system for the structure would be a static one rather than a dynamic one, even though movement is experienced, the force developed by the concrete must be balanced by the forces developed in the steel and by the frictional force developed between the slab segment and the subbase. In addition to the preceding hypothesis, the relief move-

ment experienced by elongation of the steel bar at the crack due to the strain developed is balanced by closing movement in the interior of a slab segment—reduction of tensile stresses in slab.

Formation of Cracks

The relationship between the pavement age and the average crack spacing for the test sections is shown in Figures 11, 29, and 30, the longitudinal distribution of movement between adjacent gage plugs along the pavement is shown for various ages. An analysis of the data presented in each of these figures indicates that temperature is a prime factor influencing both the movement in a slab segment and the average crack spacing during any period. The purpose of the following discussion is to analyze the interaction among the movement in a slab segment, the change in the average crack spacing, and the change in air temperature. In explaining this interaction, an approximation of the magnitudes of the longitudinal stress distribution is presented along with the effect of concrete properties on this stress distribution.

Stress Distribution.—Stress distribution in a concrete slab is related to movement. A slab segment completely restrained and subjected to a decrease in temperature would develop a uniform tensile stress in the slab. Any contractive movement occurring in the slab segment results in stress relief, and the magnitude of the stress relief is directly proportional to the movement. The partial restraint of movement that occurs at a transverse crack is due to the resistance of the steel and of the subbase; hence, a variation in the magnitude of movement is experienced in the area adjacent to the transverse crack. The magnitude of movement is inversely proportional to the distance from the transverse crack; therefore, the magnitude of the stress increases as the distance from the crack increases.

A relatively long slab would have (a) a central portion that is completely restrained (consequently, an area of constant stress), and (b) an area at each end of the slab segment that experiences a stress build-up as the distance from the crack increases. As long as the concrete is of relatively uniform strength, the central portion of a slab segment experiences a greater degree of cracking than the areas of the slab segment adjacent to the crack.

As the relative lengths of the slab segments decrease, as a result of the new cracks appearing in the slab, the slab segments will no longer have an area of constant stress. If the temperature differentials remain approximately equal during the daily cycles, the pavement will attain a stable crack pattern, because the summation of the flexural and tensile stresses in the pavement will not rupture the concrete.

Figure 32 shows the longitudinal distribution of stresses in the northbound roadway at 13 and 62 hr which are periods of minimum temperature for each cycle; hence, the period of maximum tensile stress. The magnitudes of stresses are only rough approximations arrived at by use of elastic theory, movement data, and concrete properties on this project; therefore, they were included only to serve as a basis for comparison.

Effect of Material Properties.—The two basic components of the pavement (concrete and steel) exhibit certain physical properties, but the steel's properties are relatively static, whereas some of the concrete's properties are in constant change. This change and the rates of change have pertinent effect on the formation of cracks and, hence, on the stress level in the steel. The initial ten days of pavement life is the period when the concrete properties are undergoing the greatest rate of change. The strength, the modulus of elasticity, and the thermal coefficient are increasing at various rates as the concrete ages. In general, the thermal coefficient and the modulus of elasticity are changing at a greater rate than the tensile strength, especially during the first few cycles. The rate of change of the thermal coefficient tends to stabilize within 20 to 50 hr, whereas the rate of change for the tensile strength continues over a much longer period.

The effect of these various rates of change in concrete properties is shown in Figure 32. At 13 hr the combination of the relatively high thermal coefficient and the temperature drop (approximately 10 F) has produced sufficient tensile stresses in the concrete to be at a level of the tensile strength. This, of course, is the period when the initial

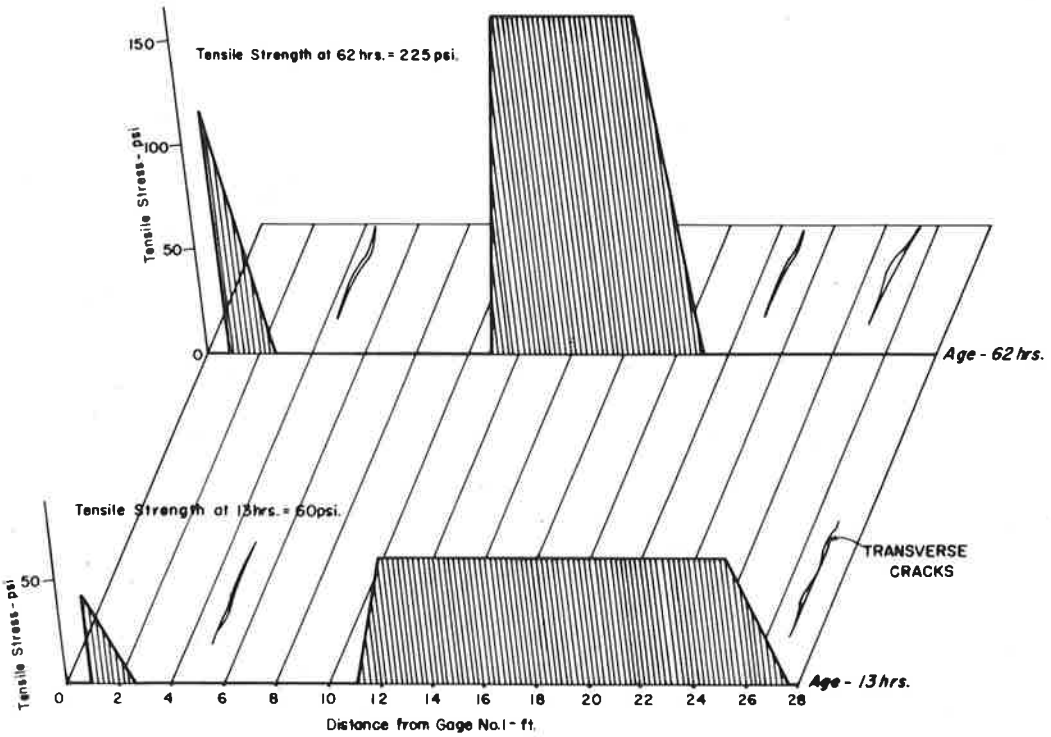

Figure 32. Stress variation along concrete, NBL (0.5 percent).

cracking of the slab occurred. In comparison, at an age of 62 hr the tensile strength is of such magnitude that an even greater temperature drop (approximately 15 F) does not produce a stress level that is near the tensile strength. This is one of the reasons why the pavement with the type III cement resulted in a much greater average crack spacing than the pavement with the type I cement. The type III (high-early strength) had such a high increase in strength during the initial few days that a much greater temperature drop is required before cracking occurs. Therefore, the wide crack spacing results in large stress levels at the crack, and this condition remains until sufficient temperature drops are experienced to produce tensile stresses in the concrete to exceed the tensile strength of the concrete. If the wide crack spacings resulted in the development of stresses that exceeded the yield point of the steel, the crack would open excessively and slab continuity would be lost.

The observations indicate that some of the desirable characteristics of concrete to be used in continuously-reinforced concrete are a low thermal coefficient and a slow gain in strength.

CONCLUSIONS

The research conducted on this project revealed that the design of the required longitudinal steel percentage for a continuously-reinforced concrete pavement is more complex than the ratio of the tensile strength of the concrete to the yield stress of the steel. Carrying the observation to its logical conclusion, the selection of a minimum steel percentage based on the performance of a pavement in one section of the country and applying it to another section is an erroneous approach. With the materials and environment in one section of the country, a fixed steel percentage might result in overdesign, whereas in another area the percentage will be insufficient.

The findings indicate that the design procedure should encompass crack spacing, temperature drop, and concrete properties, in addition to those presently considered.

Two of the more important concrete properties are the modulus of elasticity and the thermal coefficient. In general, the magnitude of these two concrete properties should be as low as possible.

The inclusion of the crack spacing in a design method points out an area where additional information is urgently needed. The factors influencing the crack spacing must be determined and evaluated. The reason why one percentage of steel results in various crack spacing under different conditions should be pursued.

In addition to the preceding hypothesis, the data from this project lead to these additional conclusions and recommendations:

1. Any future study of the factors influencing the crack spacing of continuously-reinforced concrete pavement should heed the effect of pavement age.
2. Both the 0.5 and 0.6 percent design performed satisfactorily on this project. Other factors influence steel stress and the average crack spacing more than steel percentages as long as slab continuity is maintained.
3. Each slab segment within a slab is in a continual state of fluctuation after the initial transverse cracks occur.
4. The primary factor influencing steel stresses in a given cycle is the slab temperature. The primary factor influencing the stress temperature relation between cycles is the change in crack spacing.
5. Type III cement (high-early strength) will result in much higher steel stresses than type I cement (normal) during the early life of a slab.
6. The average slab temperature gives the best prediction of steel stress and crack width.
7. The data imply that wheel loads would not be a critical factor from a steel stress fatigue standpoint as long as the slab continuity is maintained and the slab is in contact with subgrade. This observation applies solely to the design of the longitudinal reinforcing steel.

ACKNOWLEDGMENTS

The research reported in this paper was conducted on an experimental project in Walker County, Texas, on Interstate Highway 45 constructed by the Texas Highway Department and the U.S. Bureau of Public Roads. The research was under the supervision of T.S. Huff, Chief Engineer of Highway Design and general supervision of D.C. Greer, State Highway Engineer.

The authors wish to acknowledge the able assistance of C.J. Derdeyn of the Highway Design Division and W.B. Ledbetter formerly of the Highway Design Division and presently Instructor in Civil Engineering at the University of Texas.

Also acknowledgment of the help of Willard Moore and other members of the Materials and Tests Division under the supervision of A.W. Eatman for cooperation in the use of equipment and advice on instrumentation.

Thanks are also given to personnel of Highway District 17 under the direction of C. B. Thames, District Engineer, who assisted in the planning of the research phase of the project and especially to Jerry Nemec, Supervising Resident Engineer, for the splendid cooperation he arranged for with the contractor during the construction and the testing program.

REFERENCES

1. Shelby, M.D., and McCullough, B.F., "Experience in Texas with Continuously-Reinforced Concrete Pavement." HRB Bull. 274, 1-29 (1960).
2. "AASHO Interim Guide for the Design of Rigid Pavement Structures." AASHO Committee on Design (April 1962).
3. McCullough, B.F., and Ledbetter, W.B., "LTS Design of Continuously-Reinforced Concrete Pavements." Jour. Highway Div., Proc., ASCE, 86: No. HW4 (Dec. 1960).
4. Gersch, B.C., and Moore, W.H., "Flexure, Shear and Torsion Tests of Prestressed Concrete I-Beams." HRB Bull. 339, 43-66 (1962).

5. McCullough, B.F., "An Investigation of Continuously-Reinforced Concrete Pavement in Comal County, Texas." Unpublished thesis, University of Texas (1962).
6. Simpson, G., and Kafka, F., "Basic Statistics: A Textbook for the First Course." Norton (1957).
7. Lindsay, J.D., "A Ten-Year Report on the Illinois Continuously-Reinforced Concrete Pavement." HRB Bull. 214, 27-40 (1959).
8. Klieger, P., "Studies of Concrete Made With Texas Cements and Aggregates." Portland Cement Association, Skokie, Ill.
9. Jones, T.R., and Hirsch, T.J., "A Report on the Physical Properties of Concrete at Early Ages." Texas Transportation Institute, College Station (1961).
10. Lepper, H.A., Jr., and Garber, D.L., Jr., "Maryland Continuously-Reinforced Concrete Test Pavement. II. First-Year Strain Observations." HRB Proc., 40: 258-281 (1961).
11. Vetter, C.P., "Stresses in Reinforced Concrete Due to Volume Changes." Trans. ASCE, Vol. 98 (1933).
12. Perry, C.C., and Lissner, H.R., "The Strain Gage Primer." McGraw-Hill (1955).

Appendix A

INSTRUMENTATION AND WHEEL LOAD TEST DATA

The SR-4 strain gage, type A-5, 1 in. long, paper backed, was cemented to standard number 5 φ deformed steel reinforcing bars. Before attaching the gages, the bars were "turned down" on a lathe to a uniform diameter over a length of 4 in. A total of 22 gages were attached to six reinforcing bars on 20-ft centers along the bars. After the bars were prepared on the lathe each area was sandblasted with a fine sand and cleaned with acetone to remove all grease.

An epoxy adhesive, Armstrong type A-1, was used to adhere the gages to the bar. A uniform layer of adhesive, approximately ½ by 1½ by 1/32 in. thick was placed on the prepared bar area and the strain gage carefully pressed onto the adhesive. Care was exercised to insure that the longitudinal axis of the bar and the gage coincided, and that complete contact between the gage and the adhesive was obtained with no trapped air bubbles. The gages were then clamped in place and the adhesive was allowed to set for 24 hr. After 24 hr, the gages were all checked and a dike of adhesive approximately ⅛ in. high and ⅛ in. thick was formed around the gage. This was done to form a reservoir to hold the waterproofing wax. Figure 33 shows the gage and dike installation.

The gage and dike assembly was then allowed to set for a minimum of 24 hr before further treatment. After sufficient time had elapsed for the adhesive to harden, lead wires were soldered to each of the two gage resistance wires and grouped together into groups of eight lead wires to a cable and sealed in the protective plastic insulation material.

Each gage was then covered with a coating of sealing and waterproofing wax that was heated to a liquid form and applied with a small brush. The wax served the purpose of breaking any bond that might develop between the strain gage and the material used for waterproofing the gage. Any bond would result in false strain readings.

On completion of the wax coating, the entire assembly was covered with a flexible type of epoxy coating to seal and waterproof the entire assembly. Figure 34 shows a cross-section of the entire gage assembly.

The flexible epoxy was basically an epoxy resin containing a large portion of Thiokol that provided the resilient properties. The epoxy covering gained a consistency or hardness comparable to an art gum eraser, and again, a minimum of 24 hr was allowed to let the coating set up. The finished product for the waterproofing material was an impact and chemical resistant material possessing adhesion qualities to concrete and steel.

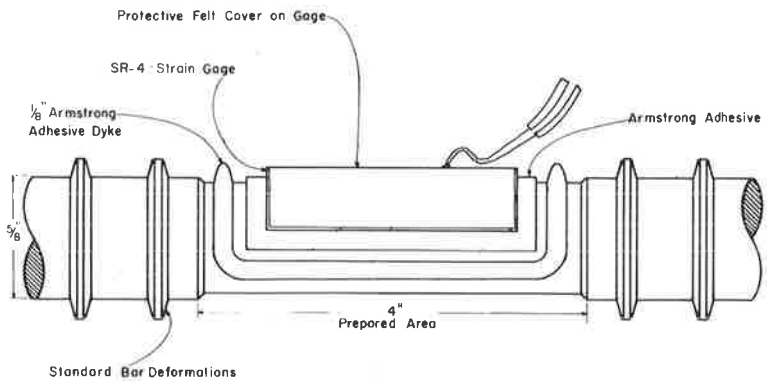

Figure 33. Gage and dike installation.

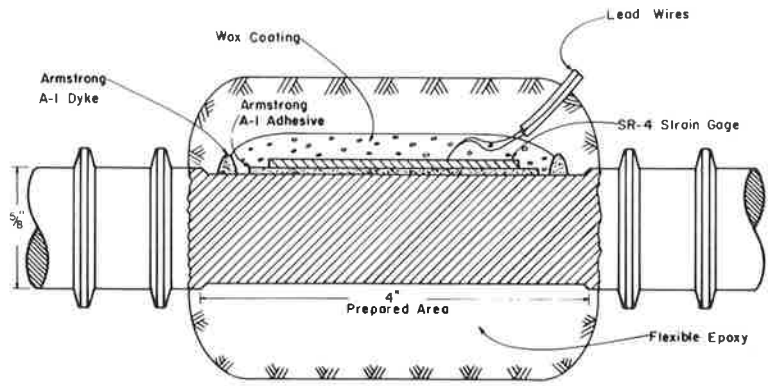

Figure 34. Cross-section of entire gage assembly.

The application of the flexible epoxy coating completed the procedure, and the reinforcing bars were ready for installation in the pavement slab.

Appendix B

STRESS CALCULATIONS

Procedure for Steel Stress Calculations

The measured steel strains are converted to stress in the following manner.

Between cracks:

$$S_g = 29.14\ \epsilon_i \times 10^6 \tag{12}$$

At cracks:

$$S_t = 22.29\ \epsilon_i \times 10^6 \tag{13}$$

in which

S_g = stress in steel at gage (psi);
ϵ_i = indicated or measured strain in bar (in./in.);

E = modulus of elasticity of steel bar (psi);
F = gage factor of strain gage being used;
ϵ_t = true strain in bar (in./in.); and
S_t = stress in typical $\frac{5}{8}$-in. φ bar (psi).

Development.—The variable resistance instrument box used on this project was calibrated to read strain directly. This calibration is based on a gage factor of 2.08. If strain gages with varying gage factors are used, the strain must be corrected by

$$\epsilon_t = \epsilon_i \frac{2.08}{F} \tag{14}$$

After obtaining the true strain in the bar, the stress in the steel is calculated by

$$S_g = \epsilon_t E \tag{15}$$

The stress obtained from Eq. 15 is the stress in the steel at the gages which is in an area of reduced cross-section. This elevated stress must be corrected to what would be experienced in a typical $\frac{5}{8}$-in. φ bar by the following (next section on steel stress correction for gages at transverse cracks gives development procedures):

$$S_t = 0.765\, S_g \tag{16}$$

For simplicity purposes the preceding equations could be reduced to one; hence, requiring only one calculation for stress. Within the mass of the concrete only Eqs. 14 and 15 should be used, whereas all three could be used when calculating the stress at a crack.

Calculating Stresses Between Cracks.—Combining Eq. 14 and 15,

$$S_g = \epsilon_i \frac{2.08}{F} E \tag{17}$$

Preliminary laboratory tests on the steel showed $E_s = 27.6 \times 10^6$ psi, and the gage factor for the gages used was 1.97. Substituting these values in Eq. 17,

$$S_g = 29.14\, \epsilon_i \times 10^6 \tag{18}$$

Calculating Stresses at Crack.—Combining Eqs. 16 and 17,

$$S_t = 22.29\, \epsilon_i \times 10^6 \tag{19}$$

Steel Stress Correction for Gages at Transverse Cracks

Before attaching the SR-4 strain gages to the longitudinal steel bars, each bar was "turned down" on a lathe to a uniform diameter over a length of 4 in. The "turning down" operation was required in order to obtain a smooth surface for cementing the gages to the bars. Therefore, each of the areas was "turned down" to approximately the same diameter for the sake of uniformity. This operational procedure resulted in a net reduction in the effective cross-sectional area of the bar.

An examination of the stress conditions in the steel bars reveals the problem created by this operational procedure. Figure 35 portrays a free body diagram of force conditions in longitudinal steel at the crack. The forces in each of the bars are approximately equal; therefore, the average strain between points of bond rupture (loss of bond) of the concrete to the steel must be equal. The necked down area must transmit the force; hence, a higher stress results in this area due to the reduced cross-sectional diameter of the bar. Correspondingly, an increase in stress results in an increased strain; therefore, the measured strain is of excessive magnitude even

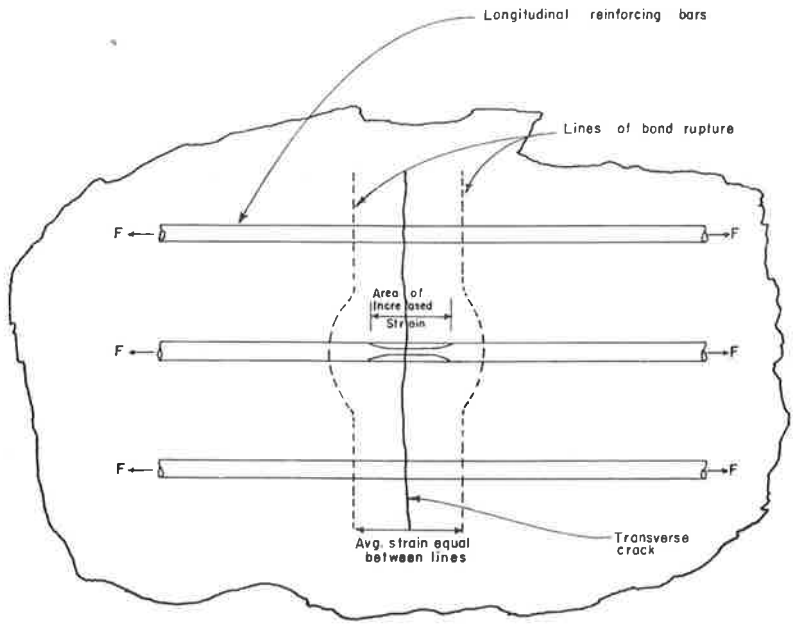

Figure 35. Free body diagram of forces present at a crack in continuously-reinforced concrete pavement.

though the average strains in all bars between points of bond rupture are equal. With this in mind, it is proposed that the measured strain be corrected by multiplying the ratio of the cross-sectional area at the gage to the normal cross-sectional area of the bars.

This correction is based on the following assumptions:

1. The point of bond rupture is outside the reduced cross-sectional area of the bar.
2. The forces in each of the bars are approximately equal.

Numerous papers on bond of concrete to steel portray the phenomenon of bond development. These papers should be referred to for the concept of bond development used in this paper. The first assumption is quite plausible because the waterproofing agent extended outside the necked-down area. If the point of rupture extended a finite distance outside the necked-down area in proportion to the force applied, the second assumption would be valid.

Correct stress is obtained by

$$S_t = S_g \frac{A_g}{A_n} \tag{20}$$

in which

S_t = correct steel stress in normal bar (psi);
S_g = stress in steel at gage (psi);
A_g = cross-sectional area of bar at gage (sq in.); and
A_n = cross-sectional area of normal bar (0.31 sq in.).

From preliminary measurements the average diameter of the necked-down area was equal to 0.549 in. (maximum departure from the average is 0.005 in.—less than 1 percent). Substituting in Eq. 20,

$$S_t = S_g \frac{(0.549/2)^2 \pi}{0.31} = \frac{0.237}{0.310} S_g = 0.765 S_g$$

Appendix C

STRESS-TIME PLOTS

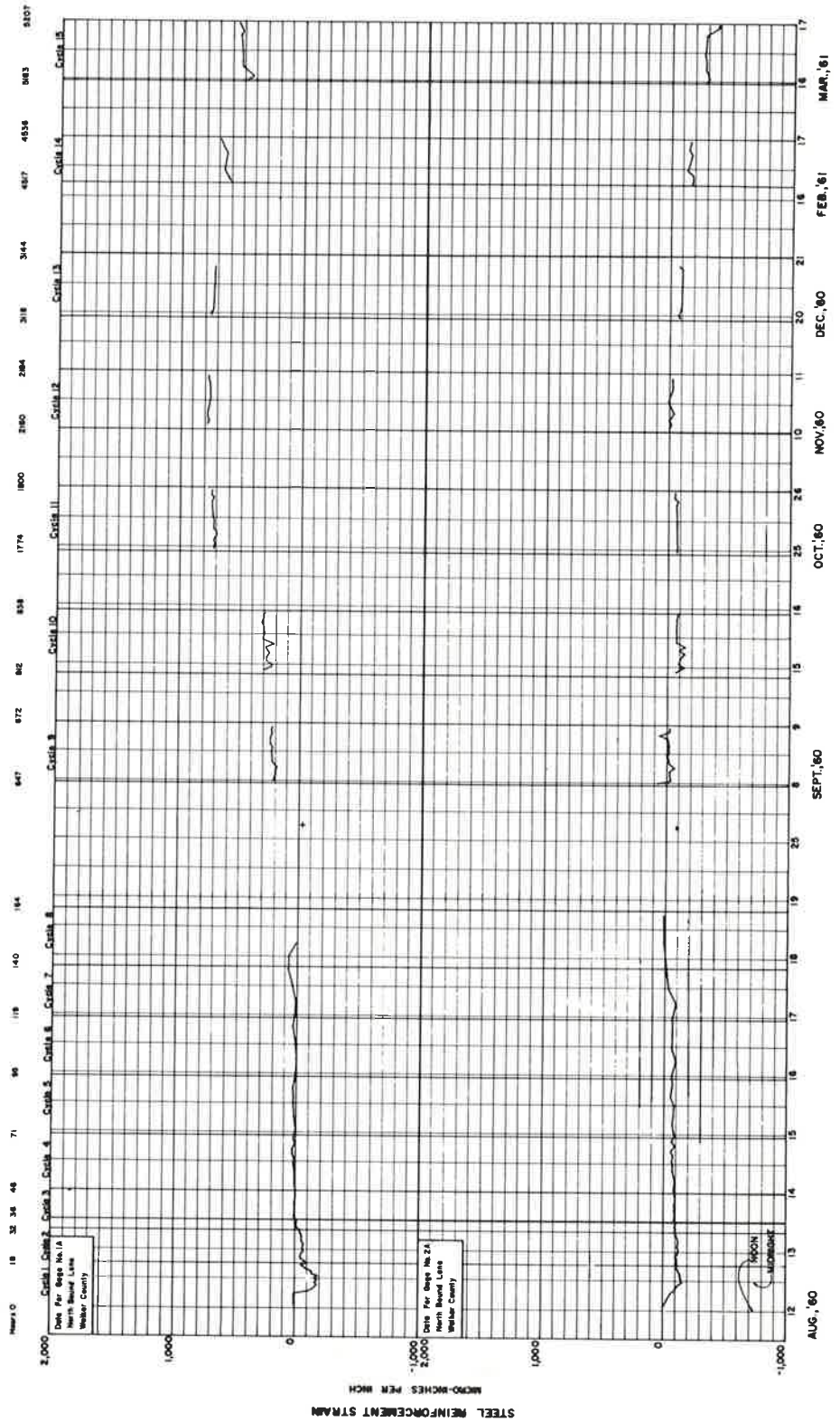

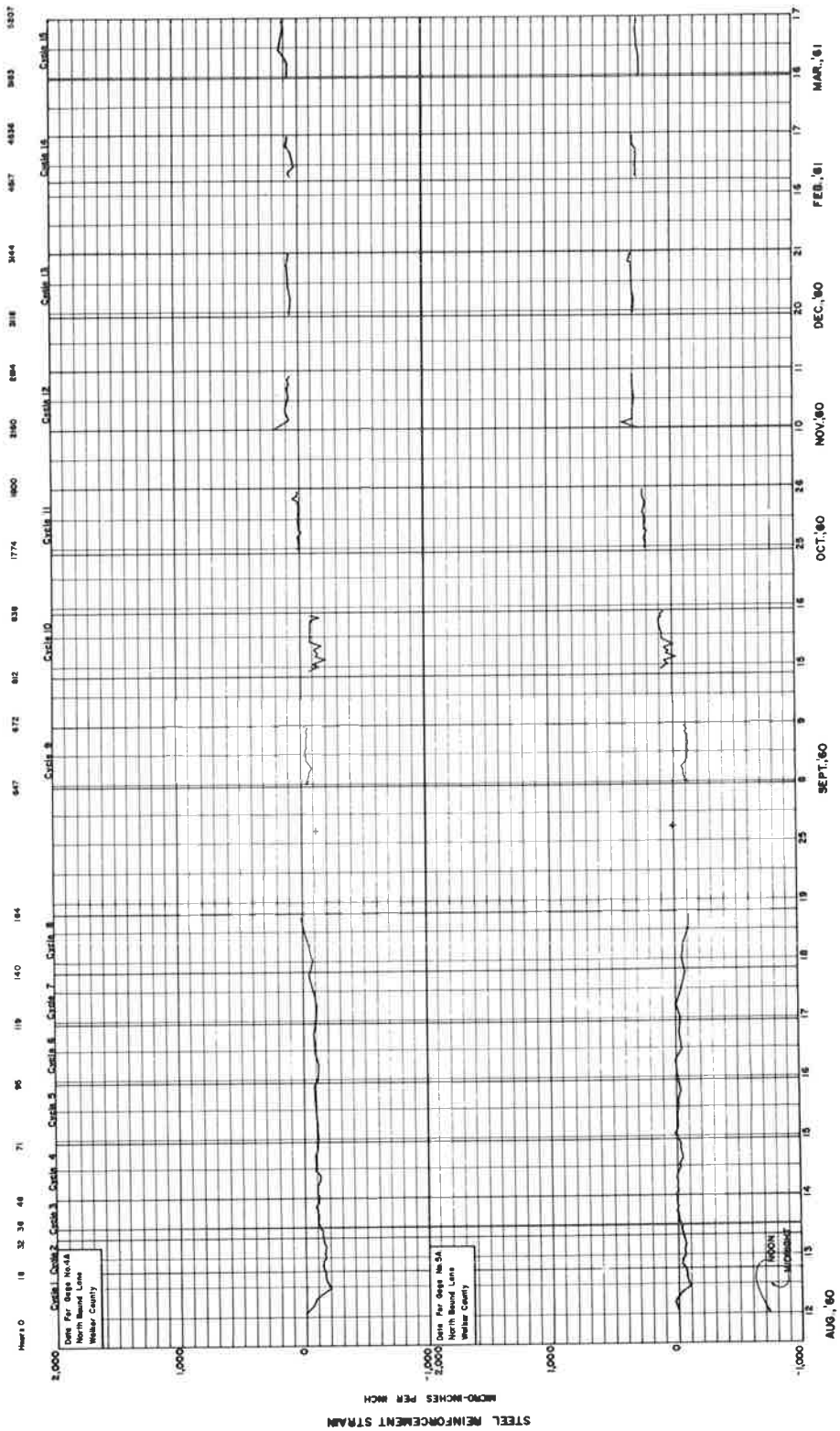
Data For Gage No.4A
North Bound Lane
Weber County
Data For Gage No.5A
North Bound Lane
Weber County
NOON
MONDAY
AUG.,'80
SEPT.,'80
OCT.,'80
NOV.,'80
DEC.,'80
FEB.,'81
MAR.,'81
STEEL REINFORCEMENT STRAIN
MICRO-INCHES PER INCH

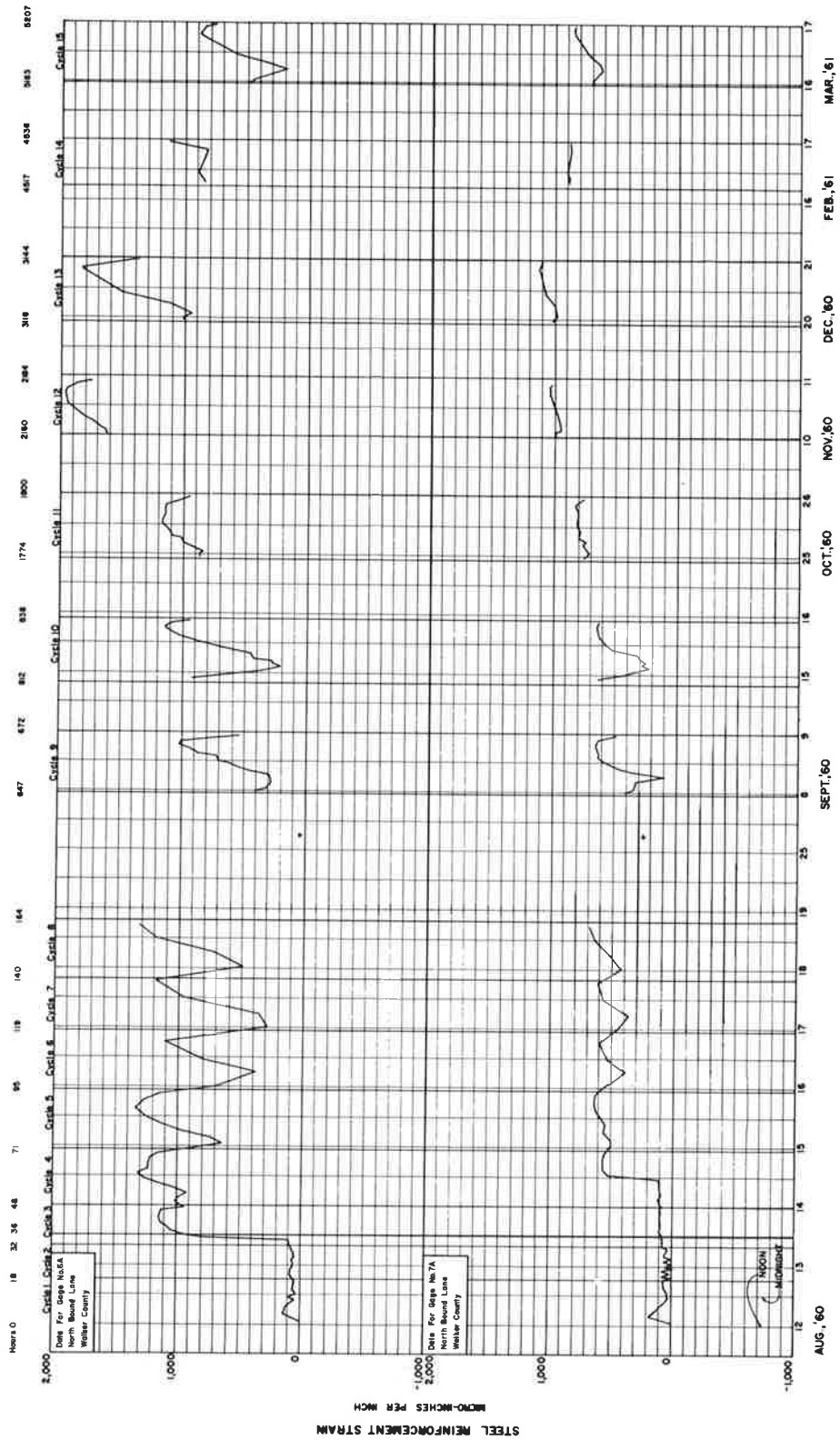
STEEL REINFORCEMENT STRAIN
MICRO-INCHES PER INCH
Data For Gage No.6A
North Bound Lane
Walker County
Data For Gage No.7A
North Bound Lane
Walker County
NOON
MIDNIGHT
AUG.,'60
SEPT.,'60
OCT.,'60
NOV.,'60
DEC.,'60
FEB.,'61
MAR.,'61


STEEL REINFORCEMENT STRAIN
MICRO-INCHES PER INCH
Data For Gage No.10A
North Bound Lane
Weber County
Data For Gage No.11A
North Bound Lane
Weber County
NOON
MIDNIGHT
AUG.,'60
SEPT.,'60
OCT.,'60
NOV.,'60
DEC.,'60
FEB.,'61
MAR.,'61

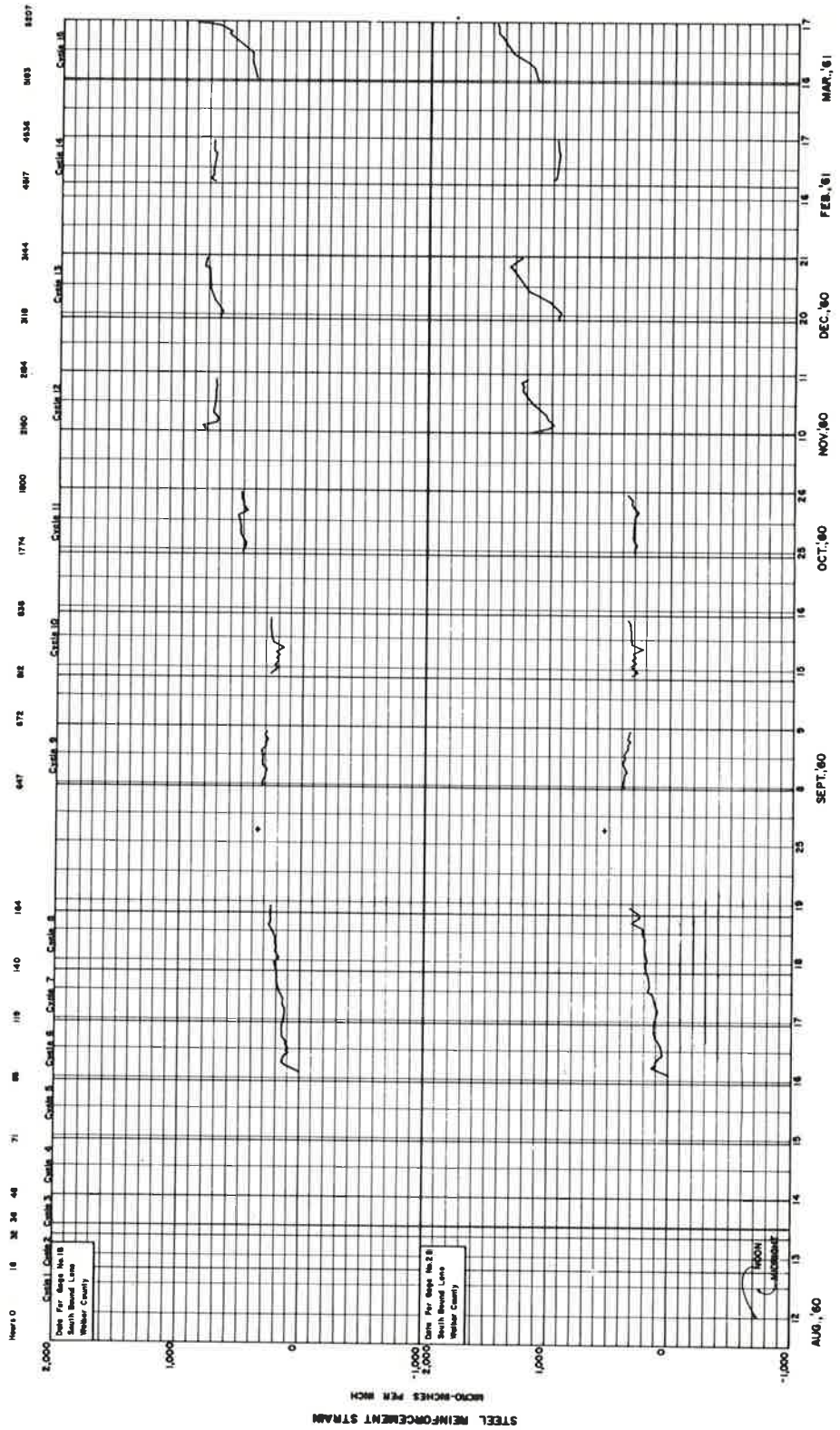
STEEL REINFORCEMENT STRAIN
MICRO-INCHES PER INCH
2,000
1,000
0
-1,000
2,000
1,000
0
-1,000
Data For Gage No.18
South Bound Lane
Weber County
Data For Gage No.28
South Bound Lane
Weber County
NOON
MIDNIGHT
AUG.,'60
SEPT.,'60
OCT.,'60
NOV.,'60
DEC.,'60
FEB.,'61
MAR.,'61

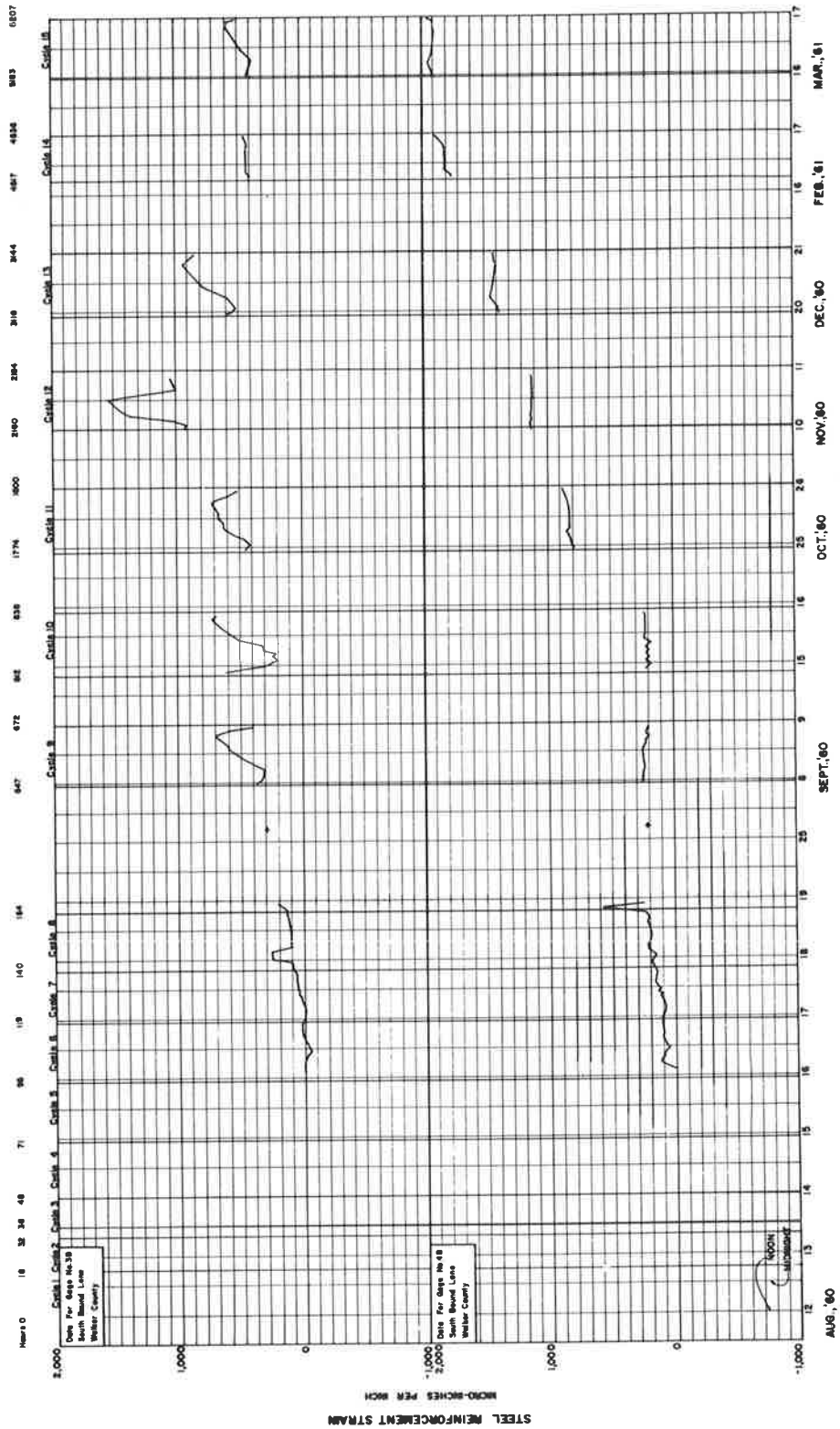
STEEL REINFORCEMENT STRAIN
MICRO-INCHES PER INCH
Data For Gage No.39
South Bound Lane
Walker County
Data For Gage No.40
South Bound Lane
Walker County
NOON
MIDNIGHT
AUG., '60
SEPT.,'60
OCT.,'60
NOV.,'60
DEC.,'60
FEB.,'61
MAR.,'61

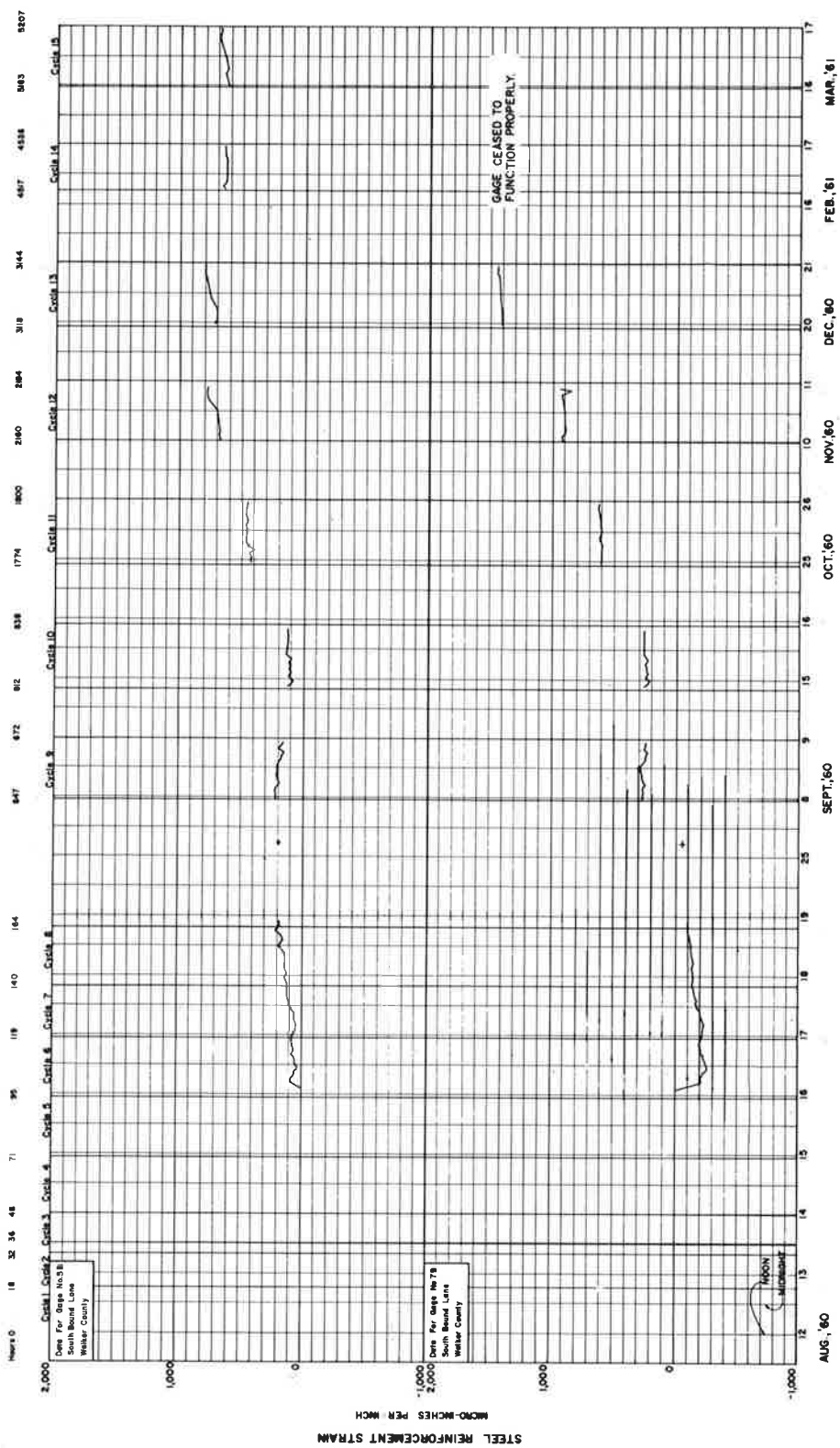
STEEL REINFORCEMENT STRAIN
MICRO-INCHES PER INCH
Data For Gage No.58
South Bound Lane
Welker County
Data For Gage No.78
South Bound Lane
Welker County
GAGE CEASED TO FUNCTION PROPERLY.
NOON
MIDNIGHT
AUG.,'60
SEPT.,'60
OCT.,'60
NOV.,'60
DEC.,'60
FEB.,'61
MAR.,'61

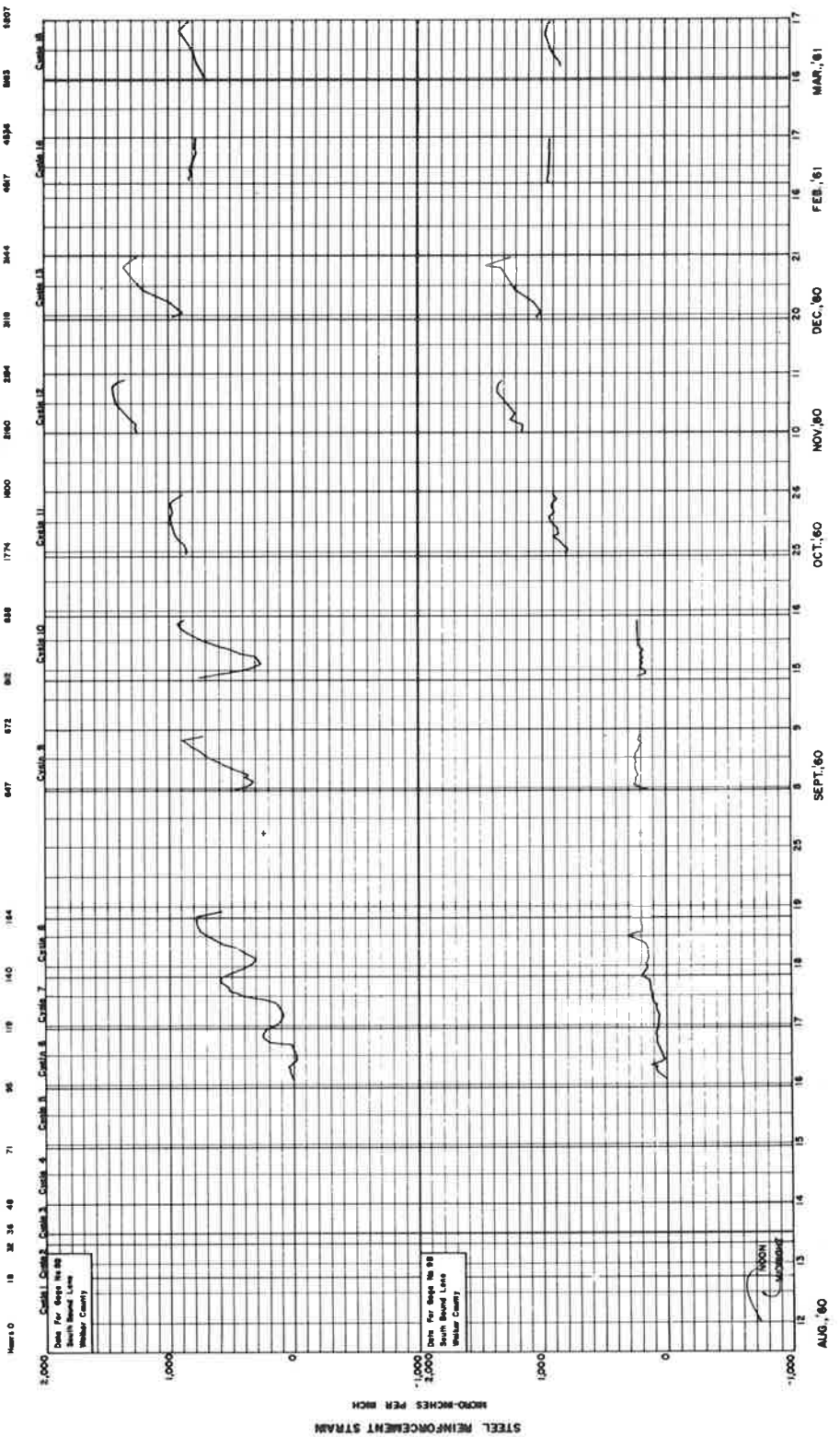
STEEL REINFORCEMENT STRAIN
MICRO-INCHES PER INCH
Data For Gage No. 88
South Bound Lane
Walker County
Data For Gage No. 89
South Bound Lane
Walker County
NOON
MONDAY
AUG., '80
SEPT.,'80
OCT.,'80
NOV.,'80
DEC.,'80
FEB.,'81
MAR.,'81

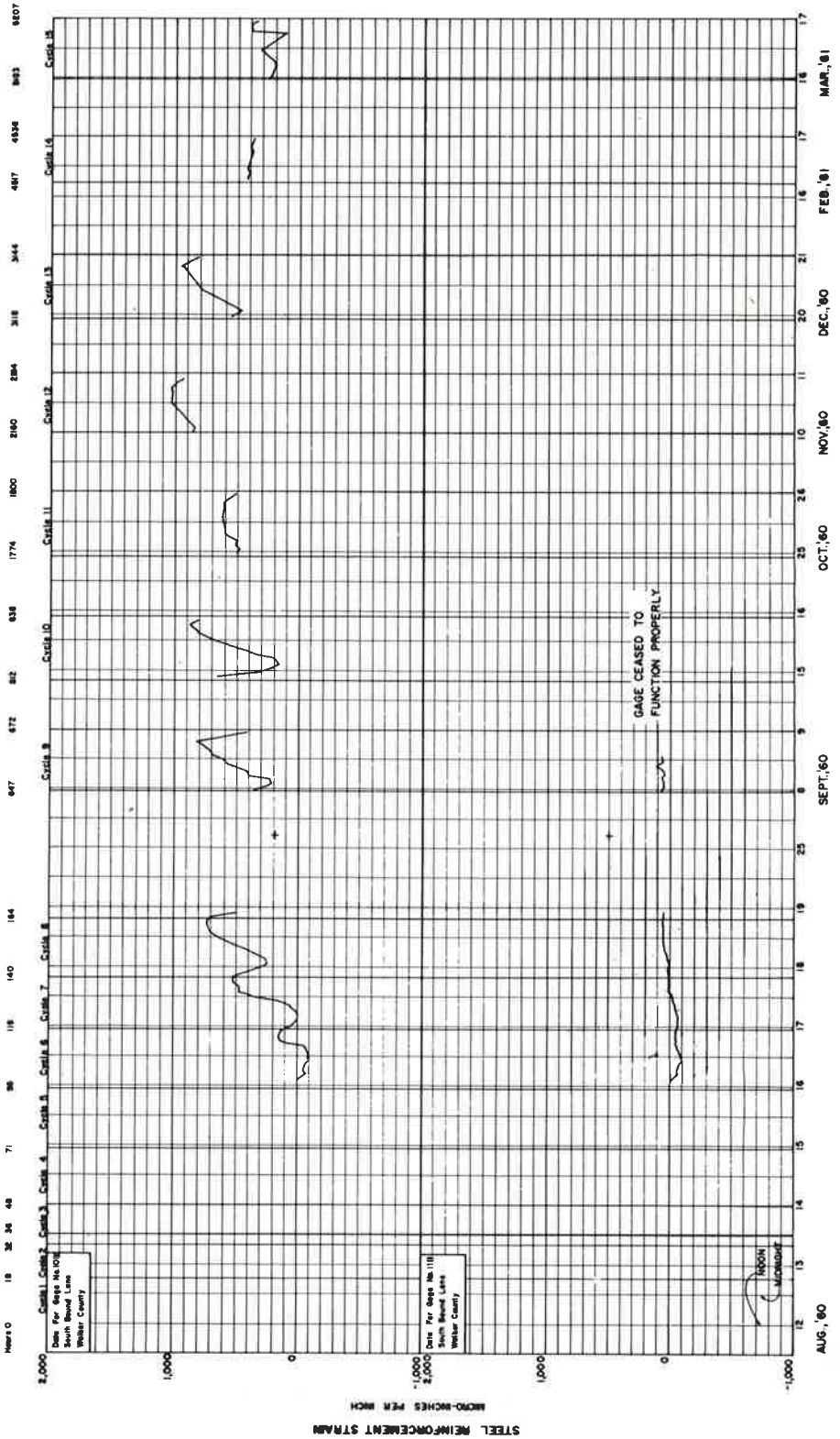
STEEL REINFORCEMENT STRAIN
MICRO-INCHES PER INCH
Data For Gage No.108
South Bound Lane
Walker County
Data For Gage No.110
South Bound Lane
Walker County
GAGE CEASED TO FUNCTION PROPERLY
NOON
MIDNIGHT
AUG.,'60
SEPT.,'60
OCT.,'60
NOV.,'60
DEC.,'60
FEB.,'61
MAR.,'61

End Anchors for Continuously-Reinforced Concrete Pavements

R.A. MITCHELL, Highway Research Engineer, Virginia Council of Highway Investigation and Research (Now with National Bureau of Standards, Washington, D.C.)

Unrestrained end sections of continuously-reinforced concrete pavements have been observed to move several inches longitudinally due to thermal, shrinkage, or swelling strains. During the last few years a number of continuous slabs have been provided with subgrade anchors of various configurations to prevent these large end movements. This paper reports an experimental and theoretical study to develop guidelines for selecting and designing a suitable end anchor system.

A full-scale experimental investigation of two different end anchor configurations—a cylindrical pile-shaped anchor and a rectangular solid-shaped anchor—was conducted. Four test anchor units were subjected to a horizontal thrust applied by a jacking frame at the pavement slab level. Two of the test units were rigidly attached to a 15-ft length of 10-in. thick slab to simulate the interacting anchor-pavement system. The other two test anchor units were without attached slab. Loads, deflections, and rotations were measured.

A theoretical analysis has been developed for the elastic and plastic range of end anchor response. The more complex theoretical solutions have been presented in the form of curves for use in design.

•A CONTINUOUSLY-REINFORCED concrete pavement slab may expand or contract due to changes in temperature, moisture, chemical reaction, or mechanical stress. The resulting movement of the slab relative to its subgrade creates frictional stresses that oppose the movement. These subgrade frictional stresses prevent the development of a part of the potential slab strain but not all of it.

The movements discussed here are longitudinal expansions or contractions at the ends of a long slab. Movements of as much as 4 in. have been observed at the ends of continuously-reinforced concrete slabs (10). Such large movements must be either restrained or accommodated by expansion joints. Expansion joints capable of accommodating such movements are rather elaborate and may require considerable maintenance expenditure.

Zuk proposed that subgrade anchors be used to prevent excessive end movement and since that time a number of end anchor systems have been built in several States. Figure 1 shows a longitudinal section of the type of system that has commonly been used. The depths of vertical anchor units have ranged from 1 to 8 ft, and the thicknesses from 1 to 2 ft. Rectangular units extending the full width of the pavement slab and vertical cyclindrical units have been used (2).

There have been instances of conventional jointed concrete pavement expanding and exerting damaging forces against bridge structures. Such forces have been known to push abutments and piers out of alignment, to shear anchor bolts, and to move superstructures. To prevent these excessive expansions some States have used subgrade anchors. Texas, for example, has installed a large number of end anchor systems

Paper sponsored by Committee on Rigid Pavement Design.

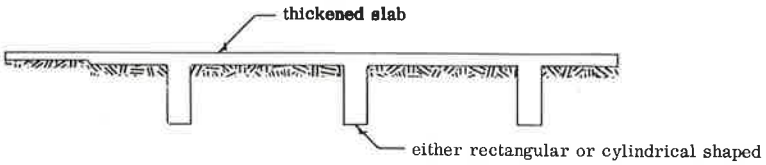

Figure 1. Longitudinal section of anchor system.

with jointed pavement as well as with continuously-reinforced pavement (4).

The study reported here was primarily concerned with subgrade anchor systems for use with continuously-reinforced concrete pavement, and the theoretical analyses and experimental investigation are discussed from that viewpoint. In a later section of the paper, subgrade anchors are discussed in relation to their possible use in jointed pavements.

The objective of the study was to develop a rational analysis of end anchor units and of systems of anchor units in series. A theoretical and an experimental investigation were conducted. In the theoretical phase the elements of the problem that are of most direct interest to the designer were considered. The experimental phase, which was considerably more limited in scope than the theoretical phase, included a full-scale field loading test of two different configurations of anchor unit.

LONGITUDINAL MOVEMENT OF PAVEMENT SLAB

Figure 2 shows some of the measurements of longitudinal movement along an experimental continuously-reinforced concrete pavement reported by Van Breemen (9). The horizontal scale represents the slab length of 5,130 ft. The vertical scale indicates the longitudinal movement of various points. Movement to the right is plotted above the abscissa. Thus, contraction of the left end is plotted above; and contraction of the right end is plotted below. The maximum movement is at each end, and the movement decreases at a decreasing rate to practically zero a few hundred feet from the end, as would be expected.

An explanation for the predominant nature of the curves in Figure 2 can be developed by examination of an idealized mechanical model. In Figure 3a the model represents one-half the length of a long slab having the following properties:

1. Uniform thickness, density, and linear elastic properties;
2. Uniform volume change due to temperature, moisture, etc., if not restrained by forces external to slab; and
3. Uniform friction coefficient relative to subgrade on which it is supported.

If there is no volume change due to temperature, moisture, etc., the only forces acting on the slab are its weight and the vertical subgrade reaction to that weight. If, however, there is longitudinal expansion or contraction of the slab, there is a uniform frictional stress throughout the region of longitudinal movements. The frictional stress acts on the slab in the direction opposite to the direction of movement.

Because the slab is assumed uniformly linear elastic, the components of horizontal strain due to different causes can be considered separately. Consider the case of the slab contracting due to temperature decrease T. The horizontal strain at any point due to temperature change is

$$\epsilon_t = -\alpha T \tag{1}$$

in which α = coefficient of thermal expansion.

If the orgin of the x-axis is at the free end of the slab, the strain due to uniform subgrade is

$$\epsilon_f = \frac{\mu w x}{AE} \tag{2}$$

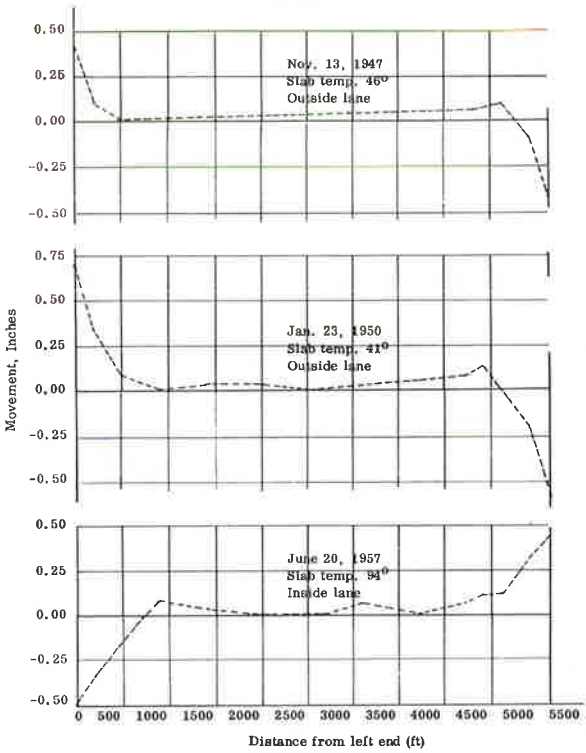

Figure 2. Movement of continuously-reinforced concrete pavement in New Jersey (9).

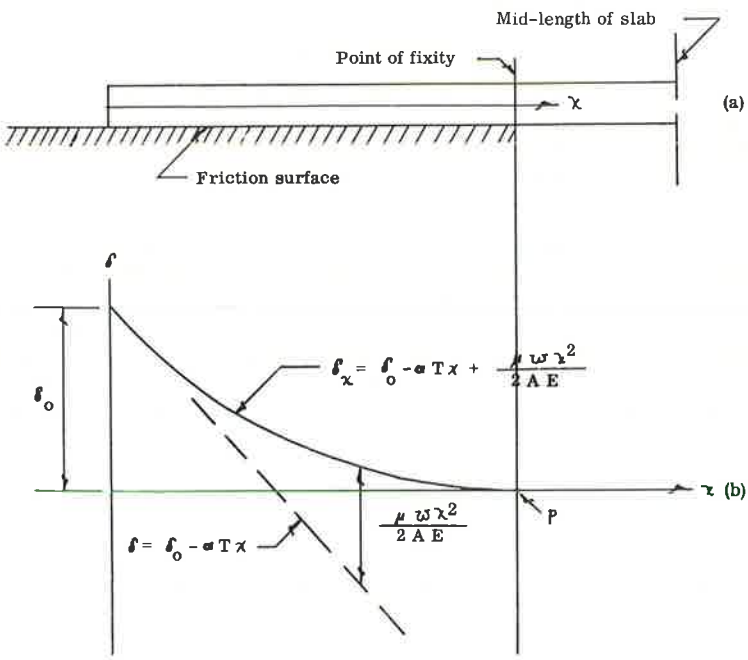

Figure 3. Idealized model of continuously-reinforced slab.

in which

μ = constant coefficient of friction;
w = slab weight per unit area;
A = slab cross-sectional area per unit width; and
E = elastic modulus.

The horizontal movement of a point on the slab relative to the end of the slab is therefore

$$\delta_{tf} = \delta_t + \delta_f = -\int_0^x \alpha T \, dx + \int_0^x \frac{\mu w x}{AE} \, dx$$

$$= -\alpha Tx + \frac{\mu w x^2}{2AE} \tag{3}$$

The total movement including the movement of the slab end δ_o is thus

$$\delta_x = \delta_o - \alpha Tx + \frac{\mu w x^2}{2AE} \tag{4}$$

This function is plotted in Figure 3b. At point x = p the curve is horizontal. Beyond that point there is no movement of the slab and no net strain. The strain due to temperature change is numerically equal (but of opposite sign) to that due to friction stress. In Figure 3b the three terms of Eq. 4 are separately indicated. The δ_x curve is tangent to the δ_t curve at x = 0, and is tangent to the x-axis at x = p. The conditions of zero strain and movement at x = p yield the two equations:

$$-\alpha T + \frac{\mu w}{AE} p = 0 \tag{5}$$

and

$$\delta_o - \alpha T p + \frac{\mu w}{2AE} p^2 = 0 \tag{6}$$

These simultaneous equations yield the solutions

$$p = \frac{AE}{\mu w} \alpha T \tag{7}$$

and

$$\delta_o = \frac{AE}{2 \mu w} (\alpha T)^2 \tag{8}$$

The amount of horizontal movement of the end of the slab could be further reduced by the addition of a horizontal force P at the slab end. The horizontal strain due to P would be P/AE and the movement of any point would be Px/AE.

This additional restraint would modify Eqs. 5 and 6 to

$$-\alpha T + \frac{P}{AE} + \frac{\mu w}{AE} p = 0 \tag{9}$$

$$\delta_o - \alpha T p + \frac{P}{AE} p + \frac{\mu w}{2AE} p^2 = 0 \tag{10}$$

The distance to the point of no movement would be

$$p = \frac{AE}{\mu w} \left(\alpha T - \frac{P}{AE} \right) \tag{11}$$

and the end movement would be

$$\delta_o = \frac{AE}{2\mu w}\left(\alpha T - \frac{P}{AE}\right)^2 \tag{12}$$

If the force P is applied at some distance h<p from the slab end the corresponding end movement would be

$$\delta_o = \frac{AE}{2\mu w}\left(\alpha T - \frac{P}{AE}\right)^2 + \frac{Ph}{AE} \tag{13}$$

If several horizontal forces were applied at various distances h_n < p from the slab end the resulting free end movement would be

$$\delta_o = \frac{AE}{2\mu w}\left(\epsilon - \sum_{n=1}^{K}\frac{Pn}{AE}\right)^2 + \sum_{n=1}^{K}\frac{Pn\,hn}{AE} \tag{14}$$

in which

ϵ = sum of strains due to temperature, moisture, etc. (i.e., αT in previous discussion);
P_n = various horizontal forces (P_1, P_2, ..., P_K); and
h_n = distances to corresponding horizontal forces (h_1, h_2, ..., h_K).

This equation for an idealized slab model is now examined in relation to the real problem of preventing excessive movement of a continuous pavement slab.

Experimental data (5) indicate that subgrade friction increases at a decreasing rate with an increasing movement of the slab (Fig. 4). Thus, Eq. 14, which was developed for a constant friction coefficient μ, would give only a rough approximation of actual end movement. In a later section of this paper an analysis is presented that takes into account this friction variation.

The last term of Eq. 14 indicates that the smaller the distance h to the point of application of a force P the more effective the force. This would be true whatever the nature of the force mechanism. If the force P is developed by passive resistance of a subgrade anchor, such an anchor would in general develop a greater force if located nearer the slab end where movement is greater. Of course, there is a limiting minimum spacing between anchor units beyond which the individual units interfere with adjacent ones. But, an anchor system is most efficient when the units are bunched at that minimum limiting spacing near the slab end. The determination of the minimum spacing is discussed later.

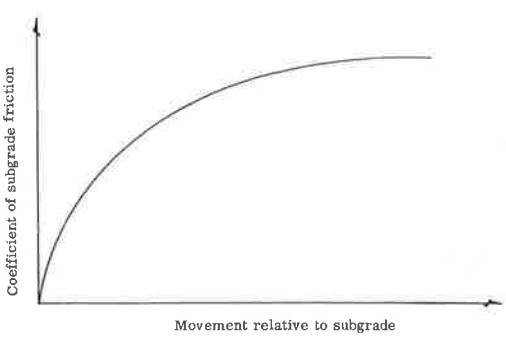

Figure 4. General nature of subgrade friction-movement relationship.

THEORY OF SUBGRADE ANCHOR RESISTANCE

The resistance of the slab to rotation of the slab anchor joint is considered first. Then the elastic and later the plastic resistance of the vertical anchor to horizontal deflection are examined. Plastic behavior is discussed particularly as it relates to minimum anchor spacing. Finally, the requirements for the bending and shear strengths of the reinforced concrete elements are considered.

The entire analysis is made for a longitudinal cross-section element of 1-in. width. A condition of plane strain is assumed to exist.

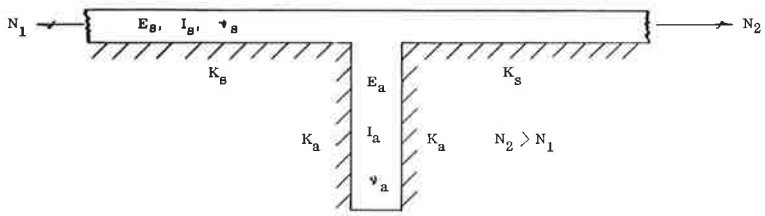

Figure 5. Assumed elastic system.

Elastic Analysis

Figure 5 shows the assumed elastic system. The symbols ν, E, I and K represent Poisson's ratio, the elastic modulus of the concrete, the moment of inertia of the concrete member, and the modulus of reaction of the subgrade soil, respectively. The subscripts s and a identify the properties of the slab and anchor, respectively. The soil modulus K is assumed to be defined by

$$p = b K_o y = Ky \tag{15}$$

in which

- p = normal pressure at soil-concrete interface due to deflection;
- y = transverse deflection of slab or anchor;
- b = width of the deflected concrete elements (1 in. for this analysis);
- K_o = soil modulus, constant ratio of pressure to deflection for any width of elements; and
- K = abbreviation for bK_o in this analysis (lb per cu in.).

It is assumed that the weight and stiffness of the system are sufficient to prevent significant vertical movement of the joint. Because $N_2 > N_1$ the slab is displaced to the right. As the top of the anchor is deflected horizontally, rotation of the anchor is partially restrained by the slab and a bending is induced at the joint. Hetenyi (3) gives a solution for the deflection of an infinitely long beam with axial load N and transverse moment M_o (Fig. 6) as

$$y = \frac{M_o}{4EI} \frac{e^{-\alpha x}}{\alpha\beta} \sin \beta x \tag{16}$$

in which

$$\alpha = \sqrt{\sqrt{\frac{K}{4EI}} + \frac{N}{4EI}}$$

$$\beta = \sqrt{\sqrt{\frac{K}{4EI}} - \frac{N}{4EI}}$$

The corresponding rotation at $x = 0$ is

$$\theta_o = \frac{M_o}{4EI\alpha} \tag{17}$$

The ratio of applied moment to rotation is

$$C = \frac{M_o}{\theta_o} = 4EI\alpha$$

$$= 4EI\sqrt{\sqrt{\frac{K}{4EI}} + \frac{N}{4EI}} \tag{18}$$

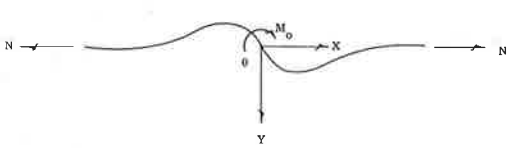

Figure 6. Infinite beam on elastic foundation with transverse applied moment.

To apply this solution to the present problem of plane strain, the effective stiffness of the slab must be modified to give

$$C = \frac{M_o}{\theta_o} = \frac{4 E_S I_S}{(1-\nu^2)} \sqrt{\sqrt{\frac{K_S (1-\nu^2)}{4 E_S I_S}} + \frac{N (1-\nu^2)}{4 E_S I_S}} \qquad (19)$$

In an effort to simplify this relationship for the present problem, the importance of N in relation to C was studied. It was found that for a wide range of N (from a tension of 60,000 psi in 0.6 percent steel to a compression of 5,000 psi in concrete) and for a wide range of other properties (that is, $\nu = 0.15$; $EI = 15 \times 10^7$ to 45×10^7 lb-in.^{2}; K = 100 to 1,000 psi) the maximum variation in C is about 10 percent. This was considered sufficient justification for dropping N in Eq. 19 to obtain

$$C = \frac{M_o}{\theta_o} = \sqrt[4]{\left[\frac{E_S t_S^3}{3 (1-\nu^2)}\right]^3} \cdot K_S \qquad (20)$$

in which t_S = slab thickness.

Figure 7 is a plot of C vs t_S for $E_S = 4 \times 10^6$ psi and $\nu = 0.15$.

There is also a question of C being reduced due to interference from an adjacent anchor unit. The slope at any point along the infinitely long beam shown in Figure 6 is (3, p. 129).

$$\theta_x = \frac{M_o}{4 EI} \frac{1}{\alpha \beta} e^{-\alpha x} (\beta \cos \beta x - \alpha \sin \beta x) \qquad (21)$$

The point at which $\theta_x = 0$, x_c, may be found by setting the right side of Eq. 21 equal to zero. This gives

$$x_c = \frac{1}{\beta} \arctan \frac{\beta}{\alpha} \qquad (22)$$

The change in N throughout the vicinity of x = 0 is assumed to be sufficiently small to permit superposition of elastic solutions. Thus, the rotation curves due to two adjacent transverse moments can be added directly to get the rotation due to the pair. By doing this, it can be readily demonstrated that, if two adjacent anchors are no closer than x_c, the rotation of one does not increase the rotation of the other and thus decrease the C-value of the other. To determine a reasonable maximum value that x_c might attain, Eq. 22 was used to determine x_c to be 52 in. for the rather extreme values: $N = 3 \times 10^3$ lb; $E_S I_S = 45 \times 10^7$ lb-in.^{2}; K = 100 psi; $\nu = 0.3$. The likelihood of anchors being placed closer than 52 in. seems rather remote.

Two solutions reported by Hetenyi (3) have been combined to give a solution for the anchor element (Fig. 8c). The equations for deflection and rotation at the point x = 0 of the anchor element loaded with the horizontal force P (Fig. 8a) are

$$y_a = \frac{2 P \beta}{K} \left(\frac{\sinh \beta H \cosh \beta H - \sin \beta H \cos \beta H}{\sinh^2 \beta H - \sin^2 \beta H}\right) = \frac{2 P \beta}{K} g_1 \qquad (23)$$

and

$$\theta_a = -\frac{2 P \beta^2}{K} \left(\frac{\sinh^2 \beta H + \sin^2 \beta H}{\sinh^2 \beta H - \sin^2 \beta H}\right) = \frac{2 P \beta^2}{K} g_2 \qquad (24)$$

in which

$$\beta = \sqrt[4]{\frac{K (1-\nu^2)}{4 EI}}$$

H = anchor depth.

The corresponding equations for the anchor element loaded with the moment Mo (Fig. 8b) are

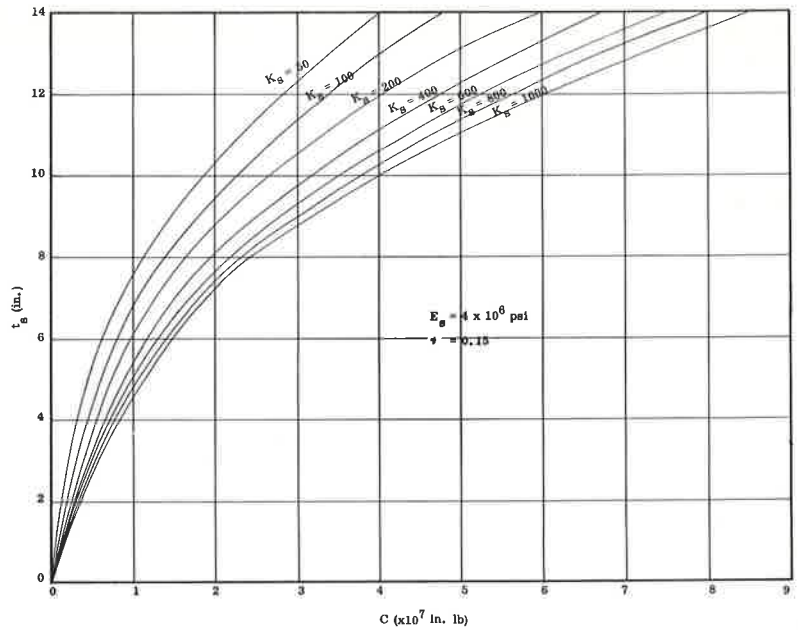

Figure 7. Moment-rotation ratio vs slab thickness.

$$y_b = -\frac{2 M_o \beta^2}{K}\left(\frac{\sinh^2 \beta H + \sin^2 \beta H}{\sinh^2 \beta H - \sin^2 \beta H}\right) = -\frac{2 M_o \beta^2}{K} g_2 \qquad (25)$$

and

$$\theta_b = \frac{4 M_o \beta^3}{K}\left(\frac{\sinh \beta H \cosh \beta H + \sin \beta H \cos \beta H}{\sinh^2 \beta H - \sin^2 \beta H}\right) = \frac{4 M_o \beta^3}{K} g_3 \qquad (26)$$

Eqs. 23 through 26 can be combined to give the deflection and rotation at x = 0 for the combined loading condition (Fig. 8c).

$$y_c = \frac{2 P \beta}{K} g_1 - \frac{2 M_o \beta^2}{K} g_2 \qquad (27)$$

$$\theta_c = \frac{4 M_o \beta^3}{K} g_3 - \frac{2 P \beta^2}{K} g_2 \qquad (28)$$

The moment and rotation at the top of the anchor are numerically equal to the moment and rotation of the slab at the joint. But the moment acting on the anchor is in the direction opposite joint rotation, whereas the moment acting on the slab is in the direction of rotation. Thus, from Eq. 20,

$$\theta_c = \frac{4 M_o \beta^3}{K} g_3 - \frac{2 P \beta^2}{K} g_2 \frac{M_o}{C}$$

or

$$M_o \left[\frac{4 \beta^3}{K} g_3 + \frac{1}{C}\right] - \frac{2 P \beta^2}{K} g_2 = 0 \qquad (29)$$

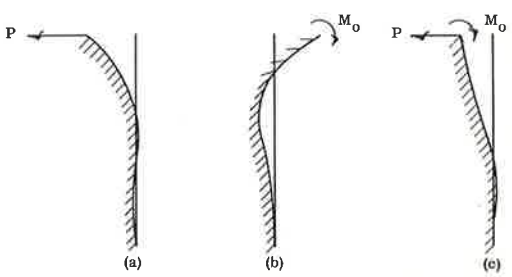

Figure 8. Elastic model of vertical anchor.

Eq. 27 can be subtracted from Eq. 29 to eliminate M_o, thus giving y_c in terms of P, β, H, K, and C as

$$y_c = \frac{2P\beta}{K_a} \left[g_1 - \frac{2\beta^3 g_2^2}{(4\beta^3 g_3 + \frac{K}{C})} \right] \tag{30}$$

This equation can be rearranged and divided by H to get

$$\frac{P}{K_a y H} = \frac{1}{2\beta_a H \left[g_1 - \frac{2\beta_a^3 g_2^2}{(4\beta_a^3 g_3 + \frac{K_a}{C})} \right]} \tag{31}$$

The subscripts a that were neglected for the derivation of Eq. 31 are inserted in the equation to avoid confusion. The functions g_1, g_2, and g_3 are functions of β_a H only. The factor y in Eq. 31 is equal to the horizontal movement of the slab at the joint, δ, and the force P is equal to the anchor force. Plots of $P/K_a H \delta$ vs H for different values of β_a and K_a/C are given in Figures 9 a-d.

An infinitely stiff anchor of any length, rigidly fixed at the pavement joint, would have the properties,

$$\beta = 0, \quad C = \infty, \quad \text{and} \quad \frac{P}{K_a H \delta} = 1$$

The curves in Figure 9 show how this quantity is decreased by a decrease in C or an increase in β_a or H. For design analysis the curves can be used to determine the anchor force P for an elastic system after the quantities δ, H, K_a, β_a, and C have been determined. A plot of β_a vs anchor thickness t_a for $E_a = 4 \times 10^6$ and $\nu = 0.15$ is given in Figure 10.

Plastic Analysis

The discussion of slab longitudinal movement showed that anchor units should be closely bunched near the slab free end. One objective of the following analysis is to determine the limiting minimum spacing beyond which closer spacing would result in no greater efficiency of the anchor system. The other objective is to determine the limiting plastic yield strength of anchor units placed at that theoretical optimum spacing. For this problem it is assumed that the anchor units are far enough apart that elastic displacement within the soil mass at one unit, due to forces exerted by other units, is insignificant.

The two adjacent anchor units shown in Figure 11a may be used as an example. If there is no horizontal movement of the anchor units, the planes ab, cd, and ef are acted on by the "at rest" earth pressure, and the shear stress along plane bd is zero. As the anchors are moved to the left the net force on plane ab is decreased, the net force on cd is increased, and shear stress is induced along at least parts of planes bd and ac. It is assumed that if movement is continued there will eventually be plastic shear flow, characterized by no increase in shear stress, along one or more of the three planes bg, bd, and dh. The precise locations and curved shapes of planes bg and dh are not specified. The assumed flow directions are shown in Figure 11a by arrows.

Figure 11b shows the net horizontal forces acting on the soil body abdc. Equilibrium conditions require that

$$S - F_t = P_p - P_a \tag{32}$$

This equation necessarily holds throughout the elastic and plastic range of response. For the limiting plastic values of P_a and P_p, designated P_a' and P_p', to develop, it is necessary that the value of $S - F_t$ be sufficiently large to hold the body abdc in equilibrium. That is, if the anchors are too close together, shear flow will develop along plane bd before it does along planes bg and dh.

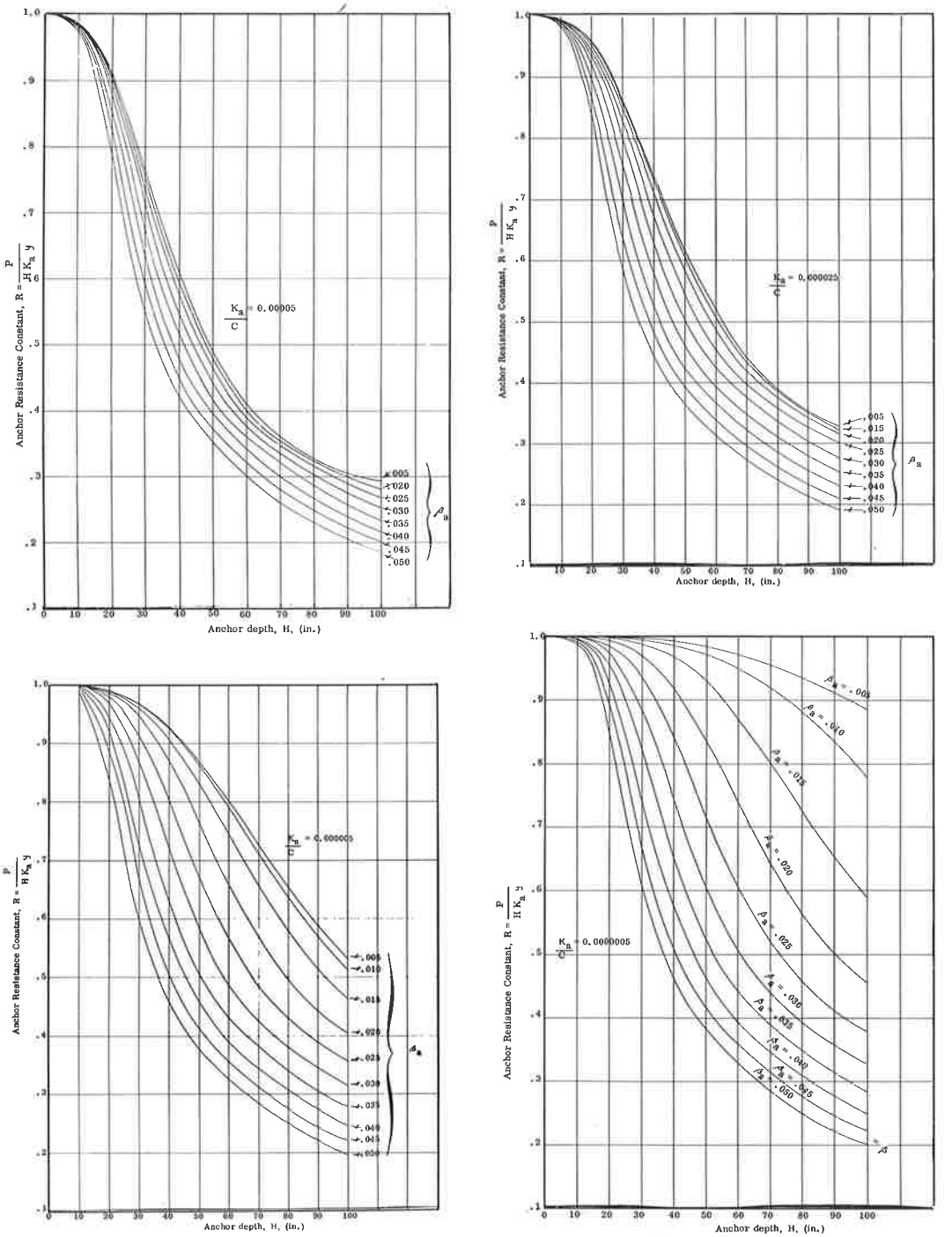

Figure 9. Resistance constant vs anchor depth.

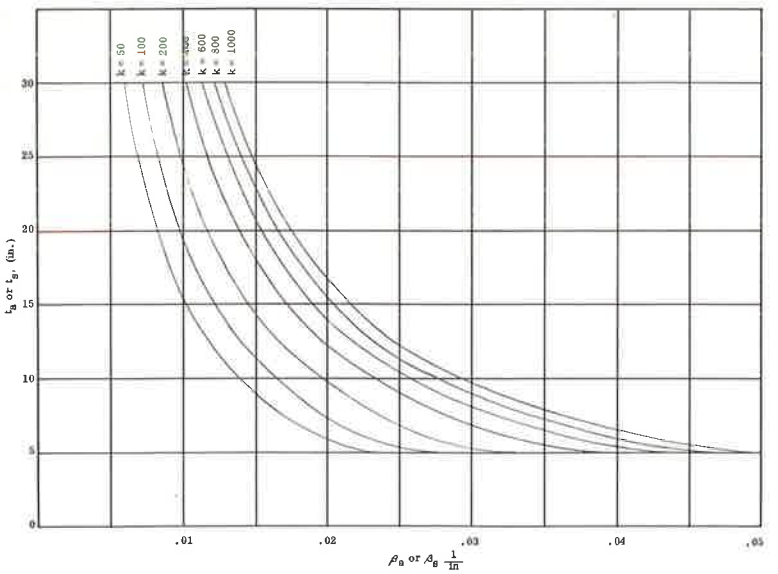

Figure 10. Characteristic β vs element thickness (slab or anchor).

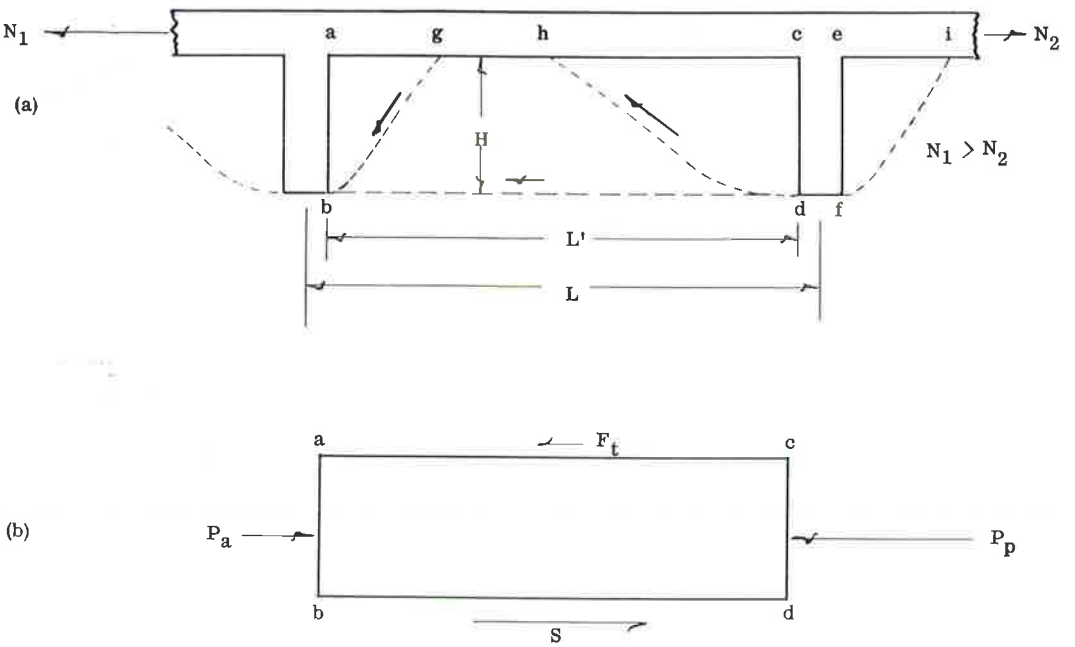

Figure 11. Plastic model of adjacent anchors.

If the subgrade soil properties are uniform and if there is plastic flow along planes bg, dh, and fi, equal forces P_a' are acting on planes ab and ef, and the net horizontal force on anchor cdfe is $P_p' - P_a'$. That is the limiting maximum force that can be developed by an anchor. If the anchor units are so far apart that plastic shear flow does

not develop along plane bd when the limiting anchor force $P_p' - P_a'$ is developed, the anchor system does not develop the full potential strength of the subgrade soil. This argument leads to the conclusion that, if movement is sufficient to develop plastic flow along either of planes bg, bd, dh, or fi, the optimum anchor spacing is that spacing at which shear flow will develop on all four planes. At that spacing the following equation will apply:

$$S' - F_t = P_p' - P_a' \tag{33}$$

in which S' = limiting plastic shear force along bd.

The force F_t acting along plane ac is assumed to be equal to the product of the slab weight and some uniform soil property constant G. The limiting shear force S' acting along plane bd is assumed to consist of a component equal to the product of the soil constant G and the weight of material above plane bd and a component that is independent of the weight of the material above bd. Thus S' may be thought of as consisting of a component F_t and a component that is independent of the slab weight, say P_h'; that is,

$$S' = P_h' + F_t \tag{34}$$

Substitution of Eq. 34 into Eq. 33 gives

$$P_h' = P_p' - P_a' \tag{35}$$

in which P_h' = component of limiting shear stress along plane bd that is independent of slab weight.

It is fully realized that the movement of a real two anchor system such as shown in Figure 11 would very likely not be characterized by shear flow initially developing along planes bg, bd, dh, and fi at the same time. Also, the rates of increase of the forces P_h, P_p, and P_a from zero to their limiting values P_h', P_p' and P_a' would in general not remain in constant ratio. Therefore, the theoretical optimum spacing of anchor units for movements large enough to induce plastic flow would not necessarily be the optimum spacing for lesser movements. And the movements of all or at least some of the units of a pavement anchor system would likely remain less than that required for plastic flow. But if the ratios of the rates of increase of P_h, P_p, and P_a are not too variable throughout their entire range, then the optimum anchor spacing throughout the range would not be too different.

The reasoning leading to Eq. 35 would seem to be valid regardless of the precise nature of the boundary conditions along the surface bacd. But to simplify the problem for a numerical parameter analysis, the following rather extreme assumptions are made.

It is assumed that the conditions at the boundary of the soil body, abdc (Fig. 12) due

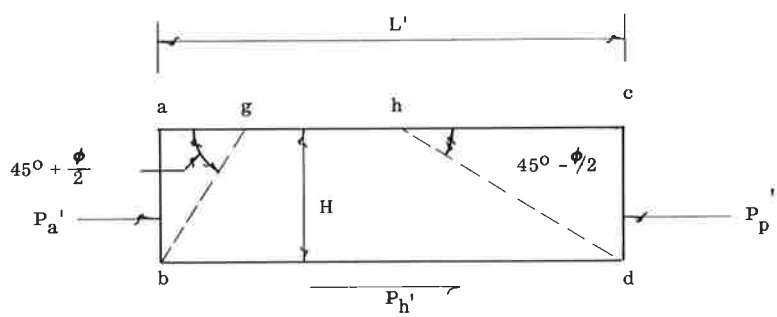

Figure 12. Soil in assumed Rankine state of plastic equilibrium between anchors.

to the weight and stiffness of the pavement slab and anchor units, are compatible with the Rankine theory of earth pressure (6, pp. 26-48). This assumption includes the conditions that there be no shear stress along planes ab and cd and that there be no stress along plane ac.

In Rankine's theory it is assumed that the limiting shear stress on surfaces of plastic shear flow is given by Coulomb's empirical equation

$$\gamma = c + \bar{\sigma} \tan \phi \tag{36}$$

in which

c = shearing resistance that is independent of effective normal stress;
$\bar{\sigma}$ = effective normal stress transferred by intergranular contact along shear plane; and
ϕ = angle of internal friction.

The theory assumes that c and ϕ are material properties that are constant for any direction of shear, for any magnitude of effective normal stress $\bar{\sigma}$, and at any point in the shear zone. This assumption is only approximately correct even if c and ϕ are selected on the basis of careful test (1, 6). But if c and ϕ are determined by tests closely approximating the stress, stress history, and moisture conditions of the anchor system subgrade, the results should be sufficiently accurate for engineering design purposes.

Figure 12 shows the soil body abdc in the assumed Rankine state of plastic equilibrium and for which Eq. 35 will be assumed to apply. There is shear flow along planes bg, dh, and bd. According to the Rankine theory (6, pp. 26-48) the inclined planes are at angles of $45^0 \pm \phi/2$ and the active and passive earth forces are

$$P_a' = \frac{\gamma_S H^2}{2 \tan^2 (45^0 + \phi/2)} - \frac{2 c H}{\tan (45^0 + \phi/2)} \tag{37}$$

$$P_p' = \frac{\gamma_S H^2}{2} \tan^2 (45^0 + \phi/2) + 2 c H \tan (45^0 + \phi/2) \tag{38}$$

Eq. 37 as written assumes that the soil can exert a normal tensile stress along the upper part of plane ab down to a depth equal $2 c/\gamma_S \tan (45^0 \text{ M } \phi/2)$. Because soil in general does not develop significant direct tensile strength it is commonly assumed that any direct tensile stress included in Eq. 37 is zero. This is accomplished by the addition of the term $2 c^2/\gamma$ to Eq. 37 (8 p. 149) to get

$$P_a' = \frac{\gamma_S H^2}{2 \tan^2 (45^0 + \phi/2)} - \frac{2 c H}{\tan (45^0 + \phi/2)} + \frac{2 c^2}{\gamma} \tag{39}$$

If the depth H is less than the quantity $2 c/\gamma_S \tan (45^0 + \phi/2)$ it is commonly assumed that the active force $P_a' = 0$.

When plane bd (Fig. 12) is in a state of plastic flow it is assumed that the shear stress is given by Eq. 36. The total shear force on plane bd is thus

$$P_S' = L' (c + \bar{\sigma} \tan \phi) \tag{40}$$

For this application it can be safely assumed that strain rate is slow enough that water pressure in the zone of shear yielding is unaffected by the shear strain. The effective normal stress $\bar{\sigma}$ is given by

$$\bar{\sigma} = \sigma - h_w \gamma_w \tag{41}$$

in which

σ = total normal stress on plane bd;

γ_w = unit weight of water; and
h_w = height of soil saturation above plane bd.

If the soil is uniformly saturated up to the subgrade surface the effective normal stress on plane bd is

$$\bar{\sigma} = H\ \gamma - H\ \gamma_w = H\ (\gamma - \gamma_w) \tag{42}$$

in which γ = unit weight of saturated soil. If the soil is unsaturated throughout the depth H the effective normal stress on bd is $\bar{\sigma} = H\ \gamma$. If $\bar{\gamma}$ designates the effective unit weight of the soil, that is $(\gamma - \gamma_w)$ for saturated soil and γ for unsaturated soil, the effective normal stress on plane bd for uniform soil conditions throughout the depth H is

$$\bar{\sigma} = \bar{\gamma}\ H \tag{43}$$

The corresponding shear force developed along bd is

$$P_s' = L'\ c + L'\ \bar{\gamma}\ H \tan \phi \tag{44}$$

By substituting Eqs. 38, 39, and 44 into Eq. 35 the optimum clear spacing between anchors L' can be determined to be

$$L' = \left\{ \frac{\frac{\bar{\gamma}\ H}{2\ c}\left[\tan^2\left(45^0 + \frac{\phi}{2}\right) - \tan^2\left(45^0 - \frac{\phi}{2}\right)\right] + 2\left[\tan\left(45^0 + \frac{\phi}{2}\right) + \tan\left(45^0 - \frac{\phi}{2}\right)\right] - \frac{2\ c}{H\bar{\gamma}}}{\frac{\gamma \tan \phi}{c} + \frac{1}{H}} \right\} \tag{45}$$

for the condition $H > \frac{2\ c}{\bar{\gamma}} \tan^2 (45^0 + \frac{\phi}{2})$.

The corresponding solution for the condition $H \leqq \frac{2\ c}{\bar{\gamma}} \tan (45^0 + \frac{\phi}{2})$ is

$$L' = \frac{\frac{\bar{\gamma}\ H}{2\ c} \tan^2\left(45^0 + \frac{\phi}{2}\right) + 2 \tan\left(45^0 + \frac{\phi}{2}\right)}{\frac{\bar{\gamma} \tan \phi}{c} + \frac{1}{H}} \tag{46}$$

Solutions to Eqs. 45 and 46 are shown in Figure 13 giving the ratio of L' to H for a wide range of values $\bar{\gamma}$, c, ϕ, and for anchor depths of 20 and 100 in. The curves for c = 0 and c = ∞ are the same for any values of H and $\bar{\gamma}$. It appears that all practical problems having H less than 100 would yield solutions within or very near the band of solutions shown in Figure 13b. Thus, according to this theory the anchors should be at least 2H apart. They could be spaced up to the vicinity of 5H for very strong soil without loss of efficiency. It is obvious that the curves in Figure 13 do not permit accurate linear interpolation, so Eq. 45 or 46 should be used for specific solutions that are not given by the curves.

If there is plastic shear flow along plane bd, the net force developed against an anchor unit such as cdfe in Figure 11a is Eq. 40. But a weakness of this analysis is that it does not predict the movement necessary to develop the full plastic resistance given by the equation. In an earlier section of this paper the elastic response of an anchor unit was analyzed. Here, the limiting case of plastic response was considered. But between the approximately linearly elastic range and the plastic flow range there is a range of behavior about which relatively little is precisely understood.

Figure 14 shows a load vs displacement curve of the type commonly assumed to exist for engineering analysis of subgrade structures. It is commonly assumed (for example, 7, p. 322) that the load-displacement curve follows a straight line such as 0_a up to a limiting elastic load P_e equal to one-half the limiting plastic load P_u. Beyond

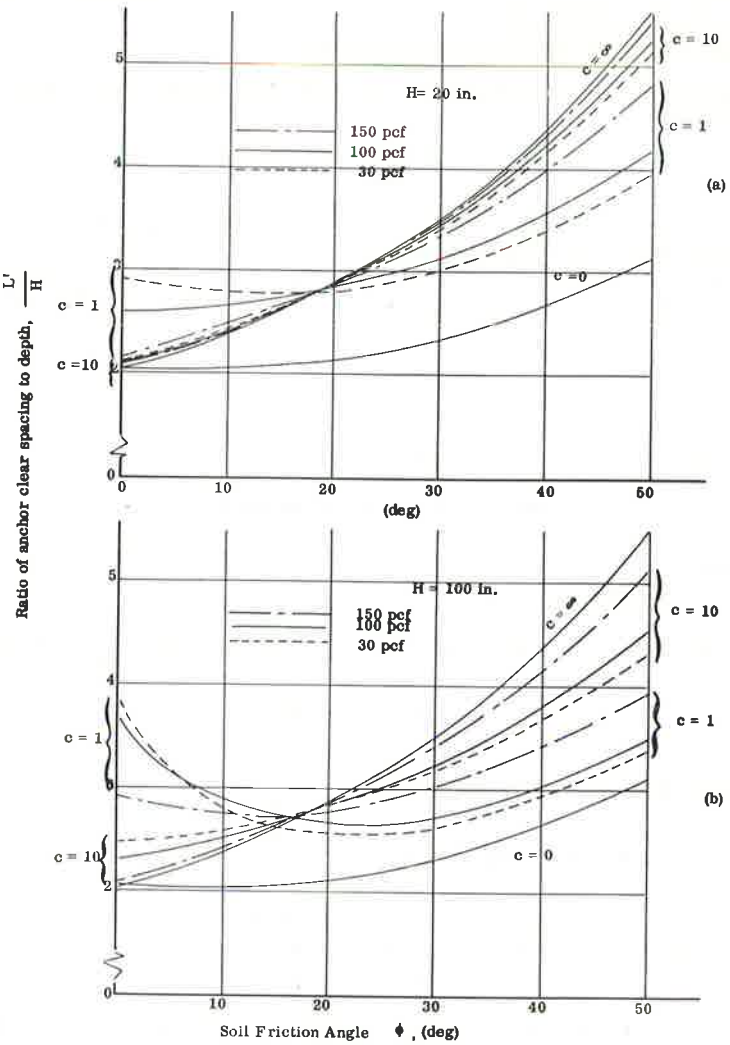

Figure 13. Theoretical optimum spacing-depth ratio for various anchor depths and soil properties.

that point, in accordance with experience, it is assumed that the curve bends appreciably to the extent that the minimum plastic displacement δ_u is several times the maximum elastic displacement δ_e. In the analysis of a pavement anchor system it is required that the anchor resistance P corresponding to a predetermined displacement δ be determined. Unless something is known of the shape of the curve bc (Fig. 14) or of the ratio of δ_u to δ_e it is proposed that the assumed anchor resistance be limited to one-half the plastic resistance. In the design procedure proposed in the next section of this paper the anchor force corresponding to a given deflection is determined by elastic analysis with the limitation that, if the force so determined exceeds one-half the limiting plastic force, the anchor resistance is taken to be one-half the plastic force.

Shear and Moment Analysis

To determine the shear and moment strength required in the anchor, the conditions

shown in Figure 15 are assumed. The force P is equal in magnitude to the anchor resistance force determined by elastic or plastic analysis as previously discussed. P is also the resultant of the subgrade horizontal pressure that is assumed to increase linearly with depth. The resulting moment at the top of the anchor, and applied to the slab, is

$$M_o = \frac{2}{3} PH \qquad (47)$$

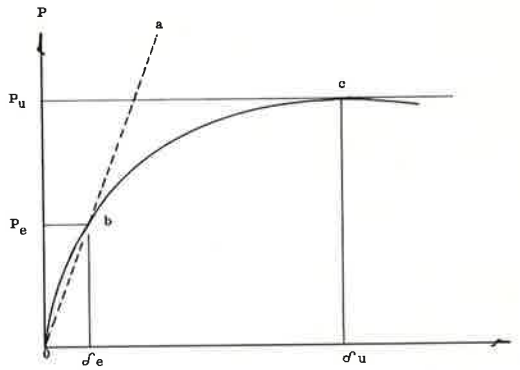

Figure 14. Load-displacement curve of type commonly assumed for engineering analysis.

The assumption of P acting at 2H/3 is rather arbitrary. P could actually act at a higher or lower point depending on anchor stiffness and soil deformation conditions. In the extreme limiting case P could act at the anchor bottom, but the assumption of P acting at 2H/3 is probably sufficiently conservative for engineering purposes.

The problem of shear and moment in the slab adjacent to the joint is more complex. It is complicated by such facts as (a) soil does not develop significant tensile strength, (b) axial loads and transverse traffic loads are acting along with anchor loads, and (c) bending and shear cracks might well develop near the joint. The complexity of the problem would seem to justify a trial and error approach; that is, design should be adjusted on the basis of careful observation of the performance of anchor joints in the field. The following analysis, based heavily on intuition and simplifying assumptions, is proposed for design guidance, subject to modification as indicated by field observations.

It is assumed that axial loads in the slab and traffic loads have negligible effect on the distribution of the shear and moment that is induced in the slab by the anchor moment. Hetenyi (3 p. 14) gives expressions for the deflection, rotation, moment, and shear of an infinitely long beam loaded with a concentrated transverse moment. His expressions, modified for plane strain conditions and with notation modified to conform with that used elsewhere in this paper, are

$$y = \frac{M_o \beta_s^2}{K_s} e^{-\beta_s x} \sin \beta x \qquad (48)$$

$$\theta = \frac{M_o \beta_s^3}{K_s} e^{-\beta_s x} (\cos \beta_s x - \sin \beta_s x) \qquad (49)$$

$$M = \frac{M_o}{2} e^{-\beta_s x} \cos \beta_s x \qquad (50)$$

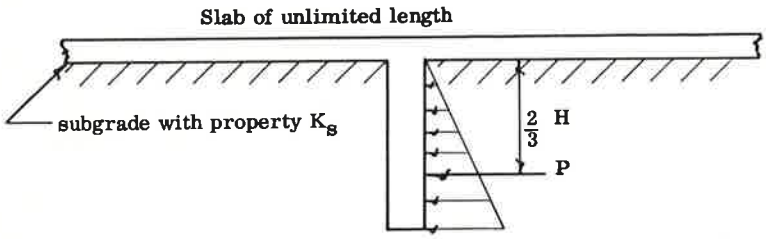

Figure 15. Assumed condition for moment and shear analysis.

$$V = \frac{-M_o}{2} \beta_S e^{-\beta_S x} (\cos \beta_S x + \sin \beta_S x) \quad (51)$$

in which

$$\beta_S = \sqrt[4]{\frac{K_S (1 - \nu^2)}{4 E_S I_S}}$$

x = distance from joint along slab.

A plot of β_S vs slab thickness t_S for $E_S = 4 \times 10^6$ psi and $\nu = 0.15$ is shown in Figure 10. Figure 16 shows the general shape of the curves corresponding to Eqs. 48 through 51. It is proposed that these four equations, with the modifications suggested in the following paragraph, be assumed to apply to the slab in the vicinity of an anchor.

Because the subgrade soil cannot actually develop tensile stress, it appears likely that the greater part of the shear and moment induced by the anchor will be balanced by the downward deflected side of the slab (Fig. 16). Therefore, it is recommended that the slab be designed to withstand double the moment and shear given by Eqs. 50 and 51. But if two adjacent anchors are closer together than two times the distance to the point of zero moment given by Eq. 50 (Fig. 16) the moment should be assumed zero midway between the anchors. It is recommended that reinforcing steel required for anchor-induced moment and shear be provided in addition to the normal continuous pavement reinforcing steel. It is also recommended that the slab thickness be sufficient to resist either the anchor-induced loads or the traffic loads, whichever is greater.

RECOMMENDED PROCEDURE FOR ANALYSIS AND DESIGN

The following paragraphs outline a recommended procedure for the analysis and design of an anchor system. At the end of this section a numerical example is presented. The reader may wish to refer to earlier sections for definitions of terms or for theoretical justification of some of the following.

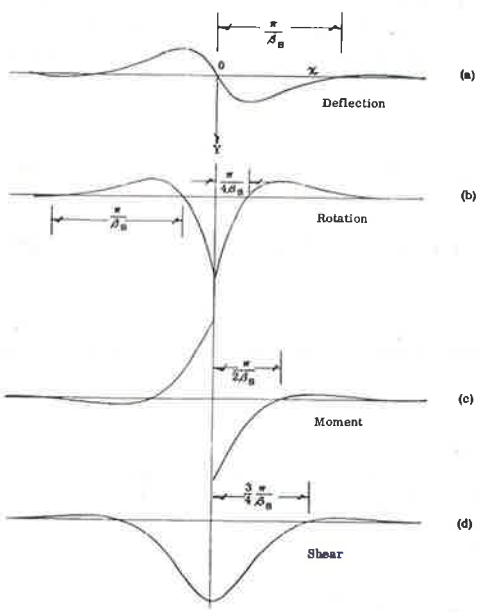

Figure 16. Response of infinite beam on elastic foundation due to transverse moment applied at x = 0.

Temperature, Moisture, or Chemical Strain. —An anchor system should be designed to accommodate a selected unit strain ϵ. This strain might be induced by changes in temperature, moisture, or chemical state of the pavement slab. A detailed study of these phenomena is beyond the scope of this paper, but considerable information on this subject is contained in the technical literature.

End Movement. —End movement δ_o should be assumed equal to the range of the expansion joint to be provided at the slab end. The greater the end movement, the smaller the required anchor forces. Thus, an expansion joint of the greatest range practical should be used.

Soil Properties. —The following properties of the subgrade soil in place must be determined or assumed:

1. Coefficient of vertical subgrade reaction under the slab, K_S.
2. Coefficient of horizontal subgrade reaction throughout the anchor depth K_a.
3. Angle of internal friction, ϕ.
4. Effective cohesion, c.

5. Effective unit weight of soil throughout the anchor depth, $\overline{\gamma}$, as defined for Eq. 43.

Subgrade Friction. —A curve of subgrade friction coefficient vs movement must be assumed.

Concrete Properties. —Poisson's ratio γ and the elastic modulus E must be determined or assumed.

Anchor Dimensions. —The selection of anchor dimensions would seem to require consideration of construction methods. Holes for cylindrical anchors can be dug with a power-driven auger. Rectangular trenches can be dug with a variety of trenching machines. Either shape can also be dug with hand tools. Of course the deeper an anchor is, the more resistance it can develop. Once the maximum bending moment and shear have been determined, the anchor dimensions should be checked for sufficiency.

Anchor Spacing. —It is recommended that the required clear spacing between anchor units be calculated using Eq. 45 or 46 or by reading directly from Figure 13. It is also recommended that the first anchor unit be located at a distance from the free end equal to the anchor depth. The latter recommendation is based more on intuition than on theoretical analysis.

Limiting Anchor Resistance. —The theoretical limiting anchor resistance P_s' can be calculated by Eq. 40. It is recommended that one-half that value be used as the maximum resisting force developed by a single anchor.

Anchor Bending Moment and Shear. —The maximum bending moment and shear in the anchor at the joint should be determined as discussed above under "Shear and Moment Analysis." The maximum shear is equal to the anchor force P. The maximum bending moment is assumed to be given by Eq. 47. At this point, the anchor dimensions should be checked for sufficiency.

Slab Thickness. —It is recommended that the slab be thick enough and reinforced enough to withstand double the moment and shear given by Eqs. 50 and 51. Steel re-

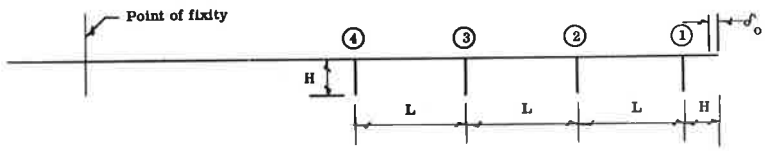

Figure 17. Line diagram of anchor system.

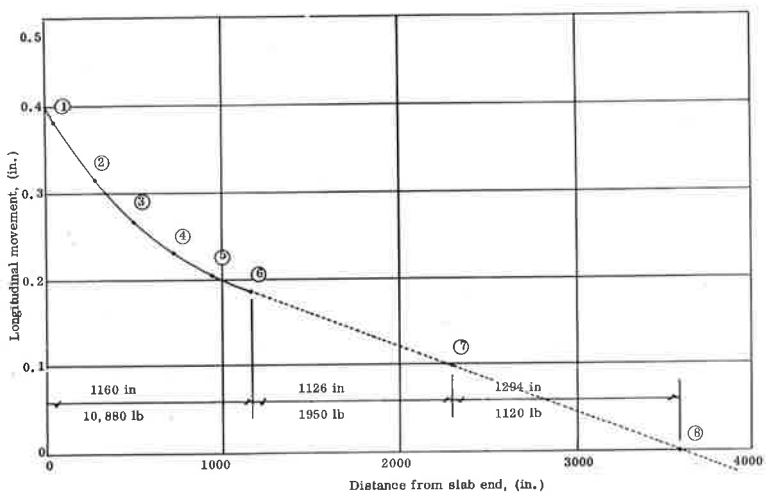

Figure 18. Longitudinal movement of slab in numerical example.

quired for anchor-induced moment and shear should be provided in addition to the regular continuous pavement reinforcing steel (the discussion under "Shear and Moment Analysis" gives further guidance on steel placement). Reinforcing steel should be checked for bond, minimum spacing, and cover before proceeding.

Joint Moment-Rotation Ratio. —A satisfactory approximation to the moment-rotation ratio C can be calculated using Eq. 20. If the concrete properties are in approximate agreement, the value of C can be read from Figure 7.

Elastic Anchor Resistance. —The value of the anchor characteristic β_a can be calculated using the definition given with Eq. 24 or it can be read from Figure 10 if the concrete properties are in approximate agreement. With βa, K_a, C, and H known, the value of the anchor resistance constant $R = P/H K_a \delta$ can be interpolated using Figure 9. The numerical example presented later illustrates interpolation among all four of the families of curves of Figure 9 to evaluate the anchor resistance constant R.

Longitudinal Movement Analysis. —After the preceding quantities have been determined the following steps can be performed to complete the anchor system analysis.

1. Determine movement δ_1 at point 1 (Fig. 17) as the end movement minus the movement at point 1 relative to the end; that is,

$$\delta_1 = \delta_0 - \epsilon H \tag{52}$$

2. Knowing R, H, K_a, and δ_1, compute the elastic resistance of anchor 1 using

$$P = R H K_a \delta_1. \tag{53}$$

The value of P must be compared to $P_S'/2$. The smaller of the two values should be used as the anchor resistance force P_1.

3. Determine movement δ_2 at point 2 (Fig. 17) as the movement δ_1 minus the movement at point 2 relative to point 1; that is,

$$\delta_2 = \delta_1 - \epsilon L + \frac{P_1 L}{AE} \tag{54}$$

4. Repeat step 2 to determine P_2.
5. Determine δ_3 to be

$$\delta_3 = \delta_2 - \epsilon L + (P_1 + P_2) \frac{L}{AE} \tag{55}$$

6. Repeat for additional anchors as necessary.
7. Plot a graph of δ vs position along slab, as in Figure 18. For a satisfactory design, the curve must become horizontal at some point at or above the horizontal axis, $\delta = 0$. If the curve becomes horizontal far above the horizontal axis, the system is overdesigned. The total axial force ΣP acting on the slab at some point beyond the last anchor unit must be equal to or greater than given by

$$\Sigma P = AE \epsilon \tag{56}$$

in which A is the cross-sectional area of that part of the slab beyond the last anchor. (A in Eq. 56 is not necessarily the same magnitude as A in Eq. 55.) That is, the total restraining force must be sufficient to develop a mechanical strain equal to the temperature, moisture, or chemical strain. The total force consists of anchor forces and the subgrade friction forces acting in the zone between the last anchor and the point of fixity. For numerical analysis, the distributed subgrade friction between the last anchor and the point of fixity can be assumed concentrated at several separate points.

Numerical Example. —The following calculations are for a system of 1-in. width. The following dimensional quantities are chosen:

End movement, $\delta_0 = 0.4$ in.

Anchor depth, H = 60 in.
Anchor thickness, t_a = 16 in. (rectangular anchor)

The following soil properties are assumed:

Horizontal coefficient, K_a = 200 psi
Vertical coefficient, K_s = 100 psi
Internal friction angle, ϕ = 32^0
Cohesion, c = 10 psi
Effective unit weight, $\bar{\gamma}$ = 120 pcf = 0.0695 pci

The following concrete properties are assumed:

Elastic modulus, E = 4×10^6 psi
Poisson's ratio, ν = 0.15
Thermal coefficient, α = 7×10^{-6} per deg. F
Unit weight, γ_c = 150 pcf = 0.0868 pci

A strain due to a pavement temperature increase of 50^0 F is assumed. Moisture and chemical strain are assumed zero. Thus the strain to be restrained is $\epsilon = 50 \times 7 \times 10^{-6} = 3.5 \times 10^{-4}$. The subgrade friction curve shown in Figure 19 is assumed.

Anchor spacing is calculated as follows:

$$\frac{2C}{\bar{\gamma}} \tan\left(45^0 + \frac{\phi}{2}\right) = \frac{2 \times 10}{0.0695} \tan\left(45^0 + \frac{32^0}{2}\right) = 512 > 60 \text{ in.}$$

Therefore, use Eq. 16.

$$L' = \frac{\frac{\bar{\gamma} H}{2c} \tan^2\left(45^0 + \frac{\phi}{2}\right) + 2 \tan\left(45^0 + \frac{\phi}{2}\right)}{\frac{\bar{\gamma} \tan}{c} + \frac{1}{H}} = \frac{\frac{0.0695 \times 60}{2 \times 10}(1.804)^2 + 2(1.804)}{\frac{0.0695}{10}(0.625) + \frac{1}{60}} = 204 \text{ in.}$$

Adding the anchor thickness of 16 in. gives a spacing L of 220 in. center to center.

Limiting anchor resistance by Eq. 40 is

$$P_s' = L'(c + \bar{\gamma} H \tan\phi) = 204(10 + 0.0695 \times 60 \times 0.625) = 2,570 \text{ lb}$$

$$\frac{P_s'}{2} = \frac{2,570}{2} = 1,285 \text{ lb} = \text{maximum shear}$$

Maximum anchor moment by Eq. 47 is

$$M_o = \frac{2}{3} PH = \frac{2}{3} \times 1,285 \times 60 = 51,400 \text{ in.-lb}$$

The 16-in. anchor thickness is sufficient.

Maximum slab moment and shear due only to M_o (that is, neglecting axial and traffic loads on slab) are assumed to be twice those values given by Eqs. 50 and 51.

$$\text{Max. } M = \frac{2 M_o}{2} = 51,400 \text{ in.-lb}$$

$$\text{Max. } V = \frac{2 M_o}{2} \beta_s = 51,400 \times 0.0164 = 843 \text{ lb}$$

The value β_s = 0.0164 per in. is taken from Figure 10, assuming a 10-in. thick slab adjacent to the anchors. A 10-in.

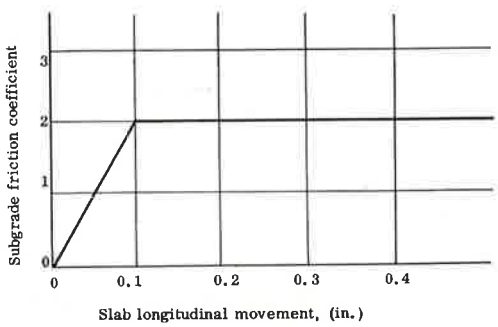

Figure 19. Assumed subgrade friction curve for numerical example.

slab can resist the moment if double reinforcing is provided near the anchor. The slab would have a theoretical shear stress due to the anchor moment, of about 103 psi, which is assumed satisfactory for this example.

Joint moment-rotation ratio C from Figure 7 is 2.27×10^7 in.-lb. The ratio

$$\frac{K_a}{C} = \frac{200 \text{ lb/in.}^2}{2.27 \times 10^7 \text{ in.-lb}} = 0.0000088/\text{in.}^3$$

From Figure 10, $\beta_a = 0.0138$ per in.

Elastic anchor resistance constant R is interpolated from Figure 9 as shown in Figure 20. For each of the four values of K_a/C plotted in Figure 9, one point is plotted in Figure 20. The values are read from Figure 9 for an H of 60 in. and are interpolated by eye for a β_a of 0.0138 per in. Thus Figure 20 is a plot of R vs K/C for an H of 60 in. and a β_a of 0.0138. The value of R for the present example is read from Figure 20 to be 0.683.

$$R = \frac{P}{H K_a \delta} = 0.683$$

thus,

$$P = 0.683 \times 60 \times 200\,\delta = 8,200\,\delta \text{ lb per in.}$$

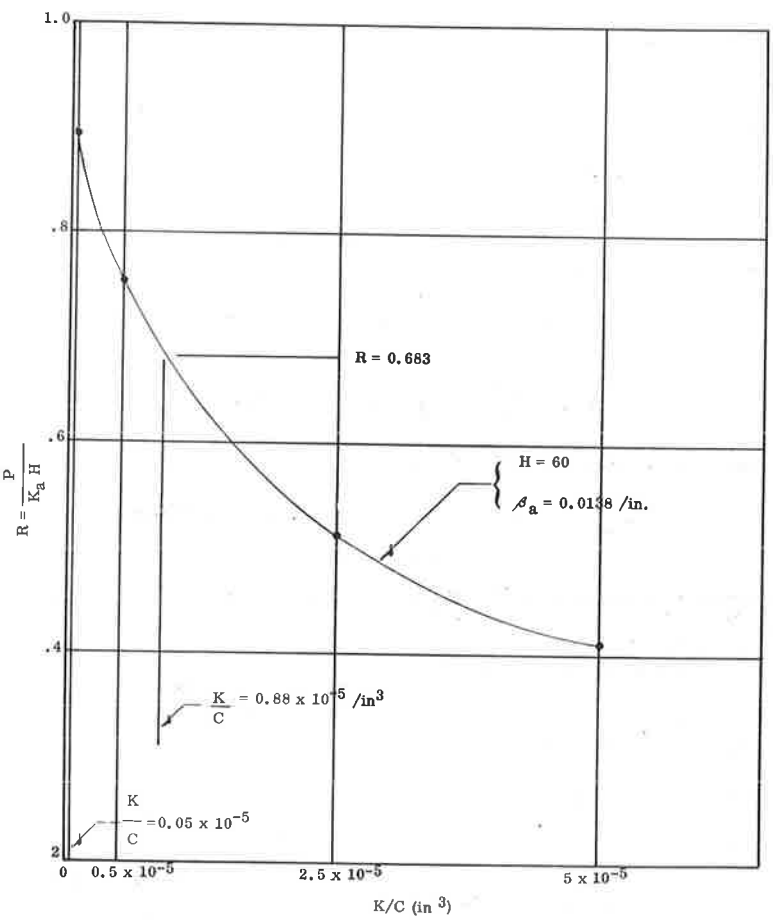

Figure 20. Longitudinal movement of slab in numerical example.

Longitudinal movement:

$$\delta_o = 0.4 \text{ in.}$$

At first anchor located H = 60 in. from the end

$$\delta_1 = \delta_o - \epsilon H = 0.400 - 0.00035 \times 60 = 0.379 \text{ in.}$$

$$P = 8,200 \times 0.379 = 3,110 \text{ lb} > \frac{P_s'}{2} = 2,570 \text{ lb}$$

therefore,

$$P_1 = 2,570 \text{ lb}$$

At second anchor located 220 in. from first anchor

$$\delta_2 = \delta_1 - \epsilon L + \left(\frac{P_1 L}{AE}\right)$$

$$= 0.379 - 0.00035 \times 220 + 2,570 \left(\frac{220}{10 \times 4 \times 10^6}\right)$$

$$= 0.379 - 0.077 + 0.014 = 0.316 \text{ in.}$$

and

$$P = 8,200 \times 0.316 = 2,590 > \frac{P_s'}{2} = 2,570 \text{ lb}$$

therefore,

$$P_2 = 2,570 \text{ lb}$$

$$\delta_3 = \delta_2 - \epsilon L + (P_1 + P_2) \frac{L}{AE}$$

$$= 0.316 - 0.077 + (2,570 + 2,570) \left(\frac{220}{10 \times 4 \times 10^6}\right)$$

$$= 0.316 - 0.077 + (5,140)\,(55 \times 10^{-7}) = 0.267 \text{ in.}$$

$$P = 8,200 \times 0.267 = 2.190 \text{ lb} < \frac{P_s'}{2} = 2,570 \text{ lb}$$

therefore,

$$P_3 = 2,190 \text{ lb}$$

$$\delta_4 = \delta_3 - \epsilon L\,(P_1 + P_2 + P_3)\ \frac{L}{AE}$$

$$= 0.267 - 0.077 + (7,330)\,(55 \times 10^{-7}) = 0.230 \text{ in.}$$

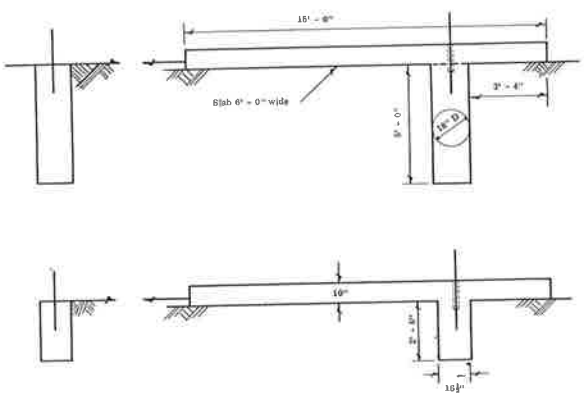

Figure 21. Four anchor units tested.

$$P_5 = 8,200 \times 0.204 = 1,670 \text{ lb}$$

$$\delta_6 = \delta_5 - \epsilon L + (P_1 + P_2 + P_3 + P_4 + P_5) \frac{L}{AE}$$

$$= 0.204 - 0.077 + (10,880)(55 \times 10^{-7}) = 0.187 \text{ in.}$$

The longitudinal movments of points 1 through 6 are shown in Figure 18. By Eq. 56 the required total restraining force, assuming a slab thickness of 10 in. throughout the pavement length, is

$$\Sigma P = A E \epsilon = 10 \times 4 \times 10^6 \times 3.5 \times 10^{-4} = 14,000 \text{ lb}$$

If a thinner pavement had been assumed outside the region of the anchors, the corresponding area would have been used to calculate the required ΣP.

Anchors 1 through 5 develop a resistance of 10,880 lb. The line from point 6 to 8 is a straight extension of the line from point 5 to point 6. The theoretical movement curve would actually fall above line 6-8. But by assuming that the movement is as indicated by line 6-8, and by assuming that the subgrade friction coefficient is as shown in Figure 19 the subgrade resistance between points 6 and 8 can be determined. Between points 6 and 7 subgrade resistance is

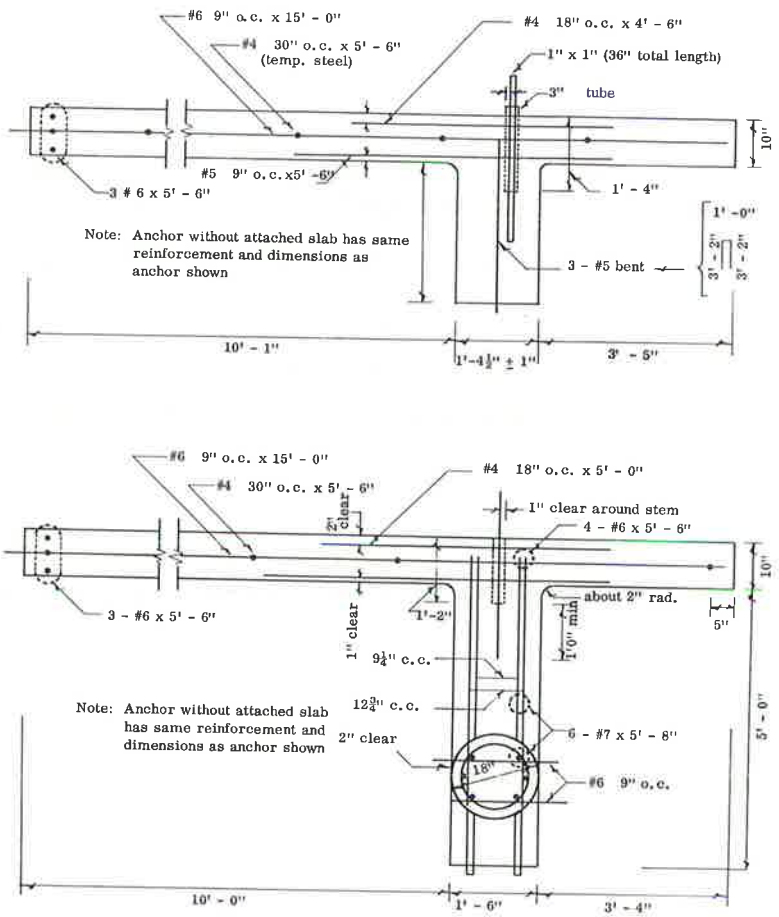

Figure 22. Structural details of test anchors.

$$P_{6-7} = 2 \times 0.0868 \times 10 \times 1,126 = 1,950 \text{ lb}$$

Between points 7 and 8 the subgrade resistance is

$$P_{7-8} = 1 \times 0.0868 \times 10 \times 1,294 = 1,120 \text{ lb}$$

Thus, the total restraining force at point 8 is

$$10,880 + 1,950 + 1,120 = 13,950 \text{ lb}$$

Because subgrade friction would actually deflect curve 6-8 upward and thus induce even greater subgrade friction, it is safe to assume the design using five anchor units is sufficient. A more precise incremental analysis between point 6 and some point of fixity beyond point 8 might even indicate that four anchor units would be sufficient. If the pavement thickness beyond the anchor region had been 8 in. rather than 10 in., a system of four anchor units would very likely have been sufficient.

FIELD EXPERIMENT

The four units shown in Figure 21 were built and tested during the summer and fall of 1961. Trenches and cylindrical holes dug with hand tools served as forms for the concrete. The two slabs were cast monolithically with their anchors. Structural details of the units are shown in Figure 22.

Known horizontal forces were applied as shown in Figure 21. Horizontal and vertical anchor movement, anchor rotation, and slab vertical deflection were measured.

Soil Properties

Subgrade soil at the test site was a brownish red clay having a fairly uniform appearance. Nine samples indicated liquid limits from 37 to 48 with a mean of 42, plasticity indexes from 16 to 25 with a mean of 21, and water contents from 17 to 33 with a mean of 28 (all in percent). One gradation analysis indicated 80 percent passing the No. 200 sieve.

The results of triaxial tests on samples taken from each anchor site are given in Table 1. Samples were taken with a 2-in. diameter split-spoon sampler. There is some uncertainty about the results for c and ϕ because they are based on tests run on but three or four different samples from each anchor site, each tested at a different chamber pressure.

A plate-bearing test was made at the site of each of the slabs. For these tests, an 18-in. diameter plate was loaded in 2,000-lb increments until a settlement of over 0.8 in. developed. The load-settlement curves are shown in Figure 23. The subgrade modulus K_0 corresponding to the straight line 0_a in Figure 23 is about 74 pci.

Loading System

The applied force was developed by a screw jack (Fig. 24) extending to develop a tensile load in a steel frame tied to two adjacent anchors. In Figure 25 load is being applied to the rectangular anchor in the foreground and to the rectangular anchor and

TABLE 1

TRIAXIAL TEST RESULTS

Anchor Site	No. of Samples	Cohesion, c (psi)	Angle of Friction, ϕ (°)	Unconfined Compressive Strength (psi)
Rectangular:				
With slab	4	9	44	41
Without slab	3	9	16	23
Cylindrical:				
Without slab	4	5	36	24
With slab	3	11	37	45

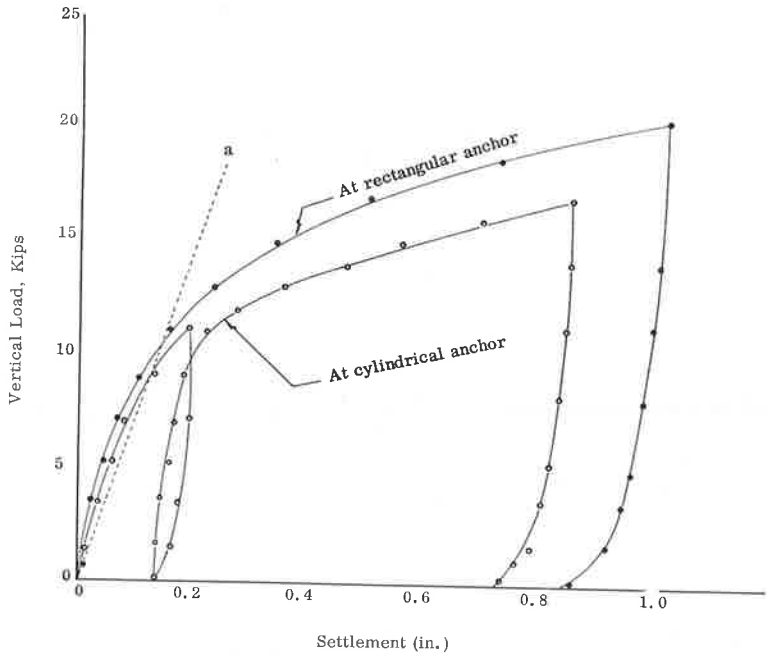

Figure 23. Load settlement curve for 18-in. circular plate bearing test.

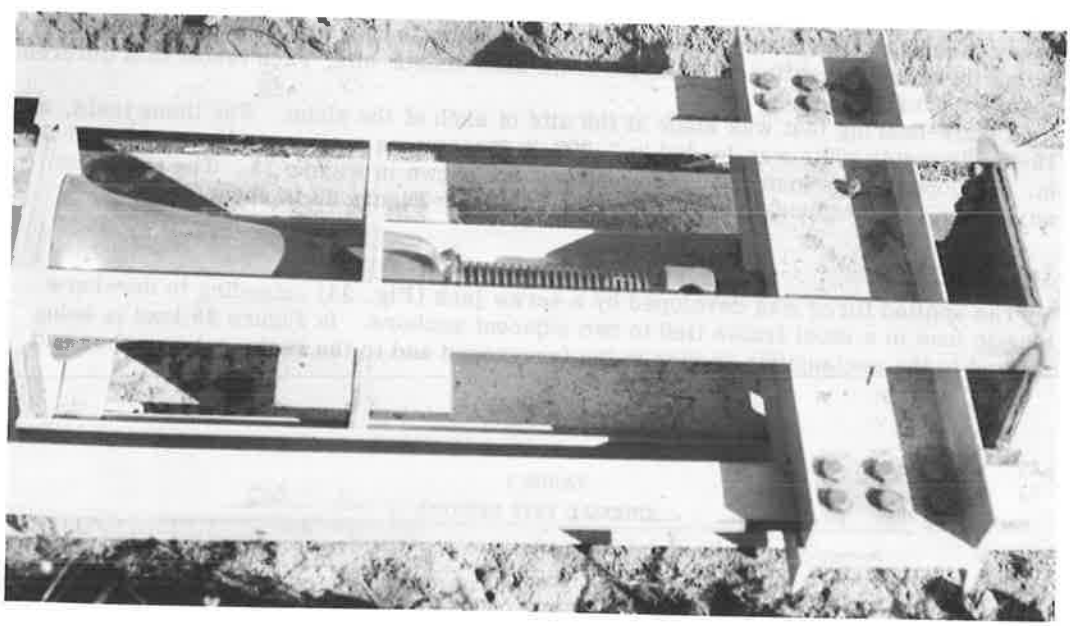

Figure 24. Screw jack for loading system.

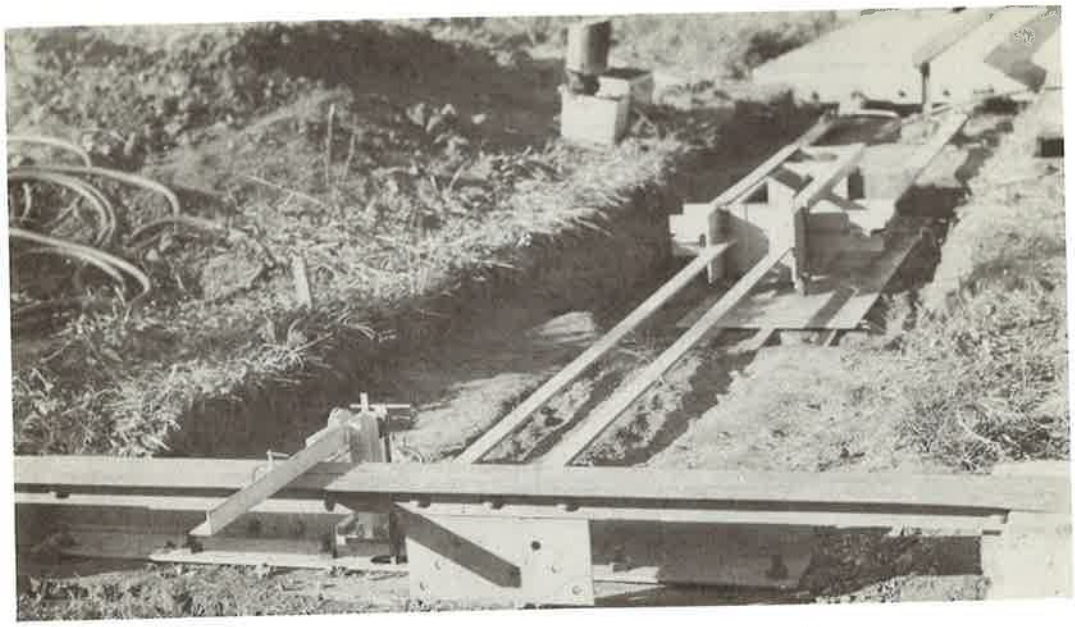

Figure 25. Load being applied to rectangular anchors.

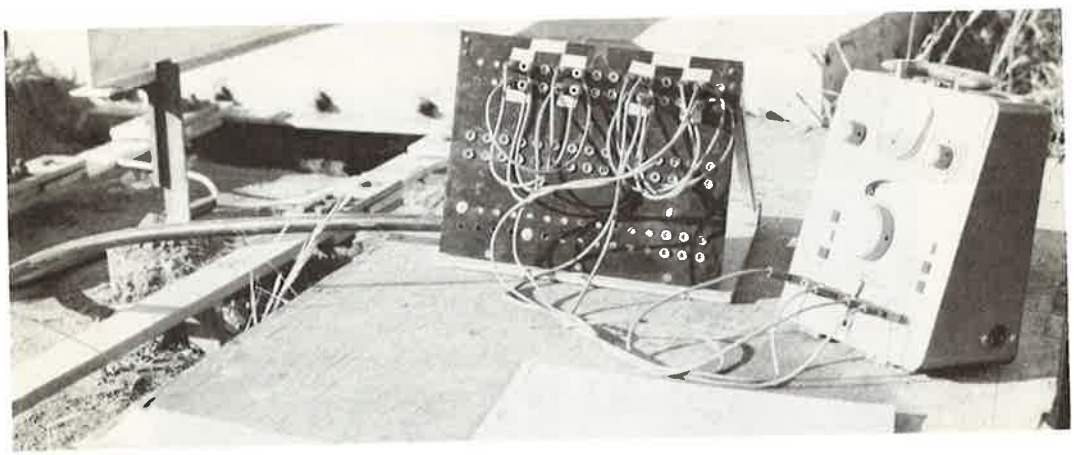

Figure 26. Load cells, wiring, and strain indicator.

slab in the background (the open crack in the soil behind the anchor is noteworthy). The tensile load in the steel frame was measured by two precalibrated load cells. The load cells were pin-connected flat bars with electrical resistance wire strain gages attached. The cells can be seen attached to the slab and long steel tensile members to the left in Figure 26.

Loads were generally applied in increments of 2,000 to 4,000 lb. The total time required for a load cycle ranged from 50 to 140 min. Peak loads were never held for more than a few minutes at the most.

Deflection and Rotation Measurements

Dial micrometers were used as shown in Figure 27 to measure deflection and rotation of the anchor units. A foot was attached at right angles to the stem of each

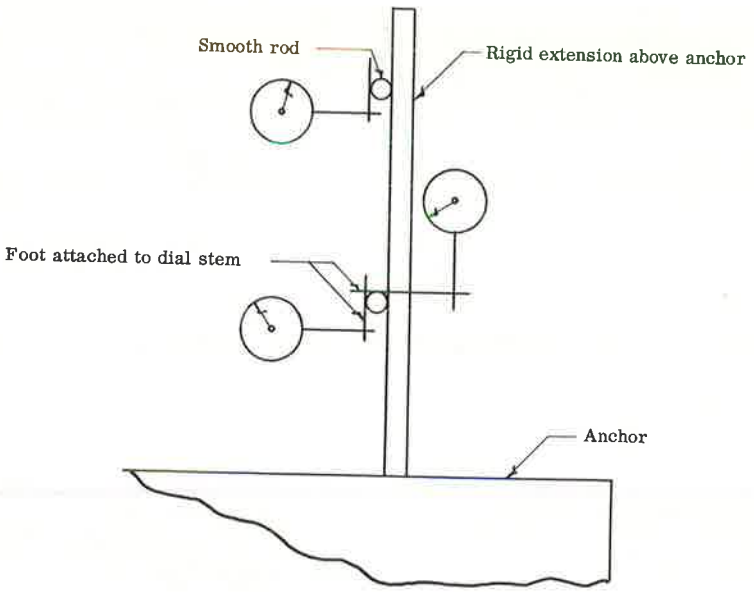

Figure 27. Schematic arrangement of dial micrometers above anchor.

Figure 28. Micrometers in position for measuring horizontal translation and rotation.

micrometer used. This foot remained in contact with a smooth horizontal cylindrical rod attached to a rigid extension to the anchor. Thus, only the horizontal or vertical component of translation of the cylindrical rod was indicated on the dial. By measuring the horizontal movement of two points, and the vertical movement of one of the points, the translation and rotation of the top of the anchor were determined. Two micrometers for measuring horizontal translation and rotation are shown in Figure 28. The vertical micrometer is hidden behind the rigid extension to the anchor.

The micrometers used to measure vertical slab deflection are shown in Figure 29. They also had feet attached at right angles to the stem. The dials indicated only the vertical component of translation of cylindrical rods attached to the slab.

Experimental Results

Figure 30 shows plots of the horizontal deflection of the top of the various test units vs the applied horizontal force. The figure shows the results for all load cycles of the units without slabs but only for one cycle each for the units with slabs.

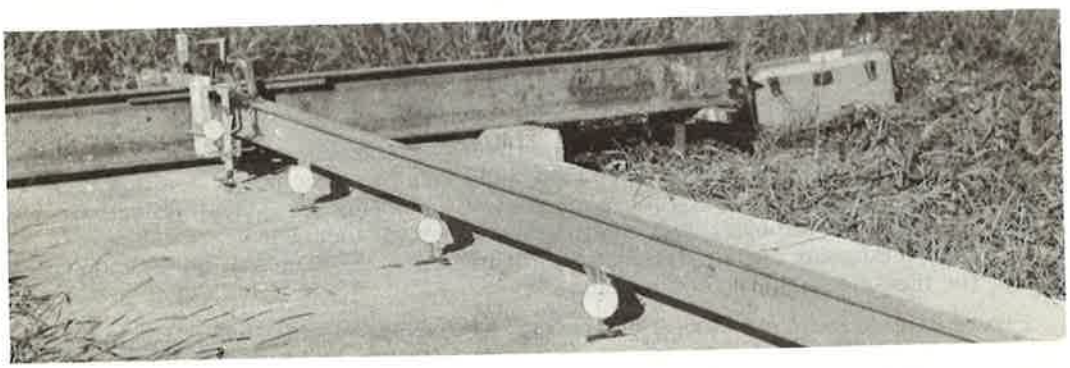

Figure 29. Micrometers in place for measuring vertical slab deflection.

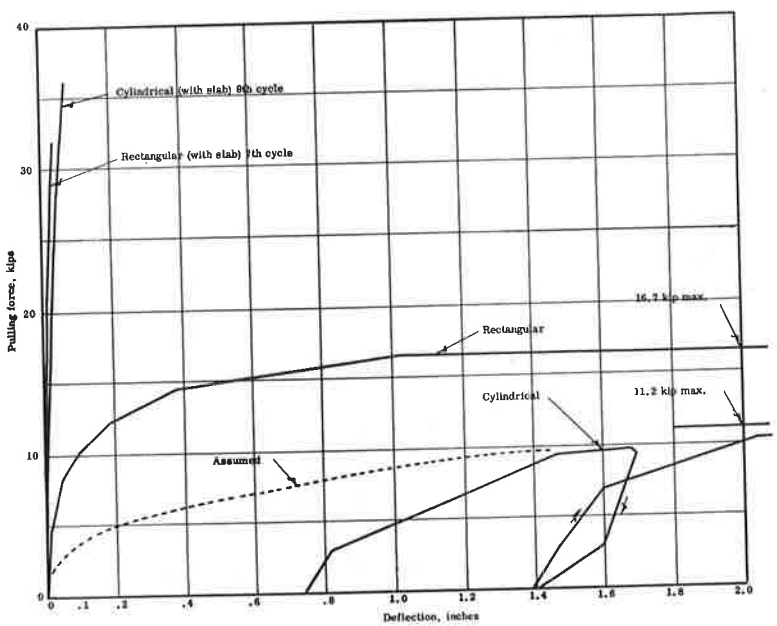

Figure 30. Load vs horizontal deflection at top of anchors.

The dashed curve in Figure 30 represents the assumed initial cycle of the cylindrical unit without slab. For that cycle, a usable load record was not obtained because of an unknown electrical resistance in the strain gage circuit. The deflections for that cycle were measured and the loads and deflections for the two subsequent cycles were determined as plotted.

The figure also suggests that there is a great difference in strength of an anchor with slab as compared to an anchor without attached slab, but the curves might be misleading without further explanation. The total horizontal force applied at the slab end is the quantity plotted in the figure. This total force no doubt included a slab subgrade friction component which unfortunately was not evaluated. Subgrade friction could conceivably account for perhaps 50 percent of the force applied to the slabs.

The resistance of the slab to rotation of the slab-anchor joint accounts for a large part of the strength of a slab-anchor combination. An infinitely stiff anchor in an elastic subgrade, if permitted no joint rotation, would be four times as strong as a similar anchor with free joint rotation. Less stiff anchors under similar conditions have a comparable strength ratio of less than four with the strength ratio decreasing as stiffness decreases. Eq. 31 is a statement of this phenomenon.

Other factors contributing to the great strength of the anchors tested with attached slabs might be (a) the confinement by the slab of the soil in front of the anchor, and (b) the decreased vertical movement of the anchor due to slab weight and stiffness.

Figure 31 shows load-deflection curves for all recorded load cycles on the two anchor units with attached slabs. The following characteristics of these curves stand out:

1. The general slopes appear to remain almost constant for subsequent load cycles.
2. On removal of load, the anchors returned almost to their initial position. Backlash in the dial micrometers could explain part of the apparent residual deflection.
3. The curves could be roughly approximated by a straight line.
4. The rectangular anchor developed about twice the resistance of the cylindrical anchor for the same amount of movement.

Figure 31 also suggests a great detraction of the experimental study. Cycle four of the cylindrical anchor and cycle two of the rectangular anchor suggest the initiation of

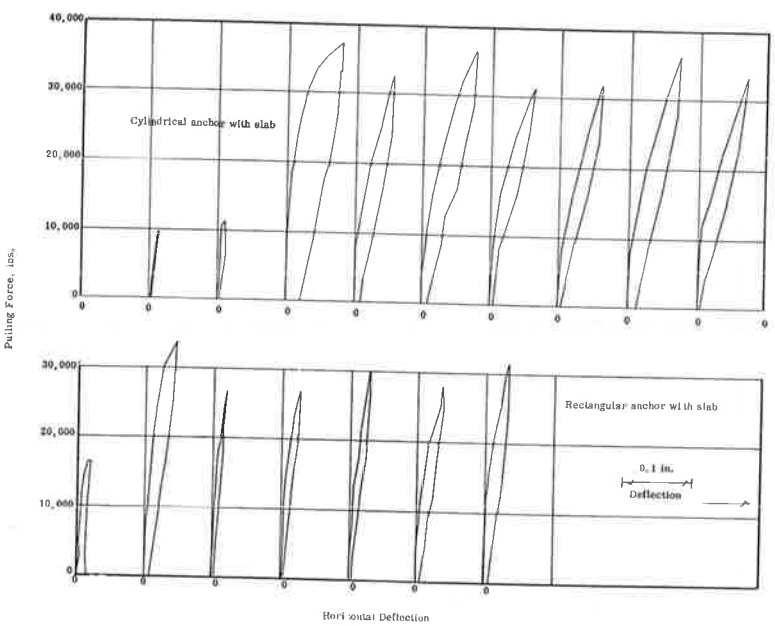

Figure 31. Load vs horizontal deflection at top of anchor with slabs.

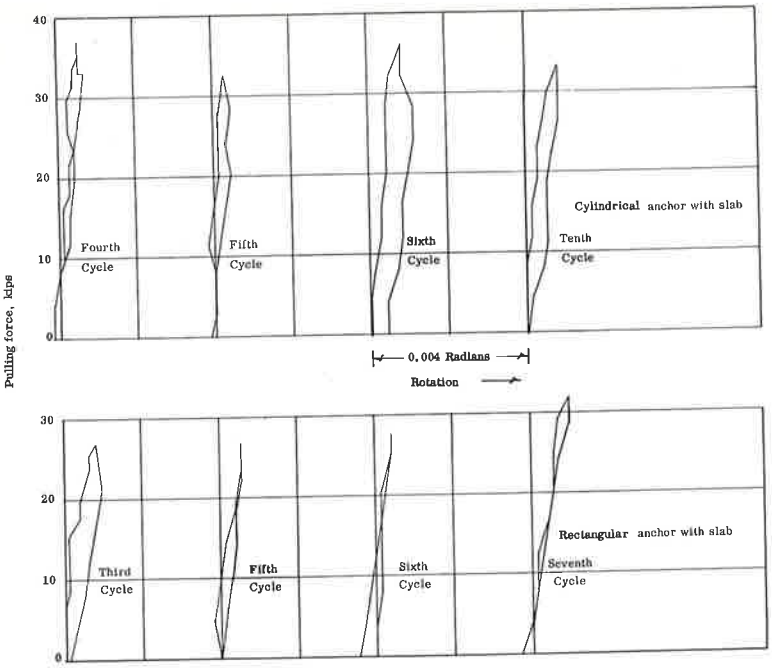

Figure 32. Some of the more characteristic load-rotation curves for anchors with slabs.

some form of plastic yielding. But due to limitations of the loading system, applied horizontal loads did not exceed about 37,000 lb. In this connection it is of interest to compare the peak load of 472 lb per in. applied to the rectangular anchor and slab with that anchor's theoretical limiting load as predicted by Eq. 44. Assuming a cohesion of 9 psi and an internal friction angle of 44^{0} as determined by soil tests (Table 1), and assuming an effective soil unit weight of 120 pcf, an L'/H ratio of about 4.5 is obtained from Figure 13. Substituting into Eq. 44 gives

$$P_S' = L' (c + \overline{\gamma} H \tan \phi) = 4.5 \times 30 (9 + 0.0695 \times 30 \times 0.965) = 1,490 \text{ lb/in. width.}$$

Thus, the maximum load applied during the test was a little less than one-third the limiting plastic resistance predicted by Eq. 44, or a little less than two-thirds the limiting values $P_S'/2$ recommended for design use.

Figure 32 shows some of the more characteristic curves of load vs joint rotation for the anchor units with attached slabs. The rotation values were obtained by dividing the difference in two horizontal dial micrometer readings by the vertical distance between micrometers (Fig. 27). The two dial readings corresponding to the maximum rotation shown in Figure 32 (6th cycle, cylindrical) were 75 and 83. The fact that rotations were determined from two readings that were fairly close together, and that either reading might be in error in either direction, would seem to explain the erratic nature of the curves.

Figure 33 shows the location of the dials

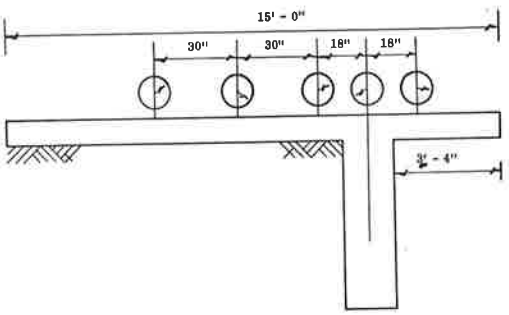

Figure 33. Vertical dial micrometer locations.

used to measure vertical slab deflection. Some representative deflected shapes are shown in Figure 34. The rotation of the top of the anchor is indicated by the downwardly extending element (the upward deflection of the anchor at the joint is noteworthy, as well as the fact that the slab just behind the anchor remained almost at right angles with the anchor, whereas there was significant bending of the slab in front of the anchor).

The curves in Figure 31 show that the rectangular anchor developed about twice the resistance of the cylindrical anchor for the same amount of slab movement. The total volume of the rectangular anchor was about 2.4 times that of the cylindrical anchor, but the cylindrical anchor contained about three times as much steel as the rectangular one. The projected area of the rectangular anchor available to induce subgrade resistance was two times the corresponding projected area of the cylindrical anchor. Thus, a comparison of resistance developed with material quantity for this particular experiment does not indicate one anchor configuration to be particularly superior to the other.

An earlier discussion of longitudinal movement indicated the advantage of developing anchor resistance as near the slab end as possible. Thus, the rectangular anchor might appear to be the better of the two tested in this experiment.

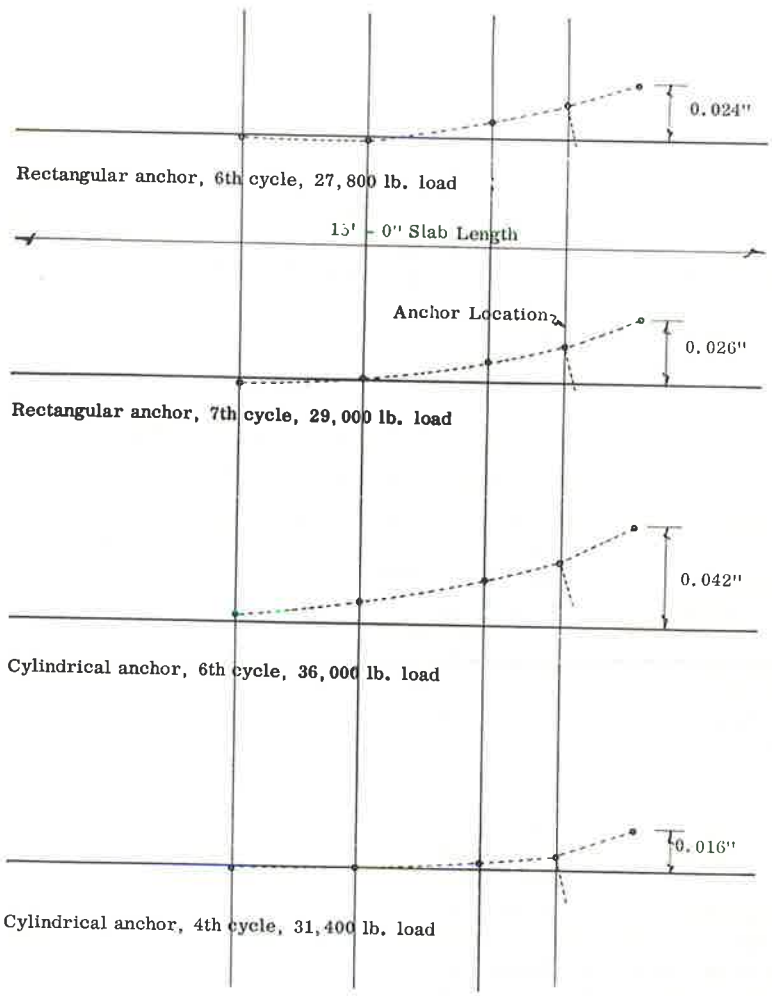

Figure 34. Representative deflected shapes of slabs.

But a general conclusion as to the better configuration, cylindrical or rectangular, cannot be made on the basis of this experiment alone. For example, the results do not indicate whether two or three cylinders of the same dimensions as the one used would be less resistant than a rectangular anchor 60 in. deep.

Significance of Results

Two items of the results are of particular significance relative to the analysis and design of an anchor system. First, the great difference in strength of the anchor units tested (Fig. 30) demonstrates the advantage of providing a rigid joint between anchor and slab. Second, the approximate linearity of the load-deflection curves (Fig. 31) would seem to justify an elastic analysis for the lower load range of anchor response.

APPLICATION TO JOINTED PAVEMENT

When the slabs of a jointed concrete pavement contract, loose soil or other foreign matter may be deposited in the open joints. When the slabs later expand, the deposited solid material may partially prevent the normal closing of the joint. Each cycle of contraction and expansion may result in a greater separation between slabs and a net increase in pavement length. This phenomenon is in contrast to that occurring in a continuously-reinforced concrete pavement whose random cracks are so narrow that very little intrusion of foreign matter takes place.

Shelby and Ledbetter (4) have reported early indications of satisfactory results using only two rectangular anchor units to restrain the ends of jointed pavements. They reason that by preventing the progressive opening of contraction cracks, from the beginning of pavement life, the growth forces are kept much lower than they would be if anchors were not provided.

Some parts of the theoretical analysis previously developed for continuously-reinforced pavement can be applied directly to jointed pavement. The conclusion that subgrade anchor units are most efficient if bunched near the pavement end would apply equally to jointed pavement. The plastic analysis for optimum anchor spacing, Eqs. 45 and 46, would be applicable. The shear and moment analysis might be of some assistance in design.

Application of the elastic anchor resistance analysis would require that longitudinal slab movement at the anchor be calculated or assumed. To adapt the longitudinal slab movement analysis to the jointed pavement problem, it would be necessary to assume the change in width of each joint as well as the pavement end movement. Short of that, it is recommended that jointed pavements be provided with, at most, only a very few anchor units at each end, and that subsequent design be adjusted as indicated by careful observation of field performance.

It is recommended that the anchor units be spaced as indicated by the plastic analysis (Eqs. 45 and 46) and that the entire group be connected by one continuous slab.

CONCLUDING REMARKS

The analysis methods just presented are believed to be suitable for design use in their present form, but they have thus far been correlated with field observations to but a very limited degree. More extensive field observations may indicate a need for modification of the analysis.

Some very useful field observations have been reported in the literature (for example, 4, 9) but further field data are needed, particularly on the performance of subgrade anchor units. It would be desirable to correlate such data with a theoretical analysis such as developed in this paper. For such a correlation, it would be necessary to determine soil and concrete properties, dimensions, temperatures, and absolute longitudinal movements at the slab end, at each anchor unit, and at other points on the pavement slab. It would be desirable to measure any significant vertical slab deflection and carefully to examine for slab cracks in the vicinity of anchor units. For such a study, more meaningful information would probably be obtained from an anchor system that permitted appreciable end movement.

ACKNOWLEDGMENTS

The following major contributions to the project are gratefully acknowledged. W. Zuk made the initial suggestion to the author that the project be undertaken. J. F. Jackson and K. E. McElroy assisted in the planning and execution of the experimental work. K. Tatlidil and G. R. Smith assisted with the many mathematical computations. The manuscript was checked by Y. N. Liu. T. E. Shelburne provided over-all support and encouragement throughout the project.

REFERENCES

1. ASCE, Proc., Research Conference on Shear Strength of Cohesive Soils (June 1960).
2. CRSI, "Design of Continuously-Reinforced Concrete Pavement for Highways." Continuously-Reinforced Concrete Pavement Bull. 1 (Dec. 1960).
3. Hetenyi, M., "Beams on Elastic Foundations." University of Michigan Press (1946).
4. Shelby, M. D., and Ledbetter, W. B., "Experience in Texas with Terminal Anchorage of Concrete Pavement." HRB Bull. 332, 26-38 (1962).
5. Teller, L. W., and Sutherland, E. C., "The Structural Design of Concrete Pavement." Public Roads (Oct. 1935).
6. Terzaghi, K., "Theoretical Soil Mechanics." Wiley (1943).
7. Terzaghi, K., "Evaluation of Coefficients of Subgrade Reaction." Geotechnique (Dec. 1955).
8. Terzaghi, K., and Peck, R. B., "Soil Mechanics in Engineering Practice." Wiley (1948).
9. Van Breemen, W., "Ten-Year Report on Experimental Continuously-Reinforced Concrete Pavements in New Jersey." HRB Bull. 214, 41-75 (1959).
10. Zuk, W., "Analysis of Special Problems in Continuously-Reinforced Concrete Pavements." HRB Bull. 214, 1-20 (1959).

Continuously-Reinforced Concrete Pavements in Pennsylvania—A Six-Year Progress Report

R. K. SHAFFER, and C. D. JENSEN, respectively, Research Coordinator and Director of Research, Materials Bureau, Pennsylvania Department of Highways

After five and six years of service life, the two continuously-reinforced concrete pavements in York and Berks Counties, Pa., have supplied data sufficient for evaluating the effects of the variables under which the pavements were constructed. These projects, on Interstate Routes 83 and 78, respectively, are located on heavily-traveled arteries where approximately one-third of the traffic is rated as heavy truck.

The background history of the two projects is reviewed briefly and the design variables of each pavement are described. Significantly different data are obtained from these variables, particularly from the season of paving.

Included are data on crack frequency, crack width, traffic count, and roughness surveys. Annual end movement and performance of the terminal joints are described.

Shortly after completion of the Berks County project, several wide cracks developed and a subsequent investigation showed these to be lap failures, for the most part. Satisfactory repairs were made, but in 1960, a portion of the 7-in. pavement had to be replaced, essentially because of foundation failure and poor subbase densification. The investigation accompanying this repair work is reported in detail.

The York County pavement to date is performing adequately. The relative performance of both pavements is discussed and a suggested design for continuously-reinforced pavements is offered.

• TWO continuously-reinforced concrete pavements in Pennsylvania have accrued five and six years of service life. Both pavements are strategically located on heavily-traveled arteries and should contribute greatly to the evaluation of the merits of continuous paving. The background history of these two projects is similar in many respects, but the performance to date is remarkably different. A complete description of construction techniques and recorded data relative to these two projects is given elsewhere (1, 2). The following is a very brief description of the important features and variables of both pavements.

The York County project, slightly in excess of 2 miles, is on Interstate 83, the Baltimore-Harrisburg Expressway, 3 miles north of York, Pa. (Fig. 1). The pavement was placed in the fall (September and October) of 1956. It is uniformly 9 in. thick and rests on a 6-in. granular subbase throughout its length. Steel reinforcement is of the bar mat type and was designed for 0.5 percent of the cross-sectional area. The mats were fabricated longitudinally with hard grade No. 5 bars and transversely with No. 3 bars. The performance to date is judged to be quite normal and acceptable by present standards.

Unfortunately, the same is not true of the Berks County project at Hamburg, Pa. When this pavement was in the embryo stage, much thought was given to design vari-

Paper sponsored by Committee on Rigid Pavement Design.

ables by Bureau of Public Roads and Pennsylvania Highway Department engineers who fully realized that failures might possibly be encouraged by the minimum design variables. Feeling that significant data would not be obtained unless a wide range of variables were included, the decision was made to permit construction of sections where assurance of adequate performance was not entirely known.

The Berks County pavement, just short of 2 miles in length, is a section of Interstate 78 and is located 2 miles east of Hamburg, Pa. (Fig. 2). The project was constructed in the spring and summer of 1957 with the exception of a short length of pave-

Figure 1. Interstate 83, Baltimore-Harrisburg Expressway, York County.

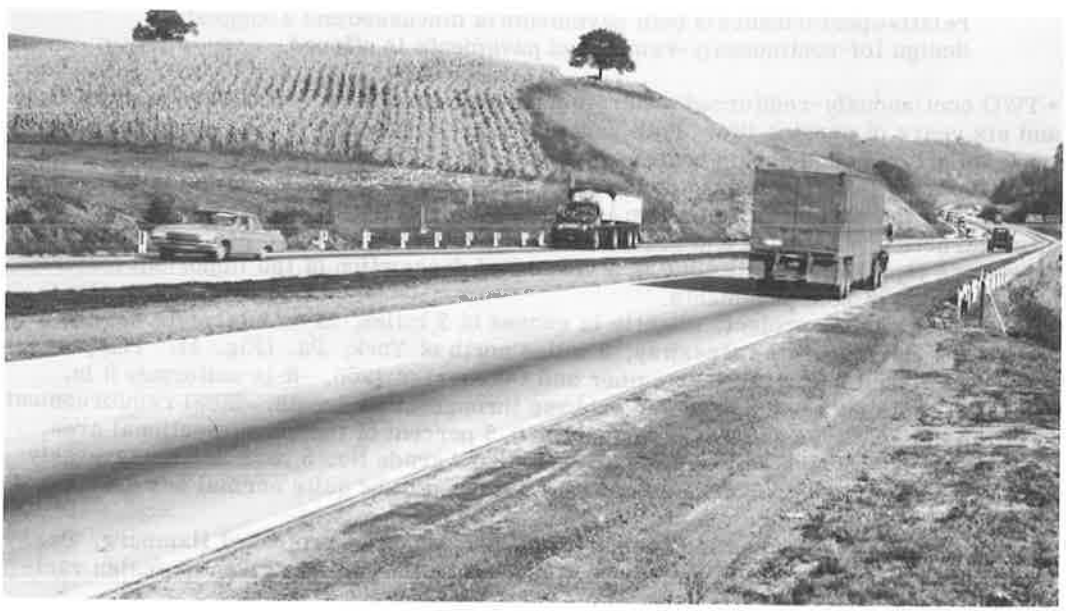

Figure 2. Interstate 78, US 22, Berks County.

ment (1,800 ft) placed in October because of a delay caused by a slide condition. Pavement thicknesses were varied to include 7-, 8-, and 9-in. depths and the subbase was designed for alternate depths of 3- and 6-in. minimums, but the final results varied erratically from the original intent as described later in this report. Reinforcing steel comprised 0.5 percent of the cross-sectional area and was of the bar mat type except for 1,000 ft of welded wire mesh.

YORK PAVEMENT

Much of the success of the York project, it is felt, can be attributed to careful workmanship, but most of all, to the time of year in which it was placed. During construction, ambient temperatures varied between an average high of 66 F and an average low of 44 F. Thus, during the critical curing period, even though the bar mats were overlapped only 20 diameters (12 in.), pavement stresses were not excessive and cracks developed in a normally expected pattern.

During the construction of both continuous pavements, Lehigh University, under a research agreement with the Commonwealth, worked in close accord with the Department of Highways and was responsible for a most comprehensive program of instrumentation. Data were obtained from brass plugs installed on each side of a plane of weakness near the edge of the pavement to measure crack openings; from resistance wire temperature gages in the pavement to indicate local temperatures; and from Bakelite SR-4 strain gages attached to the surface of the longitudinal steel reinforcing bars. These data are available in several published reports (3, 4, 5).

Records maintained by the Highway Department include crack frequency, crack width, traffic count, and roughness surveys. Crack frequency surveys were conducted weekly during the first month of pavement life, then monthly for six months, and annually thereafter. For the York pavement, it was not until the sixth year of service life that the crack pattern appeared to be leveling off. Even in the fifth year, the new cracks developing showed an increase of 25.4 percent over the total number recorded through the fourth year. However, in the sixth year, the rate of increase was only 1.5 percent.

In terms of distance between cracks, surveys indicate (Table 1) that, at the present time, the average crack spacing in the outside or traveling lane is 8.8 ft, whereas the corresponding spacing in the passing lane is 10.6 ft. There are no cracks within the first 100 ft of both ends of the continuous slabs. In the next 100 ft, an average of only 3 cracks per 100 ft is recorded, but immediately beyond 200 ft, the crack pattern is characteristic of that evidenced throughout the job, and for that matter, is consistent with the results obtained from other continuous pavements.

There has been some concern in this State over the appearance of the cracks on the York pavement, particularly the wide, irregularly spalled openings at the surface. The Materials Bureau has always felt these were only superficial and confirmed this opinion by removing a core over a typical crack. Immediately below the surface, the crack assumed hairlike proportions, and as it progressed toward the center of the core, or pavement slab, it became almost indiscernible. The true appearance of the crack, unspalled and void of traffic wear can be observed along the pavement edge. These conditions are shown in Figure 3. It is not felt that moisture of any appreciable amount can penetrate this opening.

Initial crack widths were recorded by a microscope capable of reading to thousandths of an inch, but after an invar-type gage was constructed, all subsequent readings were taken with this equipment. Unless measuring plugs have been installed in the pavement before the development of any cracking, the invar gage cannot be used to record an actual crack width, but it can be used to determine the extent to which any crack is opening or closing.

TABLE 1

CRACK FREQUENCY SURVEY, YORK PROJECT

Age (yr)	Average Distance Between Cracks (ft)			
	Northbound Lane		Southbound Lane	
	Outside	Inside	Outside	Inside
1/12	51.6	27.6	31.7	24.7
1/2	19.1	18.9	19.4	18.1
1 1/2	14.1	16.1	16.2	14.6
2	14.0	15.8	15.9	14.3
3	11.2	14.5	13.1	12.9
4	10.4	14.2	12.0	12.5
5	8.1	11.4	9.5	10.2
6	8.0	11.1	9.5	10.0

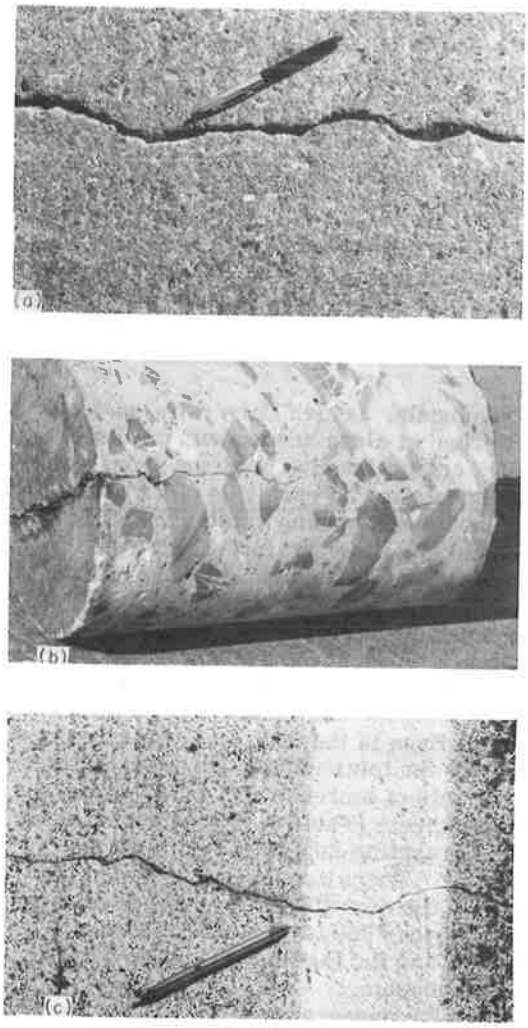

Figure 3. Typical crack on York pavement: (a) spalled appearance at surface, (b) core removed directly over crack, (c) appearance of crack at edge of pavement.

Thus it was necessary to correlate the first invar gage reading with a microscope reading taken at the same time. This was accomplished with a good measure of accuracy because the pavement was not opened to traffic for over a year and the surface condition of the crack was quite intact and unspalled.

Areas selected for crack width studies were 500-ft sections at the beginning, middle, and end of each traffic lane. Widths were recorded between brass plugs set in the pavement on both sides of the cracks and temperatures were recorded by a thermometer inserted into a 6-in., oil-filled brass tube imbedded in the concrete.

During the last 5½ years, crack width readings have been taken twice yearly during typical summer and winter variations. From a total of more than 249 measurements (Table 2), it has been observed that crack widths vary from an average of 0.004 to 0.042 in. per lane. The average crack width in the summer is 0.017 in. and in the winter it increases to 0.023 in., making a seasonal differential of approximately 0.006 in. per crack. This differential is 0.004 in. on the outside lanes and 0.008 in. on the inside lanes, indicative of the greater percentage of cracks occurring in the outside lanes. Crack widths on the first and last 500-ft sections of the continuous slabs were only slightly greater than those measured in the center section of the northbound lanes but were considerably greater in the southbound lanes for unexplainable reasons.

Pavement elongation has been negligible during five years of observation. According to data collected by Lehigh University, there was a measured growth of ¼ in. at 70°, after five years of service on the south end of the continuous pavement where a finger-type bridge expansion joint connects the project to conventional pavement. Seasonal differences in the length of the slab are not more than ⅜ in. At the north end of the project, four dowel-bar expansion assemblies were placed 61½ ft apart in the standard 10-in. pavement to allow end movement of the continuous slab. From observation it appears that the movement of the continuous pavement has influenced only the first expansion joint, and that total growth at this end has been less than at the south end. Present findings indicate that the series of four expansion joints provides a suitable end condition for the continuous reinforcement. Others have found the series of expansion joints not entirely successful. Two favorable situations however, not always available, may have been present to assure success: (a) construction in the fall of the year when low daily temperatures prevailed and (b) apparently high friction between the pavement and the base. Foundation keys or deliberately planned high friction between pavement and base are well worth considering in future designs.

Recent roughness surveys by the Bureau of Public Roads roughometer have indicated

TABLE 2

CRACK WIDTH SURVEY, YORK PROJECT

Lane	Age (yr)	First 500 Ft		Middle 500 Ft		Last 500 Ft	
		Temp. (°F)	Width (in.)	Temp. (°F)	Width (in.)	Temp. (°F)	Width (in.)
Northbound:							
Outside	1½	78	0.018	76	0.017	80	0.023
	2	55[a]	0.010	55[a]	0.010	59[a]	0.018
	2½	85	0.010	85	0.010	87	0.018
	3	37	0.017	37	0.016	32	0.025
	3½	86	0.013	81	0.013	85	0.022
	4	24	0.019	33	0.017	33	0.027
	4½	84	0.015	83	0.014	83	0.025
	5	29	0.019	34	0.016	34	0.030
	5½	85	0.017	85	0.015	86	0.028
	Avg. summer readings	84	0.015	82	0.014	84	0.023
	Avg. winter readings	30	0.018	35	0.016	33	0.027
	No. cracks surveyed	41		26		19	
Inside	1½	80	0.018	82	0.020	81	0.024
	2	57[a]	0.004	56[a]	0.012	59[a]	0.010
	2½	93	0.002	93	0.012	86	0.008
	3	32	0.015	32	0.023	40	0.017
	3½	86	0.005	81	0.014	85	0.011
	4	24	0.017	33	0.023	33	0.020
	4½	84	0.007	83	0.015	83	0.014
	5	29	0.018	34	0.026	34	0.026
	5½	85	0.012	85	0.018	86	0.018
	Avg. summer readings	86	0.009	85	0.016	84	0.015
	Avg. winter readings	28	0.017	33	0.024	36	0.021
	No. cracks surveyed	36		23		29	
Southbound:							
Outside	1½	76	0.024	80	0.013	87	0.012
	2	60[a]	0.032	59[a]	0.001	60[a]	0.021
	2½	90	0.033	94	0.002	95	0.022
	3	35	0.039	35	0.007	39	0.027
	3½	86	0.037	81	0.003	85	0.026
	4	24	0.043	33	0.008	36	0.030
	4½	84	0.039	83	0.005	83	0.028
	5	29	0.045	34	0.009	34	0.037
	5½	85	0.044	85	0.005	86	0.031
	Avg. summer readings	84	0.035	85	0.006	87	0.024
	Avg. winter readings	29	0.042	34	0.008	36	0.031
	No. cracks surveyed	34		25		24	
Inside	1½	78	0.015	84	0.011	85	0.014
	2	60[a]	0.026	59[a]	0.001	60[a]	0.021
	2½	86	0.002	88	0.000	88	0.020
	3	35	0.032	35	0.008	39	0.029
	3½	86	0.024	81	0.002	85	0.023
	4	24	0.033	33	0.009	36	0.028
	4½	84	0.023	83	0.002	83	0.023
	5	29	0.034	34	0.010	34	0.032
	5½	85	0.029	85	0.004	86	0.026
	Avg. summer readings	84	0.023	84	0.004	85	0.021
	Avg. winter readings	29	0.033	34	0.009	36	0.030
	No. cracks surveyed	43		30		26	

[a]Not included in average, being neither typical winter or summer temperature.

that the York continuous pavement shows no increase in surface roughness after five years of service. Relative roughness measured an average 110 units per mile. Surprisingly, the inner lanes showed a 5 percent lower reading than the outside lanes. The riding quality of adjacent standard pavement was slightly better, however, at 95 units per mile.

Traffic on the York pavement in the last three years has increased over 20 percent (Table 3 and Fig. 4). Surveys taken as late as September 1962 reveal that the average daily traffic is now running over 10,600 vehicles, 24 percent of which can be classified as heavy truck traffic. Information is not available relative to the amount of truck

TABLE 3

TRAFFIC COUNT, YORK AND HAMBURG PROJECTS

Classification	Traffic Count						
	York Project			Hamburg Project			
	1959	1961	1962	1958	1959	1961	1962
Passenger vehicles	7,316	7,758	7,526	4,413	5,716	5,645	6,148
Light trailers, pick-ups, panels	-[a]	455	569	190	-[a]	311	299
2- and 3-axle trucks[b]	408	701	703	416	369	400	473
3- and 4-, or 5-axle semitrailers[c]	838	1,504	1,815	3,275	3,044	3,104	3,613
Busses	39	40	28	16	12	14	11
Total	8,601	10,458	10,641	8,310	9,141	9,474	10,544

[a] Included in passenger vehicles.

[b] Maximum gross weights: 33,000 lb for 2-axle, 47,000 lb for 3-axle.

[c] Maximum gross weights: 50,000 lb for 3- and 4-axle, 60,000 lb for 5-axle.

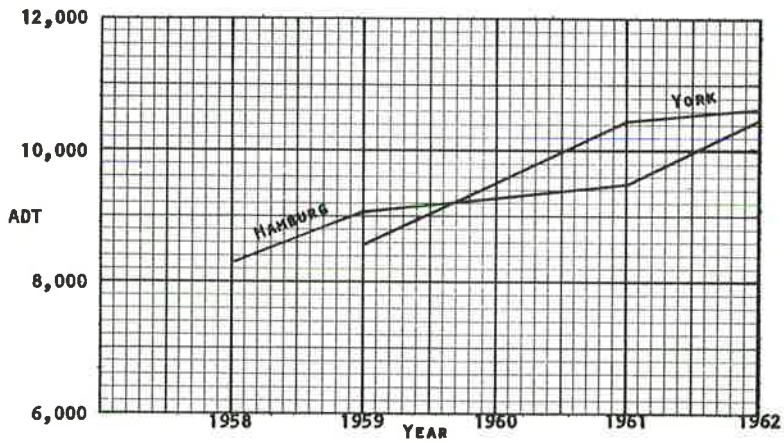

Figure 4. Traffic count, both pavements.

traffic in each lane, however every observation indicates that a very large percentage uses the outside lanes. There is every indication that traffic will substantially increase in each succeeding year as more connections are completed on the Interstate System.

Thus it can be said that the York pavement is behaving as a continuous pavement should: crack widths and frequency are within accepted tolerances and appear to have stabilized. The riding quality is satisfactory, no unusual conditions have been found to exist, and no maintenance has been required since the pavement was placed. It would be expected that many satisfactory years of service will be obtained from the York pavement.

HAMBURG PAVEMENT

The pavement at Hamburg is of a different breed, stemming partly from design variables as mentioned before. There have been a number of interesting conclusions reached and some very successful repairs have been made which will be of interest to those whose continuous pavements are giving similar difficulty.

The project was placed under entirely different weather conditions than the York job,

which was constructed in the fall. During the period from May through July 1957 concrete was placed on the Hamburg pavement under temperatures ranging from an average low of 67 F to an average high of 85 F. In an 1,800-ft section placed in October of the same year, the corresponding average temperatures were 42 and 64 F.

The number of cracks appearing in the Hamburg pavement was significantly greater than that at York, being as much as 85 percent greater in surveys conducted up through one year. The frequency of cracking was always greater in the area comprising the beginning of the day's pour, but this effect leveled out after the first year or so. During the first year, the cracking encountered in the section placed in October was only one-half that recorded on the rest of the pavement, indicating the effect which is exerted by the season of paving. Even today, after five years, the crack pattern is considerably lower in this particular section.

As given previously in Table 1, the average distance between cracks at York ranged from 8.0 to 11.1 ft. At Hamburg, this same spacing varies from 4.9 to 8.5 ft (Table 4). The spacing between cracks in the inside lanes is an average 1½-ft longer than in the adjacent outside or travel lane. There is no appreciable difference in the average crack spacing of the 7- and 8-in. deep sections, but the 9-in. pavement shows a marked increase in distance between cracks. Average distance between cracks in the 7- and 8-in. pavements is 6.2 ft, and in the 9-in. pavement, it is 7.5 ft. But in the 9-in. section placed in October, the spacing is 8.9 ft which compares favorably with the data recorded at York.

Crack widths were also recorded at Hamburg on 100-ft sections at the beginning, middle, and end of each pavement thickness. From a total of 325 plugged cracks, readings indicate that average summer widths are 0.018 in. and average winter readings are 0.023 in. These figures, shown in Table 5, correspond almost identically

TABLE 4

CRACK FREQUENCY SURVEY, HAMBURG PROJECT

Pavement Thickness (in.)	Age (yr)	Average Distance Between Cracks (ft)			
		East Lane		West Lane	
		Outside	Inside	Outside	Inside
7	1/12	10.6	12.6	14.3	12.4
	½	8.2	9.2	8.1	8.8
	1	6.2	8.5	7.1	8.5
	2	5.8	8.0	6.4	8.1
	3	5.2	7.9	5.8	8.0
	4	-[a]	-[a]	5.1	7.0
	5	-[a]	-[a]	4.9	6.6
8	1/12	11.8	15.2	16.5	16.7
	½	8.9	9.6	7.9	8.8
	1	7.8	8.7	6.9	8.6
	2	7.3	7.6	6.4	8.1
	3	6.8	7.5	6.0	7.9
	4	6.4	7.0	5.4	7.1
	5	6.3	6.7	5.3	6.9
9	1/12	24.1	21.0	9.2	13.1
	½	16.8	14.1	8.0	8.4
	1	14.6	13.1	7.6	8.0
	2	11.2	10.2	7.5	7.8
	3	9.6	9.9	7.3	7.6
	4	8.2	8.8	6.4	7.4
	5	8.1	8.5	6.2	7.1

[a] Pavement replaced 1960.

TABLE 5

CRACK WIDTH SURVEY, HAMBURG PROJECT

Lane	Age (yr)	7-In. Pavement						8-In. Pavement						9-In. Pavement					
		1st 100 Ft		Mid 100 Ft		Last 100 Ft		1st 100 Ft		Mid 100 Ft		Last 100 Ft		1st 100 Ft		Mid 100 Ft		Last 100 Ft	
		Temp. (°F)	Width (in.)	Temp. (°F)	Width (in.)	Temp. (°F)	Width (in.)	Temp. (°F)	Width (in.)	Temp. (°F)	Width (in.)	Temp. (°F)	Width (in.)	Temp. (°F)	Width (in.)	Temp. (°F)	Width (in.)	Temp. (°F)	Width (in.)
East:																			
Outside	½	50[a]	0.012	50[a]	0.013	50[a]	0.018	50[a]	0.014	50[a]	0.017	54[a]	0.020	71[b]	0.011	52[a]	0.013	52[a]	0.018
	1	65[a]	0.008	65[a]	0.011	65[a]	0.020	64[a]	0.012	64[a]	0.015	64[a]	0.017	78	0.012	72[a]	0.011	72[a]	0.012
	1½	58[a]	0.011	58[a]	0.015	58[a]	0.021	56[a]	0.010	56[a]	0.017	56[a]	0.020	85	0.021	66[a]	0.014	58[a]	0.023
	2	86	0.011	86	0.016	86	0.019	86	0.017	86	0.019	86	0.022	34	0.032	86	0.016	86	0.022
	2½	37	0.015	37	0.019	37	0.023	37	0.023	37	0.023	37	0.027	92	0.022	37	0.019	37	0.026
	3	74	0.012	74	0.018	74	0.022	80	0.020	80	0.020	80	0.024	-	-	92	0.018	92	0.030
	4	-c	-c	-c	-c	-c	-c	84	0.021	84	0.022	84	0.024	32	0.034	80	0.020	80	0.034
	4½	-c	-c	-c	-c	-c	-c	24	0.026	24	0.026	24	0.030	80	0.024	32	0.024	32	0.033
	5	-c	-c	-c	-c	-c	-c	80	0.025	80	0.022	80	0.025	-	-	84	0.019	84	0.034
Avg summer readings		80	0.012	80	0.017	80	0.021	83	0.021	83	0.021	83	0.024	81	0.018	86	0.018	86	0.030
Avg winter readings		37	0.015	37	0.019	37	0.023	31	0.025	31	0.025	31	0.029	33	0.033	35	0.022	35	0.030
No. cracks surveyed		11		10		9		8		8		10		14		9		4	
Inside	½	36	0.018	36	0.017	36	0.016	40[a]	0.017	40[a]	0.016	40[a]	0.014	73[b]	0.012	35	0.019	42	0.023
	1	84	0.013	84	0.014	84	0.014	84	0.013	84	0.012	84	0.010	78	0.019	91	0.011	91	0.018
	1½	50[a]	0.015	50[a]	0.020	50[a]	0.017	60[a]	0.016	60[a]	0.014	60[a]	0.014	85	0.026	54[a]	0.018	54[a]	0.025
	2	86	0.016	86	0.018	86	0.018	84	0.017	84	0.014	84	0.013	34	0.039	84	0.015	84	0.024
	2½	28	0.022	28	0.025	28	0.024	28	0.025	28	0.020	28	0.019	92	0.030	28	0.022	28	0.026
	3	74	0.018	74	0.020	74	0.020	80	0.019	80	0.016	80	0.016	-	-	92	0.018	92	0.026
	4	-c	-c	-c	-c	-c	-c	84	0.021	84	0.016	84	0.017	80	0.048	80	0.020	80	0.029
	4½	-c	-c	-c	-c	-c	-c	24	0.027	24	0.025	24	0.025	83	0.037	32	0.025	32	0.033
	5	-c	-c	-c	-c	-c	-c	80	0.034	80	0.018	80	0.019	-	-	84	0.021	84	0.033
Avg summer readings		81	0.016	81	0.017	81	0.017	82	0.021	82	0.015	82	0.015	82	0.029	86	0.017	86	0.026
Avg winter readings		32	0.020	32	0.021	32	0.020	26	0.026	26	0.023	26	0.022	34	0.039	32	0.022	34	0.027
No. cracks surveyed		9		9		8		5		10		9		8		6		3	
West:																			
Outside	½	42[a]	0.013	70[a]	0.008	70[a]	0.011	70[a]	0.009	73[a]	0.012	64[a]	0.011	63[a]	0.011	63[a]	0.012	54[a]	0.008
	1	92	0.011	92	0.008	92	0.014	92	0.012	92	0.014	92	0.012	92	0.012	92	0.013	92	0.011
	1½	76	0.012	76	0.009	76	0.015	65[a]	0.013	65[a]	0.014	73	0.013	73	0.013	73	0.013	76	0.011
	2	87	0.015	87	0.012	87	0.017	87	0.016	92	0.019	92	0.016	92	0.017	92	0.015	92	0.015
	2½	32	0.016	32	0.015	32	0.019	32	0.018	32	0.023	32	0.020	32	0.024	32	0.019	32	0.016
	3	74	0.017	74	0.014	74	0.019	80	0.016	80	0.021	80	0.019	92	0.022	92	0.017	92	0.016
	4	84	0.020	84	0.015	84	0.019	84	0.017	84	0.022	84	0.021	80	0.024	80	0.019	80	0.019
	4½	32	0.031	32	0.016	32	0.023	24	0.022	24	0.029	24	0.027	32	0.031	32	0.023	32	0.019
	5	84	0.022	84	0.017	84	0.021	80	0.019	80	0.023	80	0.022	84	0.025	84	0.019	84	0.020
Avg summer readings		83	0.016	83	0.013	83	0.018	85	0.016	86	0.020	84	0.017	86	0.019	86	0.016	86	0.015
Avg winter readings		32	0.024	32	0.016	32	0.021	28	0.020	28	0.026	28	0.024	32	0.028	32	0.021	32	0.018
No. cracks surveyed		7		12		11		10		11		8		13		12		9	
Inside	½	58[a]	0.007	58[a]	0.012	58[a]	0.011	64[a]	0.010	64[a]	0.008	64[a]	0.008	70[a]	0.010	68[a]	0.012	68[a]	0.008
	1	92	0.010	92	0.013	92	0.011	92	0.012	87	0.010	87	0.005	91	0.011	91	0.013	91	0.011
	1½	68[a]	0.012	68[a]	0.014	68[a]	0.012	68[a]	0.012	80	0.010	80	0.006	72[a]	0.012	72	0.014	72	0.015
	2	92	0.014	92	0.017	92	0.016	92	0.016	92	0.013	92	0.016	92	0.014	92	0.020	92	0.016
	2½	32	0.017	32	0.024	32	0.021	34	0.021	34	0.020	34	0.020	34	0.018	34	0.025	34	0.021
	3	74	0.016	74	0.019	74	0.018	80	0.018	80	0.017	84	0.017	92	0.016	92	0.022	92	0.020
	4	84	0.016	84	0.020	84	0.019	84	0.018	84	0.018	84	0.018	80	0.017	80	0.025	80	0.025
	4½	32	0.021	32	0.026	32	0.026	24	0.026	24	0.028	24	0.026	32	0.023	32	0.031	32	0.029
	5	84	0.018	84	0.021	84	0.021	80	0.020	80	0.020	80	0.019	80	0.019	82	0.026	84	0.028
Avg summer readings		85	0.015	85	0.018	85	0.017	86	0.017	84	0.015	85	0.014	87	0.015	87	0.021	88	0.020
Avg winter readings		32	0.019	32	0.025	32	0.024	29	0.024	29	0.024	29	0.023	33	0.021	33	0.028	33	0.025
No. cracks surveyed		11		11		11		10		9		2		10		9		9	

[a]Not included in average being neither typical winter or summer temperature.

[b]Placed October 1957, 100-ft continuous brass plugs, 10-in. centers.

[c]Pavement replaced November 1960.

with those at York. There is a noticeable tendency for the cracks to creep in width over a period of years so that the readings recorded at five years are now approximately double the widths taken at six months. There is very little difference to be found in the variation of crack widths in the 7-, 8-, and 9-in. sections. In the westbound lanes, for example, an average of all cracks recorded shows a summer opening of 0.017 in. for the 7- and 8-in. pavements and 0.018 in. for the 9-in. pavement. Winter readings are correspondingly close. There is a very slight tendency for the crack widths to be narrower in the 7-in. section. It must be remembered that the first 100 ft of the 7-in. pavement and the last 100 ft of the 9-in. pavement as given in Table 5 are the actual ends of the pavement. All other beginning, middle and end 100-ft sections are contained within these extremities. A variation between summer and winter readings averaged 0.005 in. for the 7-in. pavement, 0.004 for the 8-in., and 0.007 for the 9-in. concrete. The difference between crack widths in the inside and outside lanes is not significant.

It might be mentioned that the temperatures appearing in the tables throughout this report are air temperatures inasmuch as the early readings were recorded as such be-

fore installation of the brass thermometer well, and there was no desire to confuse the issue by switching from one method to the other. An accurate record has been kept, however, of both methods and it has been found that, in the summer, concrete temperatures averaged 3° higher than air temperatures, whereas in the winter, there was practically no difference.

When the 1,800-ft section of 9-in. pavement was placed in October, brass plugs for crack width measurements were installed in the fresh concrete on 10-in. centers for a distance of 100 ft to permit true readings of crack widths as they developed. Precise readings were taken between each set of plugs the first two days after placement and at regular intervals thereafter. It has been encouraging that these readings correspond quite favorably with those where the initial width readings were obtained by microscope.

There is very little evidence to indicate what effect subbase depth had on pavement performance. If cracking is of significance, it can be reported that there is a slight trend indicating that fewer cracks have developed over the 6-in. subbase than over the 3-in. This is apparent for all three pavement depths. There is no evidence to prove that the wire mesh section performed any better or worse than adjoining bar mat sections.

The volume of traffic has increased tremendously at Hamburg and shows every indication of continuing so. In the past four years, an increase of 27 percent in total vehicular traffic has been noted (Table 3 and Fig. 4). Present average daily traffic is now over 10,500 vehicles of which 39 percent is heavy truck.

Recent roughometer surveys with the BPR unit showed a reading of 93 units per mile for the 9-in. pavement, 104 units for the 8-in. pavement, and 113 units for the 7-in. section. This is compared to an average reading of 76 units per mile for adjacent, standard pavement on the same route.

End movement of the pavement slab ranges from ¾ to 1 in. At the end of two years, permanent growth or creep has been approximately ¼ in. The elaborate bridge-type finger joint, built over a box culvert with drainage through the shoulder, has performed quite satisfactorily; however, it is felt that such expense need not be incurred and that the series of expansion joints, or such devices where 1½ to 2 in. of movement is provided, are adequate.

PAVEMENT REPAIR

Shortly following the completion of the Hamburg project, generally within three months, it became evident that a number of cracks were becoming unusually wide; some of them measuring ¼ to ½ in. at the surface (Fig. 5). An investigation conducted in the spring of 1958, when sufficient pavement was removed at the edge of the roadway to expose the steel, revealed in three instances that there was no overlap of reinforcing steel at all. At two locations, the wide cracks were not at overlaps. The average lap of steel in the remaining ten areas was 7½ in., ranging from 3 to 11 in. The specifications covering this project did not require the bar mats to be tied. It is apparent that this requirement should have been specified and certainly should be written into future contracts involving continuously-reinforced pavements.

After determining the cause of the cracking, arrangements were made to repair the defective areas. It was essential that the work be performed carefully. To insure this, detailed construction specifications were written. The concrete pavement repairs consisted of removal of the existing pavement, restoration of the continuity of the longitudinal reinforcing steel, and replacement of the pavement with high-early strength cement concrete.

In repairing the steel, No. 5 deformed steel bars of the same quality as the existing steel were required for splicing and were of sufficient length to provide an 18-in. overlap at both ends. The steel was welded at the center of the lap with a ½-in. bead, on one side only, for a length of 5 in. No. 3 transverse bars were placed and tied to the longitudinal bars in accordance with the pattern of the original bar mats.

Of 13 such areas repaired, only one patch was not successful. After four years, these repairs (Fig. 5) are performing adequately, and although new cracks have formed in the longer patches, they are of a pattern typical of a normal continuous pavement. The

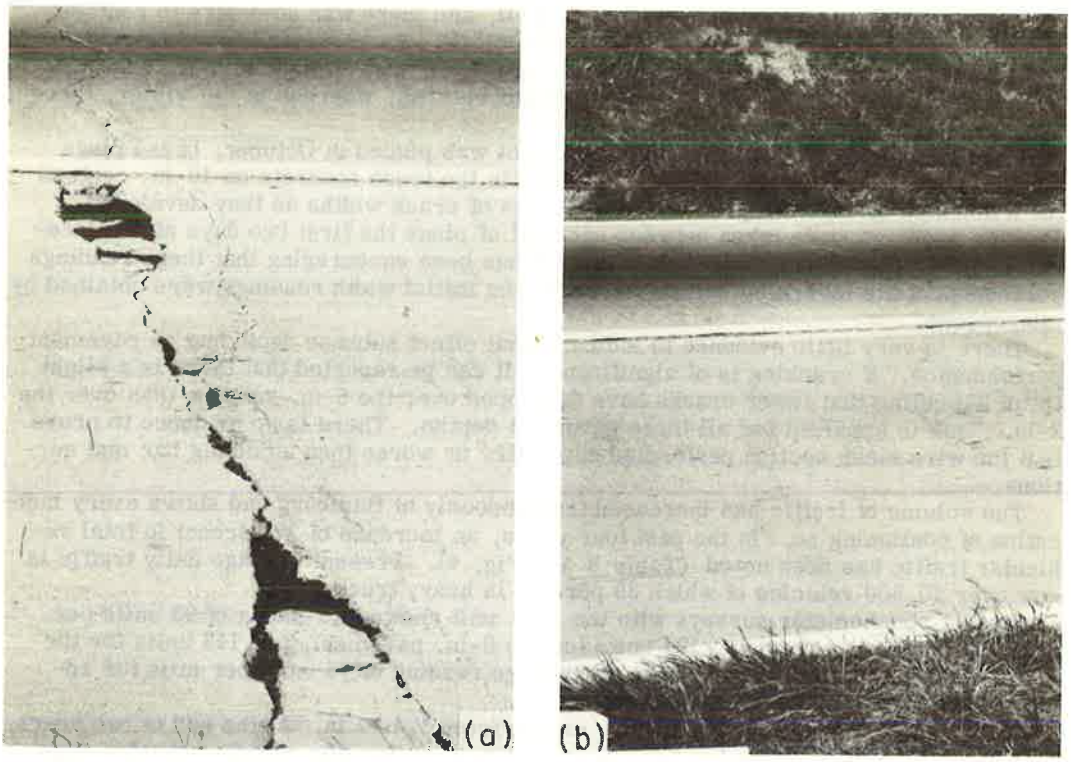

Figure 5. Hamburg pavement: (a) appearance of typical wide crack, (b) patched area after 4 year's service.

success of the repair operation has established a repair method that is apparently satisfactory and can be used where abnormal cracks develop on continuous pavements.

As if the crack failures were not sufficient trouble for the maintenance department, signs of major distress began appearing in the eastbound 7-in. lanes in 1959. More large cracks developed in several locations and these areas deteriorated progressively until large portions of the concrete, comprising as much as 200 sq ft, were broken, disintegrated, and were noticeably below original grade. The broken concrete constituted a hazard to traffic and had to be patched repeatedly with bituminous material. A typical area is shown in Figure 6. In addition to this type of failure, longitudinal cracking was encountered in several locations, primarily near these distressed areas and always within 6 to 8 in. of the center longitudinal joint. Pumping was evident along the edge of the outside traffic lane.

It was apparent that these failures were becoming worse. In the spring of 1960, the laboratory recommended that the 7-in. eastbound lanes be replaced. Bureau of Public Roads concurrence was secured, considering the major research aspect of the joint venture. A contract was awarded in September 1960 for the replacement of 5,340 sq yd of concrete with standard reinforced pavement, 10 in. in depth. Work commenced on October 19, 1960, when the contractor began breaking the concrete in the eastbound lane between stations 168 + 96 and 188 + 97.5, a distance of approximately 2,000 lineal feet.

The concrete on the inside lane shared none of the distress of that in the outside lane and was, in fact, in excellent condition. Much thought was given to the possibility of salvaging the inside lane, but considering the difficulty of joining two lanes of different thicknesses, the idea was dropped in favor of replacing both lanes.

The investigation, conducted in connection with the repaving, paralleled the earlier findings: The average overlap of steel was 10½ in., the average depth was 3¼ in.

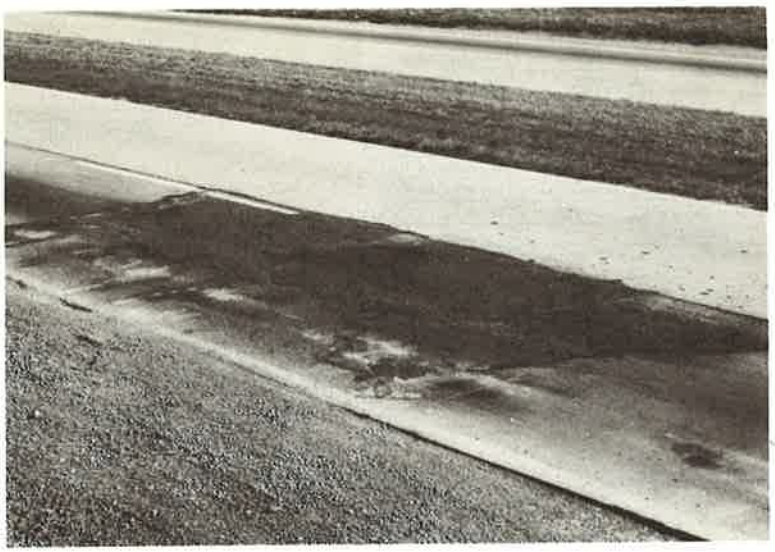

Figure 6. Failure in 7-in. pavement, Hamburg.

The overlap of steel ranged from 8 to 13 in., and the range in depth was from 2¾ to 3¾ in., measured from the top of the steel. Many of the steel bars were broken in the areas where pavement damage was the worst. There is no doubt that the overlap (12 in.) of steel on this project was inadequate and that the large transverse cracks and subsequent breaking of concrete between two such parallel cracks were probably the beginning of many of the failures. The majority of these areas occurred at an overlap. The quality of the concrete removed appeared to be sound and revealed an excellent distribution of aggregates.

SOIL INVESTIGATION

On October 19, 20, and 21, 1960, a soil investigation was conducted between stations 169 and 189, eastbound lanes, by the laboratory field soils office in cooperation with the Research Unit. The removal of the roadway section down to the subgrade provided an opportunity to investigate the subbase, subgrade, and drainage to determine if any or all of these were contributing factors to the failure of this section.

Records from construction included the following data for the eastbound lanes:

1. A soil survey with 5 soil classifications, 3 compaction tests, and 2 CBR tests (Fig. 7).
2. Sand cone density checks of the subgrade, 8 tests (Table 6).
3. Thickness measurements of the subbase every 50 ft (Fig. 8).
4. Sand cone density checks of the subbase, 4 tests (text).

Additional data obtained by the special investigation included the following:

1. Five soil gradations each for the subbase and subgrade with moisture content determinations (Fig. 7; Table 7).
2. Two sand cone density checks of the subgrade (Table 6).
3. Two holes drilled for ground water level.

Subbase

The subbase material for this project was a run of mill crushed limestone meeting the specification requirements of gradation A or B (Table 8). Of the initial 15 samples taken from the source of supply, three failed to meet specifications (two with 1 percent

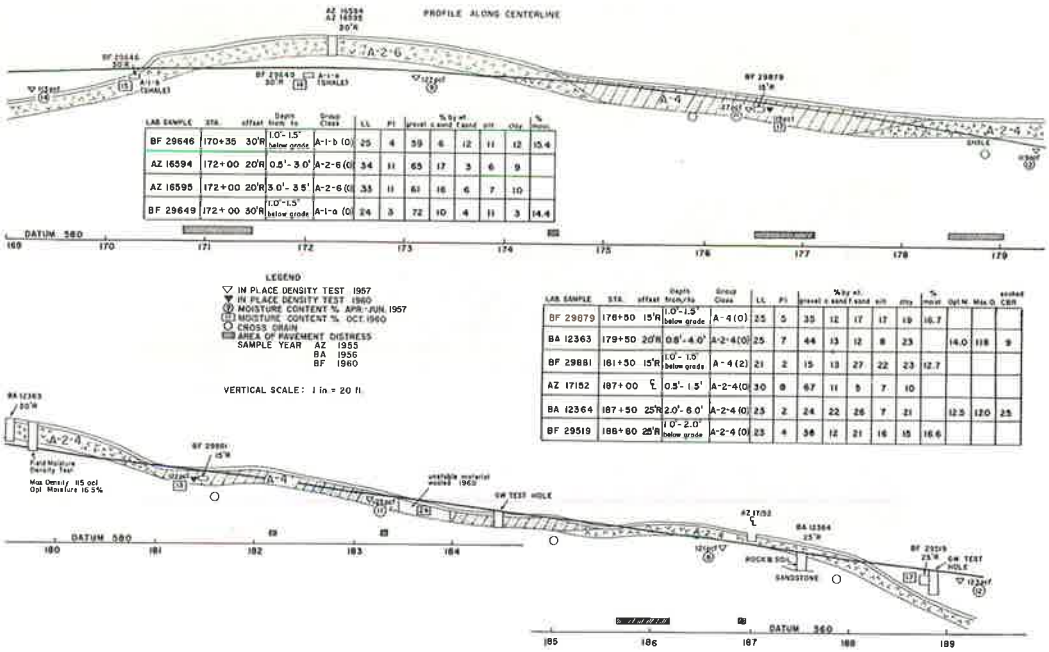

Figure 7. Soil survey, Hamburg project, stations 169 to 189.

TABLE 6

SAND CONE DENSITY TESTS ON SUBGRADE

Date	Station	Actual Density (pcf)	Percent Compaction Based on 117 pcf
May 1957	169 + 20	112.8	96.4
	173 + 06	127.0	108.5
	176 + 50	126.9	108.5
	179 + 40	118.8	101.5
	183 + 20	123.4	105.5
	186 + 72	120.9	103.3
	189 + 10	108.1	92.4[a]
	189 + 10	123.0	105.1
Oct. 1960	176 + 50	118.5	101.0
	181 + 50	121.8	104.0

[a] Rerolled; see following test.

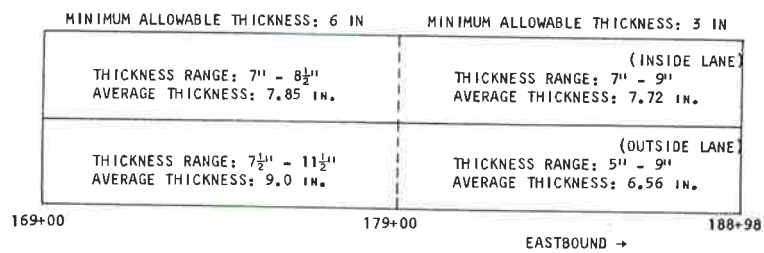

Figure 8. Thickness measurements of subbase.

TABLE 7

TESTS ON SUBBASE SAMPLES[a], 1960

Station	LL (%)	PI (%)	Aggr. (%)	C. Sand (%)	F. Sand (%)	Silt (%)	Clay (%)	Moist (%)	Remarks
170 + 35	23	3	73	10	5	7	5	9.4	Upper 3½ in. of 6½-in. thick subbase meets spec. gradation B
170 + 35	24	3	79	8	3	8	2	8.4	Lower 3 in. of 6½-in. thick subbase meets spec. gradation B
172 + 00	24	4	76	9	3	7	5	9.3	Meets spec. gradation B
176 + 50	23	2	62	16	5	10	7	9.2	Fails to meet specifications, excessive fines
181 + 50	23	3	68	11	5	10	6	11.1	Fails to meet specifications, excessive fines
188 + 80	22	2	72	13	5	7	3	7.3	Meets spec. gradation A

[a]Of 15 samples taken from source at time of construction, 12 met subbase specifications (2 samples contained 16 percent passing No. 200 sieve and 1 sample had plasticity index of 7 percent). Permeability test of a blend of samples listed showed a low permeability: 4.3×10^{-4} cm per sec at 20 C.

TABLE 8

SUBBASE GRADATIONS AT CONSTRUCTION-1957

Property	Average Gradation (%)	Specification Limits (%)	
		Gradation A	Gradation B
Sieve Size:			
3-in.		100	
2½-in.	100	-	100
1½-in.	95	40-90	-
¾-in.	74	-	40-90
No. 4	37	-	-
No. 10	25	15-50	15-70
No. 40	13	-	-
No. 200	9	0-15	0-15
LL	22	30[a]	30[a]
PI	3	6[a]	6[a]

[a]Maximum material passing No. 40 sieve.

excess of minus 200 material, and one with a plasticity index in excess by 1). Excessive amounts of shale were noted in two of the original samples. Generally, most of the original subbase samples met gradation B. The average PI for the 15 samples was 3 and the average percent of minus 200 was 9.6. The gradations made after three years of service, shown in Table 7, show no increase in the plasticity index but the average percent of minus 200 material is 13.5. This increase of 4 percent in the subbase in the failed section could be due to (a) finer subbase used in the failed section, (b) a gain of fines as a result of the use of screenings on the surface, (c) disintegration of "shaley" sand while in service, or (d) degradation of the subbase due to compaction.

The subbase thickness is quite variable and is in excess by a considerable amount from the minimum called for in the contract. The proposal called for 1,000 ft with a minimum subbase depth of 6 in. from station 169 + 00 to 179 + 00 and 1,000 ft with a minimum depth of 3 in. from station 179 + 00 to 189 + 00. The extensive irregularities in subbase depth as shown in Figure 8 could be expected to result in differential densification and nonuniformity, all of which is aggravated by traffic compaction.

Compaction figures for the subbase indicate possibly less compaction for the failed section. The sand cone apparatus, however, is not very satisfactory for so granular a material; therefore, the results are questionable. On the basis of 133 pcf as 100 percent AASHO T-99 density, four tests taken at the time of construction on the failed section showed an average of 78.5 percent compaction (range of 69 to 89 percent). In contrast, 34 other tests on the subbase of the eastbound lane showed an average of 88

percent, with only six below 78.5 percent. This indicates a possibility of less compaction for the failed stretch, providing a consistent testing method was used.

At the time of this investigation, the subbase contained a considerable amount of free water, especially in the bottom 2 or 3 in. The average moisture content was a high 9.1 percent.

Intrusion of the subgrade into the subbase does not appear to have occurred. Pumping does seem to have been a problem for this failed section, especially at station 176 + 50 where silt had intruded into the bituminous patching material. Frost heaving effects were not evaluated by the research unit but the subbase contained sufficient fines and enough moisture to have heaved.

Subgrade

The entire length of the failed section is in a shallow cut. The overburden is shallow (approximately 3 ft in thickness) and is derived from the steeply-dipping underlying Martinsburg shale which is somewhat sandy in this area. The original soil profile showed A-2-6 soil through most of the failed section with A-2-4 soil present at the eastern end. Later investigation showed the A-2-4 soil to be of greater extent with A-4 soil at the surface. CBR tests of the A-2-4 subgrade showed the stability of this material to be fair to excellent.

Eight density tests were taken in the cut section with the sand cone density apparatus at the time of construction. An average density of 117 pcf was taken as 100 percent AASHO T-99 density. The results of these tests are shown in Table 6. They indicate that satisfactory compaction was obtained for the upper part of the subgrade. Two density checks made in October 1960 indicate that satisfactory density is still present; however, at station 176 + 50, an 8-pcf loss indicates that some softening had taken place at this location.

Three moisture-density tests taken on the eastbound lane in the failed section at station 179 + 50 and 187 + 50 showed an optimum moisture average of 14.3 percent and a maximum density of 115 to 120 pcf. Moisture contents from the sand cone tests taken in April and May 1957 averaged 11.0 percent for the subgrade. The moisture determinations taken at the time of this investigation showed an average moisture content of 15.1 percent. At station 176 + 50, the upper part of the subgrade showed a gain of 6 percent in moisture. At stations 183 + 50 to 184 + 00, where the moisture content was 24 percent, the subgrade was wasted to a depth of $2\frac{1}{2}$ ft before the present reconstruction.

Fine grade material appears to be A-4 material which could be frost susceptible. The soil survey indicates that not much thickness of this material should have been used. It may have been used in the vicinity of stations 181 + 00 to 181 + 50 and 183 + 50 to 184 + 50.

Drainage

The longitudinal drain was placed at a depth of 3 to 4 ft below grade in shale, generally running below the center of the shoulder. After three years in service, the drain pipe, when ripped up, showed no staining from water or sediment in the pipe. The high moisture content in the subbase would indicate that this drain was not functioning for the following possible reasons: (a) irregularities of the bottom surface of the subbase causing ponding of the water, and (b) cutting off the access of the water to the longitudinal drain as a result of redressing the shoulders. The free water allowed to stand in the subbase could definitely contribute to pumping, excessive frost heave and softening of the subgrade at station 176 + 50.

Cross-drainage pipes (five for the failed section) have kept the side ditches from filling with water or sediment as intended. However, with the strike of the Martinsburg shale paralleling the roadway in this section and the rock dipping very steeply to the south, transverse movement of water in the rock subgrade would be difficult. Therefore, it is quite possible that water could be ponded in the soil subgrade at its contact with the upper irregular surface of the rock. Two shallow ground water holes as shown on the soil profile failed to locate the ground-water table.

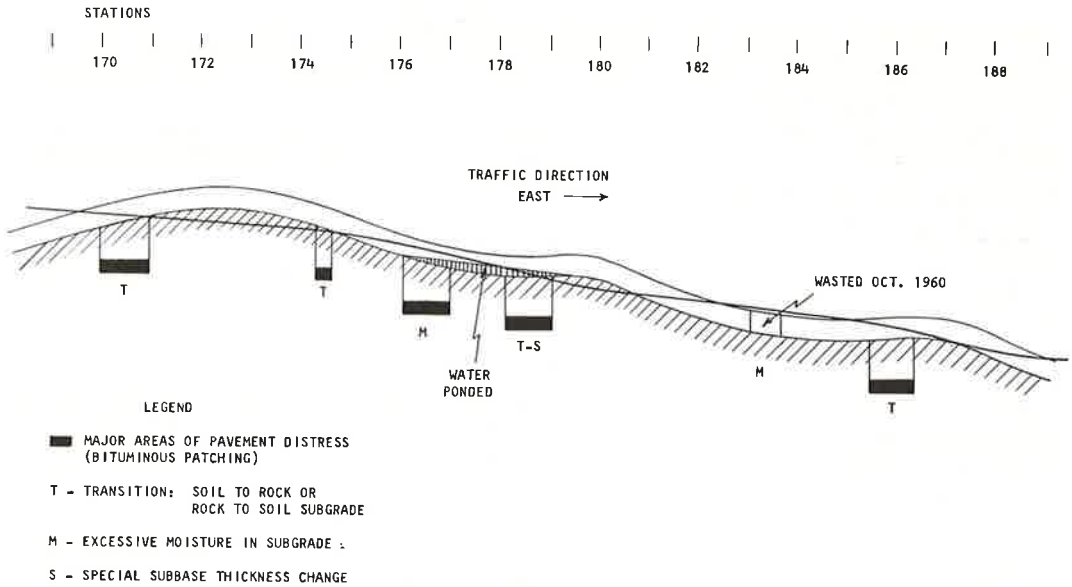

Figure 9. Failed section showing major areas of pavement distress.

SUMMARY OF SOIL INVESTIGATION

The grade line skirts along the original ground line making deeper cuts through three knobs (station 171 + 00 to 174 + 00, 178 + 50 to 181 + 00, and 186 + 00 to 188 + 00) into rock. This causes a non-uniformity of bearing of the subgrade as shown in Figure 9. The transition of soil to rock in the western flank of each knob is an area of pavement distress. At the transition of rock to soil coming out of a 7-ft cut at station 174 + 50, pavement failure was also present. At station 178 + 50 to 179 +00, the abrupt change in the subgrade is also in the area of the thickness change of the subbase, possibly further aggravating the non-uniform bearing condition.

In between the three knobs are two pockets of the natural soil derived from the Martinsburg formation below. Where this soil overburden is at its greatest depth below grade (stations 176 + 50 to 177 + 20 and 183 + 50 to 184 + 00) and where surface rolling would have the least effect at depth, unstable conditions exist in the subgrade. This is caused by excessive moisture with a resulting softening of the subgrade.

Compaction control was adequate and the type of subgrade was not poor, but the nonuniformity of the subgrade bearing was too great for the bridging action of the 7-in. pavement. This condition, aggravated by the overlap problem plus repeated application of heavy axle loads, was undoubtedly the cause of failure. If the grade line had either been lower or higher with a more uniform subgrade present, and drainage had functioned properly, it is believed that a well-constructed roadway of 7-in. continuously-reinforced pavement would not have failed at this location.

RECOMMENDATIONS

The current status of the two continuous pavements in Pennsylvania is that one project is performing as a normal member of the continuous pavement family, but there is also a problem pavement. From this situation, however, the department has learned how to repair crack failures satisfactorily and has obtained much valuable information concerning the design of continuously-reinforced pavements.

If the construction of another continuous pavement were to be considered, the following elements of design would probably be required:

1. A 6-in., well-compacted subbase.

2. A pavement depth of 9 in., certainly no less than 8 in.
3. Reinforcing bars of 20- to 30-ft lengths, set on chairs, staggered, and overlapped a minimum of 18 in. (for No. 5 bars) or alternate designs of prefabricated bar mats or welded wire fabric with adequate lap specified.
4. Reinforcing steel designed at 0.6 percent unless a steel with increased yield strength is employed. (The 0.5 percent at York was apparently satisfactory because of the lower temperature during time of construction.)
5. The use of inexpensive expansion joints at the ends of the pavement with the possible addition of foundation keys or built-in friction.

There is no assurance that this will be a perfect pavement, but it does embody the best design based on present knowledge.

ACKNOWLEDGMENT

The authors wish to acknowledge the assistance of the Material Bureau's soil engineering department and particularly the work of W. G. Wigginton, who was responsible for the soil investigation and supplied much of the data presented in that connection.

REFERENCES

1. Witkoski, F. C., and Shaffer, R. K., "Continuously-Reinforced Concrete Pavements in Pennsylvania." HRB Bull. 214, 80-97 (1959).
2. Witkoski, F. C., and Shaffer, R. K., "Continuously-Reinforced Concrete Pavements in Pennsylvania." HRB Bull. 238, 1-19 (1960).
3. Taylor, I. J., Liebig, J. O., Jr., and Eney, W. J., "Experimental Pavement on U. S. Route 22 in Berks County, Pennsylvania." Lehigh University Fritz Engineering Laboratory Report 256.9 (1962).
4. Taylor, I. J., "Experimental Pavement on U. S. Route 111 in York County, Pennsylvania." Lehigh University Fritz Engineering Laboratory Report 256.11 (1962).
5. Taylor, I. J., "Supplemental Report on the Hamburg Paving Project." Lehigh University Fritz Engineering Laboratory Report 256.13 (1962).

Maryland's Two Continuously-Reinforced Concrete Pavements—A Progress Report

ALLAN LEE, Chief, Research Section, Maryland State Roads Commission

• IN RECENT YEARS the Maryland State Roads Commission has constructed two highway projects using continuously-reinforced concrete paving. Both of these projects are located along the Baltimore-Harrisburg Expressway. This expressway is part of the Interstate System, Route I-83, and in Maryland extends from the Baltimore Beltway, just north of the Baltimore City line, northward to the Pennsylvania line.

The first of these projects was constructed under contract B-578-31, and its pavement slabs were placed during June and July 1959. Paving occupies both the northbound and southbound roadways of this divided highway. Northbound and southbound roadways terminate at a common northern point, but the southbound roadway extends farther to the south than the northbound roadway. Total length of southbound roadway including bridges, control section, etc., is about 4.1 mi, whereas the length of the northbound roadway is about 2.6 mi. This project extends from the vicinity of the town of Hereford northward to the vicinity of the town of Parkton (Fig. 1). Its northern terminal is about 20 mi north of the Baltimore City line.

The second project was built under contract B-578-53. It occupies the southbound roadway only of the Baltimore-Harrisburg Expressway. Its northern terminal directly joins the southern limits of paving of the southbound roadway of contract B-578-31. The south limit of this project is near the Shawan Road Interchange (Fig. 2). The length of the project including structures, control section, etc., is about 6.8 mi. All of the paving for this project was placed between late September and mid-October 1960.

Subsequently in this report, the first job is referred to as Project 31, and the second one as Project 53.

A report covering materials, design, construction, and early test observations for Project 31 was presented by the writer at the January 1961 meeting of Highway Research Board, and is included in the Proceedings of the 40th Annual Meeting.

BASIC FACTORS

Complete details of the experimental features of Project 31 were presented in the report mentioned. A brief review of these features follows.

Nine sections of continuously-reinforced pavement, varying in length from 1,800 to 4,150 ft, are included in the project. In the southbound roadway three sections were joined together with continuous longitudinal steel for a total length of 9,750 ft. Two lengths of conventional jointed pavement are included as control sections, 1,900 ft long in the southbound roadway and 2,850 ft long in the northbound roadway.

The continuously-reinforced pavement is 8 in. thick, founded on a granular-type subbase of 6-in. minimum thickness. In "normal sections" the subbase extends entirely under the shoulder and drains into the surface drain ditch. In "superelevated sections" it drains into a longitudinal underdrain placed along the low side at least 1 ft outside of the edge of the concrete pavement.

The control sections are 9-in. thick, jointed at 40-ft centers, and founded on a granular subbase of the same thickness and details as noted.

Paper sponsored by Committee on Rigid Pavement Design.

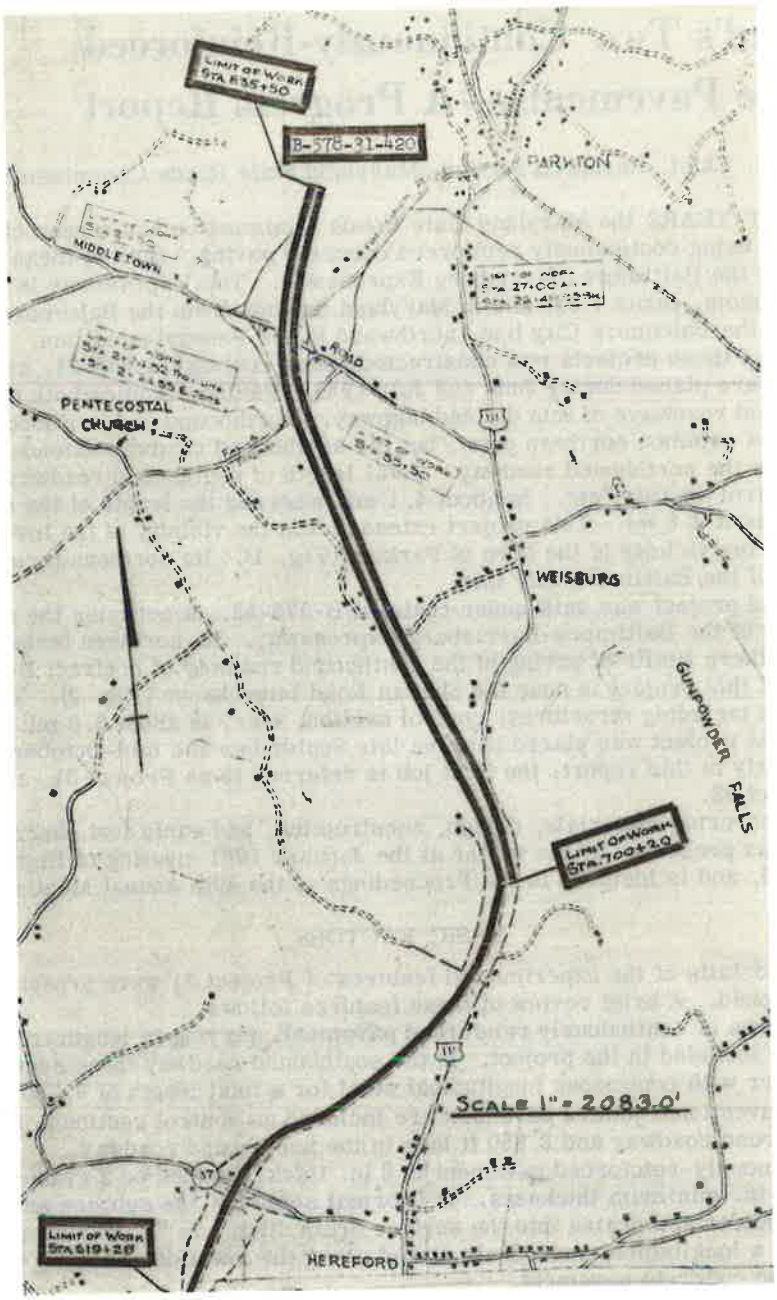

Figure 1. General location of experimental continuously-reinforced concrete pavement, Project 31.

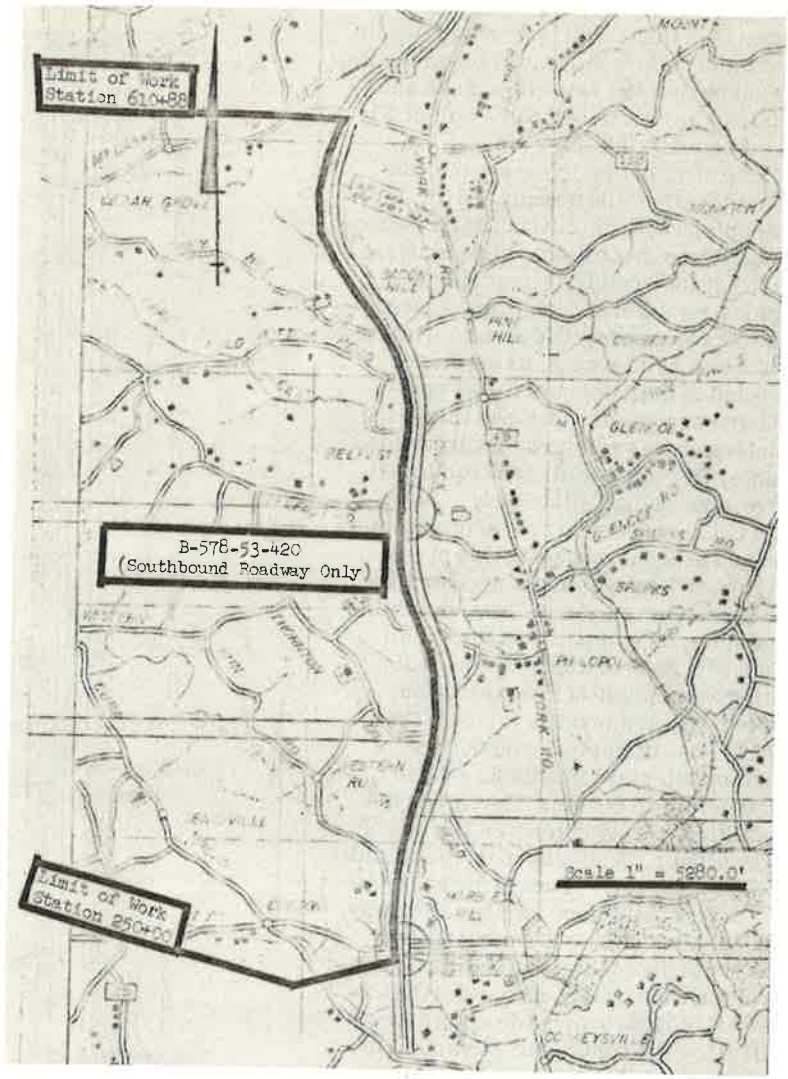

Figure 2. General location of experimental continuously-reinforced concrete pavement, Project 53.

The reinforcing in the continuously-reinforced sections consists of bar mats, and is varied both as to size of bar and percentage of steel. Number 5 bars were placed in percentages of 0.5, 0.6, and 0.7, whereas in several sections the percentage of steel was held at 0.5 but bar sizes were varied between No. 4, No. 5, and No. 6.

Three types of terminal joints were used at the ends of the continuously-reinforced sections of pavement. One type was the Goodrich rubber joint of 9 cells; another a fabricated steel plate type; and the third a "bituminous" type consisting of steel angles armoring the slab ends, and the open joint between slabs filled with a bituminous and cork mixture.

The location of test sites, steel percentages, etc., for Project 31 are shown in Figure 3.

Project 53 contains only a nominal program of experimental features. The continuously-reinforced pavement sections on this project are also 8-in. thick, varying

in length from about 3,700 to 6,500 ft, except for one short section less than 600 ft long which ties into existing pavement at the south end of the project.

A granular subbase of the same thickness and lateral dimensions as described for Project 31 also was placed beneath this pavement.

A 2,000-ft long control section using the conventional jointed construction was placed for performance comparison with the continuously-reinforced sections. It was made 9-in. thick and was provided with the granula subbase described.

The continuously-reinforced sections of pavement on this project were provided almost in their entirety with bar mat reinforcing, using No. 5 bars at 0.6 percent of the pavement cross-sectional area. There was one exception to this—a 2,000-ft subsection was reinforced with welded wire fabric mats. Percentage of steel remained at 0.6, the wire size being 6/0.

Three different arrangements of terminal jointing were also used in connection with this project. The Goodrich rubber joint was again used on this project, but in somewhat smaller size, consisting of a 6-cell assembly, as compared to the 9-cell used for Project 31. A second arrangement of terminal jointing was the use of a series of four ordinary doweled type transverse joints. The dowels were of $1\frac{1}{4}$-in. diameter, and the preformed expansion material 1 in. thick. These joints were 20 ft center to center. The third type of terminal jointing was suggested by a Bureau of Public Roads' engineer. A subslab 6 in. thick and 10 ft long was placed directly beneath the roadway slab. A 10-in. deep wide-flange steel section was embedded 2 in. into this subslab, so that its top flange was flush with the roadway surface. The inside contours of the wide-flange shape and the top of the subslab were coated to provide a positive joint which will allow the continuous pavement to withdraw from the steel shape. Details of this type of joint are shown in Figure 4.

Three 12- by 12-in. lugs cast integrally with the pavement slab were used at several terminals of continuously-reinforced concrete sections in an effort to eliminate or reduce end movements. Figure 5 shows the details of these lugs. The location of continuously-reinforced sections, control section, terminal joints, etc., is shown in Figure 6.

It was previously noted that Project 31 paving was placed during June and July of 1959, and that for Project 53 was placed between late September and mid-October 1960. It does not seem necessary to present a detailed daily temperature log in this progress report, but some general differences in temperature for the two periods should be mentioned. During the paving period for Project 31 extreme variations occurred. A very cool period occurred during June, whereas in July high sum-

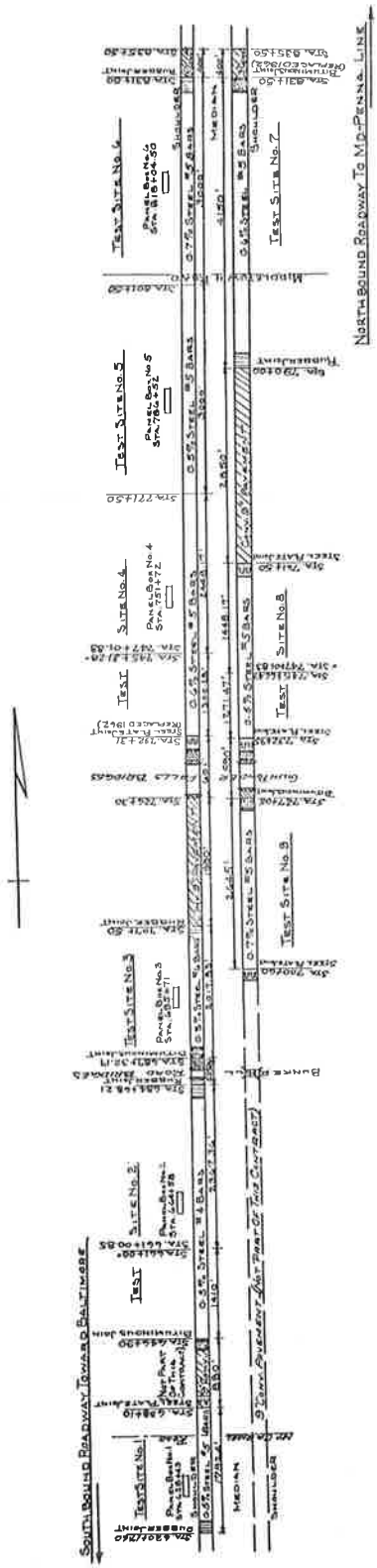

Figure 3. Location of experimental features, Project 31.

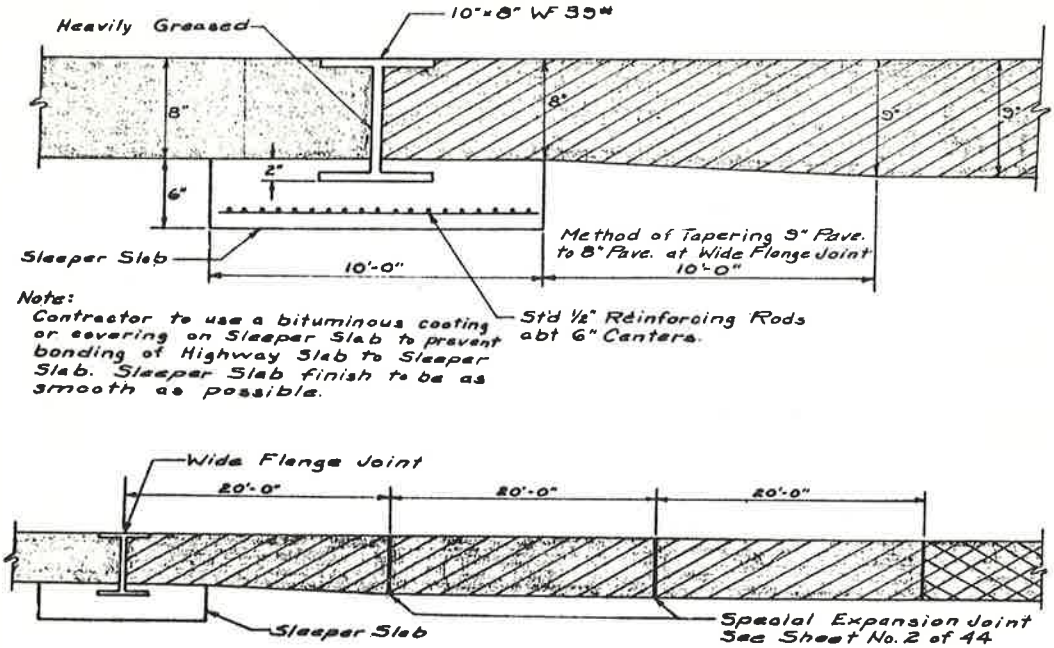

Figure 4. Wide-flange joint detail (not to scale).

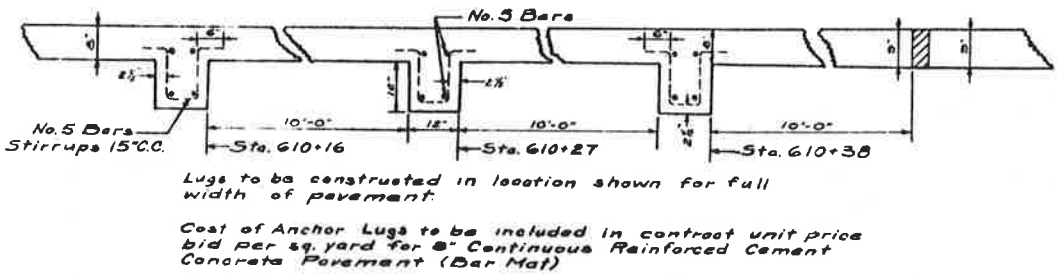

Figure 5. Details of 12- by 12-in. reinforced concrete anchor restraining lugs (not to scale).

mer temperatures, high winds, and low humidities were experienced. On the other hand, Project 53 was paved during a period of what might be described as ideal Fall weather. Very little variation in temperature occurred at any period during the paving and there was even very little variation between day and night temperatures.

It is well to emphasize some variations in design and construction between the two jobs. Project 31 used only 20 diameters lap for the bar mats. There was no attempt to stagger the ends of the mats. Only one paver was used. It placed the first lift of concrete for about 80 ft, then backed up, and placed the second lift after the steel was in place. The only vibration consisted of two internal vibrators along the inside faces of the steel forms.

For Project 53 the length of splice for bar mats was increased to 25 diameters. (The lap for the welded wire mats was in accordance with recommendations of the proponents of this material. The end transverse wire in one mat was placed in the same vertical plane as the adjoining mat.) Two pavers were used, and the complete width of the two separate lifts of concrete was thoroughly vibrated, using internal vibrators. A stagger of 2 ft was provided at the ends of adjacent mats.

TRAFFIC DATA

Very heavy interstate trucking has developed along this expressway. The Traffic Bureau of this Commission provides an annual report of axle loads of various magnitudes using the facility. This report is developed in conjunction with the Traffic Bureau's loadometer study. The latest study was made for a 24-hr period on July 17, 1962. During that period the total traffic was 6,434 vehicles, 1,993 of them being commercial vehicles, and 4,441 being passenger cars. The axle frequency weight distribution is given in Table 1.

CRACK PATTERNS

The January 1961 report stated that detailed crack surveys were made in the central 500-ft region of each of the continuously-reinforced sections of Project 31. A crack survey along similar lines has been carried out for Project 53. The cracks in the central 500 ft of sites 1, 2, 3, 5, and 6 have been recorded. Site 4 was subdesignated 4-BM and 4-WWF due to the fact that both bar mat and welded wire fabric reinforcing were used. The crack survey in this length of continuously-reinforced pavement covers 600 ft, about 300 ft in each of the bar mat and wire fabric reinforced areas. In addition, detailed crack surveys for 250 ft at each end of site 1 have been recorded. This was intended to ascertain any difference in crack spacing and patterns between the north end equipped with integral lugs, and the south end which did not have them. The short length of continuously-reinforced pavement south of Shawan Road Bridge has not been observed in detail for crack spacing.

The January 1961 report further explained that a crack is counted if it extends at least three-fourths of the distance between pavement edges; and also, if two closely spaced transverse cracks join to extend entirely across the pavement.

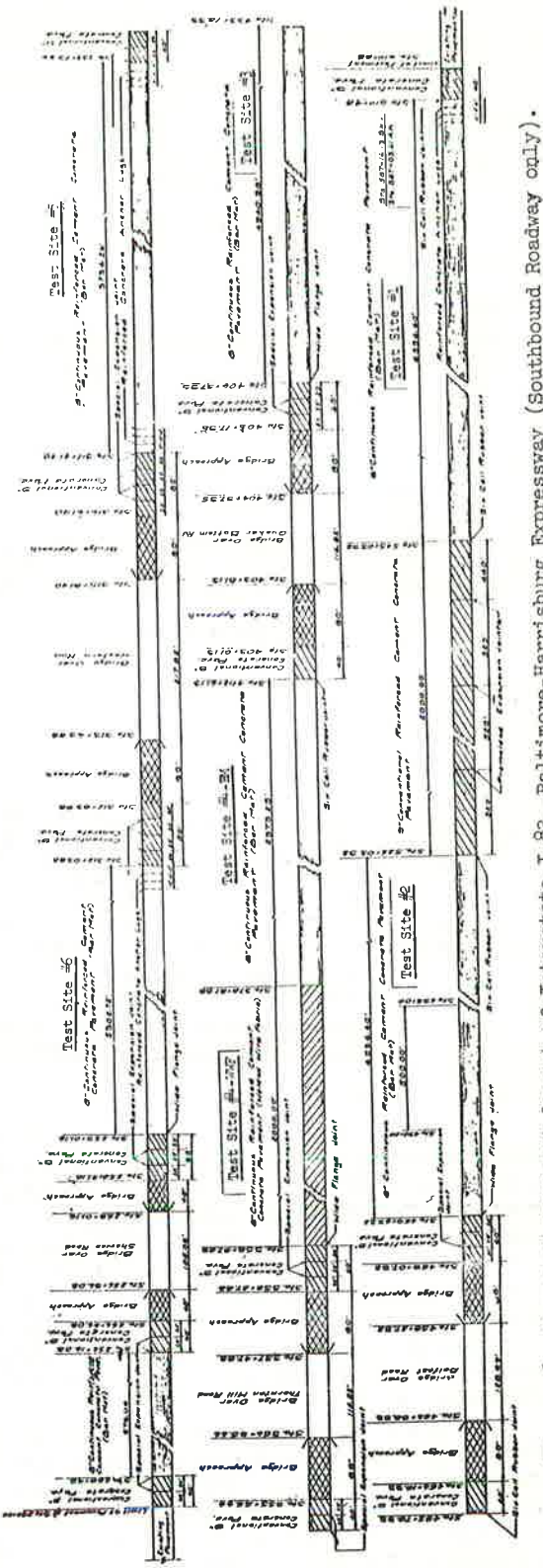

Figure 6. Proposed pavement layout of Interstate I-83—Baltimore-Harrisburg Expressway (Southbound Roadway only).

TABLE 1

AXLE FREQUENCY WEIGHT DISTRIBUTION ALL LOADED AND EMPTY COMMERCIAL VEHICLES BALTIMORE-HARRISBURG EXPRESSWAY INTERSTATE 83 NORTH OF MT. CARMEL RD.[a]

Axle Weight (lb)	Number of Vehicle Axles							
	Panel Pick-ups	Single-Unit Trucks			Tractor Semitrailer			Total
		2-Axle		3-Axle Dual-Tired	2-Axle Tractor		3-Axle Tractor	
		Single-Tired	Dual-Tired		1-Axle Trailer	2-Axle Trailer	3-Axle Trailer	
Under 8,000	588	92	516	45	193	1,434	34	2,902
8,000 - 8,499	-	-	47	-	45	331	3	426
8,500 - 8,999	-	-	7	4	14	172	11	208
9,000 - 9,499	-	-	11	-	20	181	-	212
9,500 - 9,999	-	-	7	-	11	97	-	115
10,000 - 10,999	-	-	29	4	37	172	11	253
11,000 - 11,999	-	-	7	4	14	88	3	116
12,000 - 12,999	-	-	18	14	17	163	6	218
13,000 - 13,999	-	-	18	5	40	159	11	233
14,000 - 14,999	-	-	4	-	25	203	22	254
15,000 - 15,999	-	-	4	5	25	225	8	267
16,000 - 16,999	-	-	7	-	8	305	8	328
17,000 - 17,999	-	-	15	-	6	216	3	240
18,000 - 18,999	-	-	-	-	3	208	-	211
19,000 - 19,999	-	-	-	-	3	79	3	85
20,000 - 21,999	-	-	7	-	20	115	8	150
22,000 - 23,999	-	-	7	-	11	141	3	162
24,000 - 25,999	-	-	-	-	-	35	6	41
26,000 - 27,999	-	-	-	-	-	4	-	4
Projected axles	588	92	704	81	492	4,328	140	6,425
Vehicles counted	294	46	352	27	164	1,082	28	1,993
Vehicles weighed	19	19	97	6	58	245	10	454

[a]24-hour period, Tuesday, July 17, 1962, with 1,993 commercial vehicles, 4,441 passenger cars, and 6,434 total traffic.

Table 2 has been prepared to present some information on transverse crack spacing for the projects. The data contained in this table leads to the following observations:

1. Practically no cracks occurred in Project 31 during the third year of pavement life.
2. At the end of three years, the crack spacing in the comparative sections of Project 31 reinforced with 0.5, 0.6, and 0.7 percent longitudinal steel averaged 6.3, 4.8, and 3.5 ft, respectively.
3. At the end of three years, the crack spacing in the comparative sections of Project 31 reinforced with 0.5 percent longitudinal steel consisting of Nos. 4, 5, and 6 bars averaged 5.8, 6.5, and 7 ft, respectively.
4. At the end of two years, the over-all average crack spacing for all sections of Project 31 reinforced with 0.6 percent steel consisting of No. 5 bars was about the same as that for all comparable sections of Project 53.
5. The integral concrete lugs in Project 53 had little effect on crack spacing normal to a free end area.

CRACK WIDTHS

The January 1961 report described a comprehensive program of crack width measurements taken at the pavement surface along Project 31. These measurements were in central areas, in areas near free ends, and in areas following transverse construction joints, for each of the nine continuously-reinforced sections.

A limited program of crack width measurements has been carried on for Project 53. In the portion of section 4 reinforced with bar mats (4-BM) an area near the transition point to wire fabric reinforcing was recorded. Also crack widths in an end area, and following a transverse construction joint were recorded for this 4-BM section. In the wire fabric-reinforced length (4-WWF) crack width measurements were recorded near the free end, and in the area close to the transition point to bar mat reinforcing.

Observed crack width measurements are given in Table 3. The portion of the table pertaining to Project 31 includes only those observations made after September 1960, as this date and all previous observations were included in the January 1961 report. The measurements for cracks in Project 53 are all which have been made so far—February and August of 1961, and March and September of 1962.

From the data in Table 3, a brief analysis of the crack widths recorded in 1962 for Project 31 follows:

1. During the March 1962 readings, the average measured crack widths in the central 500-ft areas ranged from 0.0100 to 0.0260 in.
2. A total of 36 cracks in the central 500-ft areas of the nine test sections (four in each section) have been observed for surface width during the life of this pavement. Thirty-two of them (about 90 percent) exhibited a width of less than 0.03 in. during the March 1962 readings.
3. A comparison of all recorded crack widths, in the central 500-ft areas, for the several steel percentages, observed during the March 1962 and September 1962 readings is given in Table 4.
4. The average widths of all cracks in the several "areas" or "zones" selected for observation, were of the following magnitudes during the March 1962 readings: in the central 500-ft areas, 0.0183 in.; in the end areas 500 ft ± from a free end, 0.0153 in. in areas following a transverse construction joint, 0.0173 in.

FAILURES AND POSSIBLE CAUSES

The January 1961 report in connection with Project 31 emphasized the extreme care with which this project was built, and the excellent cooperation of the contractor knowing that it was an experimental project. Despite these efforts toward excellent construction, a number of failures have developed in Project 31. Before the project was opened to traffic, a crack of such magnitude occurred in one area that it was deemed advisable to have it repaired by the contractor before he left the job. Subsequently, a number of additional cracks about which it was felt that it was unwise to leave were

TABLE 2

CRACK SPACING, CENTRAL 500 FT OF EACH SECTION

Project	Location	Reinforcing		Approx. Age (mo)	Avg. Crack Spacing (ft)
		Percent	Bar No.		
31	Site 1	0.5	5	12	7.25
				15	7.14
				27	6.50
				39	6.50
	Site 2	0.5	4	12	6.33
				15	6.17
				27	5.81
				39	5.81
	Site 3	0.5	6	12	7.46
				15	7.35
				27	6.95
				39	6.95
	Site 4	0.6	5	12	5.00
				15	5.00
				27	4.71
				39	4.71
	Site 5	0.5	5	12	7.25
				15	7.25
				27	7.14
				39	7.14
	Site 6	0.7	5	12	3.97
				15	3.85
				27	3.43
				39	3.31
	Site 7	0.6	5	12	5.21
				15	5.15
				27	4.80
				39	4.80
	Site 8	0.5	5	12	5.90
				15	5.78
				27	5.37
				39	5.37
	Site 9	0.7	5	12	4.00
				15	3.93
				27	3.67
53	Site 1:			39	3.67
	N[a]	0.6	5	7	12.50
				13	11.35
				24	11.35
	C[b]			7	3.50
				13	3.18
				24	3.14
	S[c]			7	11.35
				13	10.85
				24	10.00
	Site 2	0.6	5	7	4.62
				13	4.46
				24	4.46
	Site 3	0.6	5	7	6.50
				13	6.18
				24	6.10
	Site 4:				
	BM[d]	0.6	5	7	5.20
				13	4.95
				24	4.80
	WWF[e]	0.6	-[f]	7	13.45
				13	11.30[g]
				24	10.88
	Site 5	0.6	5	7	4.39
				13	4.35
				24	4.35
	Site 6	0.6	5	7	7.25
				13	7.14
				24	7.14

[a] 250 ft at north end where lugs were provided.
[b] 500 ft at center.
[c] 250 ft at south end, no lugs.
[d] 317 ft near center, reinforced with bar mats.
[e] 283 ft near center, reinforced with welded wire fabric.
[f] 6/0 wires.
[g] Wide crack spacing in Site 4-WWF probably due to occurrence of several major transverse cracks which, in effect, broke area down into several short lengths of continuously-reinforced pavement.

TABLE 3

OBSERVED CRACK WIDTHS

Project	Section No.	Central 500-Ft Area					End Area 500 Ft ± from Free End					Following Transverse Construction Joint				
		Station	Crack Width (in.)				Station	Crack Width (in.)				Station	Crack Width (in.)			
			Feb. 1961	Sept. 1961	March 1962	Sept. 1962		Feb. 1961	Sept. 1961	March 1962	Sept. 1962		Feb. 1961	Sept. 1961	March 1962	Sept. 1962
31[a]	1	627+10	0.0172	0.0207	0.0220	0.0256	632+99	0.0161	0.0155	0.0197	0.0188	624+11	0.0215	0.0212	0.0304	0.0262
		+30	0.0182	0.0216	0.0255	0.0294	633+07	0.0155	0.0160	0.0195	0.0268	+20	0.0435	0.0502	0.0565	0.0600
		+49	0.0238	0.0122	0.0313	0.0217	+18	0.0189	0.0189	0.0243	0.0244	+39	0.0208	0.0248	0.0272	0.0244
		+64	0.0125	0.0145	0.0161	0.0176	+35	0.0083	0.0215	0.0147	0.0188	+77	0.0190	0.0228	0.0230	0.0196
	2	666+35	0.0204	0.0175	0.0228	0.0218	678+99	0.0227	0.0217	0.0245	0.0200	660+06	0.0153	0.0144	0.0203	0.0190
		+48	0.0254	0.0264	0.0295	0.0287	679+08	0.0148	0.0146	0.0184	0.0176	+19	0.0116	0.0109	0.0152	0.0174
		+61	0.0126	0.0099	0.0118	0.0126	+15	0.0264	0.0227	0.0287	0.0248	+30	0.0136	0.0107	0.0156	0.0118
		+98	0.0238	0.0245	0.0281	0.0260	+21	0.0235	0.0230	0.0265	0.0262	+38	0.0085	0.0081	0.0133	0.0177
	3	693+48	0.0138	0.0156	0.0186	0.0193	702+18	0.0205	0.0159	0.0222	0.0198	699+38	0.0133	0.0127	0.0165	0.0127
		+66	0.0126	--[b]	0.0158	0.0048	+39	0.0193	0.0163	0.0214	0.0153	+41	0.0105	0.0034	0.0097	0.0100
		+82	0.0548	0.0183	0.0555	0.0274	+50	0.0259	0.0035	0.0169	--[c]	+43	0.0236	0.0200	0.0296	0.0284
		694+08	0.0102	--[b]	0.0140	0.0080	+60	0.0130	0.0102	0.0195	0.0176	+80	0.0272	0.0250	0.0302	0.0279
	4	749+01	0.0217	0.0201	0.0217	0.0210	739+01	0.0068	0.0040	0.0084	0.0090	755+51	0.0174	0.0115	0.0129	0.0160
		+06	0.0213	0.0056	0.0094	0.0138	+21	0.0231	0.0086	0.0129	0.0161	+57	0.0128	0.0101	0.0103	0.0167
		+33	0.0092	0.0038	0.0074	0.0108	+28	0.0136	0.0036	0.0055	0.0045	+62	0.0102	0.0072	0.0152	0.0084
		+51	0.0204	0.0163	0.0189	0.0198	+35	0.0148	0.0047	0.0091	0.0143	+72	0.0276	0.0149	0.0189	0.0152
	5[d]	782+75	0.0305	0.0365	0.0445	0.0432						797+76	0.0181	0.0100	0.0127	0.0074
		+82	0.0157	0.0086	0.0123	0.0122						798+15	0.0196	0.0098	0.0126	0.0116
		+92	0.0201	0.0131	0.0184	0.0148						+30	0.0334	0.0211	0.0241	0.0311
		783+04	0.0146	0.0088	0.0159	0.0974						+42	0.0474	0.0100	0.0242	0.0160
	6	812+63	0.0069	0.0029	0.0055	0.0051	826+27	0.0231	0.0133	0.0180	0.0144					
		+93	0.0165	0.0083	0.0124	0.0110	+37	0.0028	0.0023	0.0044	0.0093					
		813+28	0.0134	0.0083	0.0103	0.0101	+79	0.0171	0.0139	0.0147	0.0195					
		+44	0.0223	0.0113	0.0118	0.0138	827+61	0.0202	0.0144	0.0162	0.0255					
	7	808+08	0.0208	0.0078	0.0129	0.0103	825+81	0.0155	0.0109	0.0128	0.0158	799+94	0.0199	0.0105	0.0052	0.0053
		+30	0.0094	0.0047	0.0091	0.0060	+93	0.0241	0.0095	0.0122	0.0092	800+05	0.0202	0.0141	0.0193	0.0169
		+44	0.0178	0.0111	0.0157	0.0113	826+31	0.0107	0.0072	0.0076	0.0106	+13	0.0324	0.0186	0.0228	0.0245
		+59	0.0190	0.0059	0.0097	0.0042	+76	0.0146	0.0097	0.0111	0.0084	+23	0.0217	0.0147	0.0134	0.0152
	8	747+06	0.0251	0.0131	0.0155	0.0159	739+89	0.0218	0.0104	0.0129	0.0162	760+27	0.0106	0.0071	0.0082	0.0066
		+80	0.0336	0.0190	0.0254	0.0219	740+59	0.0134	0.0086	0.0097	0.0122	+47	0.0016	--[b]	0.0013	0.0000
		748+87	0.0490	0.0258	0.0359	0.0330	+70	0.0334	0.0464	0.0312	0.0233	+53	0.0032	0.0006	0.0017	0.0052
		749+06	0.0177	0.0104	0.0132	0.0168	741+38	0.0233	0.0126	0.0166	0.0144	+56	0.0030	0.0052	0.0076	0.0052
	9	710+96	0.0207	0.0117	0.0145	0.0151	705+53	0.0096	0.0044	0.0065	0.0084	723+70	0.0179	0.0121	0.0133	0.0171
		711+40	0.0124	0.0042	0.0097	0.0060	+86	0.0098	0.0074	0.0075	0.0100	+83	0.0148	0.0126	0.0125	0.0180
		+84	0.0108	0.0047	0.0084	0.0085	706+35	0.0122	0.0075	0.0099	0.0086	724+10	0.0167	0.0079	0.0133	0.0075
		712+16	0.0115	0.0083	0.0087	0.0093	+54	0.0094	0.0019	0.0055	0.0063	+27	0.0454	--[c]	--[c]	--[c]
53[f]	4-BM	378+92	0.0250	0.0224	0.0278	0.0234	396+85	0.0200	0.0330	0.0336	0.0379	399+02	0.0650	0.0777	0.0803	0.0849
		379+07	0.0300	0.0304	0.0371	0.0374	+91	0.0200	0.0308	0.0359	0.0365	+05	0.0300	0.0310	0.0415	0.0365
		+17	0.0700	0.0685	0.0748	0.0745	397+00	0.0400	0.0581	0.0573	0.0548	+09	0.0500	0.0482	0.0533	0.0512
		+27	0.0150	0.0149	0.0208	0.0208	+21	0.0200	0.0214	0.0271	0.0273	+11	0.0300	0.0217	0.0261	0.0265
		+44	0.0040	0.0029	0.0091	0.0091	+33	0.0150	0.0159	0.0193	0.0210	+22	0.0300	0.0276	0.0311	0.0342
		+50	0.0750	0.0674	0.0694	0.0683	+45	0.0400	0.0284	0.0355	0.0296	+37	0.0350	0.0360	0.0400	0.0418
	4-WWF[g]	377+94	0.0400	0.0490	0.0495	0.0494	363+57	0.0200	0.0221	0.0226	0.0258					
		378+15	0.0100	0.0150	0.0204	0.0209	+76	0.0040	0.0005	0.0030	0.0088					
		+27	0.0080	0.0045	0.0139	0.0151	+93	0.0030	0.0011	0.0059	0.0155					
		+36	0.0350	0.0334	0.0361	0.0354	364+05	0.0100	0.0186	0.0194	0.0099					
		+57	0.0100	0.0155	0.0183	0.0189	+27	0.0050	0.0023	0.0207	0.0055					
		+71	0.0140	0.0160	0.0247	0.0234	+63	0.0070	0.0073	0.0173	0.0090					

[a] Averages:

Section	Crack Width (in.) March 1962	Sept. 1962
0.5%	0.0236	0.0249
0.6%	0.0131	0.0123
0.7%	0.0102	0.0099

[b] "Minus" width indicated, evidently instrument error.

[c] Patched area, plugs removed during repair operations.

[d] No free end in section.

[e] Data for following a transverse construction joint same as that for 500 ft from free end. Set of 4 cracks is common to end area and following construction joint.

[f] Averages:

Reinforcement	Crack Width (in.) March 1962	Sept. 1962
Bar mat	0.0398	0.0389
Wire fabric	0.0272	0.0272

[g] A transverse construction joint did not occur.

TABLE 4

CRACK WIDTHS 1962

Percent Long. Steel	Crack Width (in.) March 1962	Sept. 1962
0.5	0.0236	0.0249
0.6	0.0131	0.0123
0.7	0.0102	0.0099

repaired by cutting out sections of concrete slab, welding in new bars if necessary, recompacting the subbase, and repouring the slab.

An inspection during the latter part of October 1962 indicated a total of 39 "areas" along both roadways of Project 31 where repairs as described had been made, or were scheduled to be made within a few weeks. Twenty-six of these repaired "areas", or two-thirds of the total, occurred at laps in the bar mats. It will be remembered that bars were spliced only 20 diameters for this project. An "area" in this case is the length of patching measured longitudinally along the roadway by the width of the travel lane in which the patch occurs. The longitudinal dimensions of the patched areas varied from slightly more than 2 ft to just under 10 ft. During this inspection most of the repaired areas were in satisfactory condition.

As these areas were being repaired, samples of the concrete removed were carefully examined. It is believed that the principal cause of failure was probably a lack of bond between the two lifts of concrete pavement and between the concrete pavement and the reinforcing steel. As reported in January 1961 only one paver was used on this project. It moved ahead some 75 or 80 ft in placing the first lift, then backed up and after the steel was in place advanced to place the second lift. Concrete was of a low slump and no vibration was used except the usual two internal vibrators along the face of the steel forms. As previously mentioned, extreme temperature ranges and periods of high winds occurred during the paving of this project.

Also on Project 31 there have been some failures of terminal joints. One of these was in connection with the bituminous joint. The armoring angle on one side of a joint began to "bang" severely under the heavy truck traffic using the roadway. Attempts were made to correct this condition by drilling and plug welding to the anchors embedded in the concrete. However, this was not successful and it was found necessary to remove the top flange of the angle completely and cover the entire area with bituminous concrete. A subslab was not used under this joint and the failure was evidently due to welded anchors breaking under traffic. Also one of the fabricated plate type of terminal joints showed extreme distress under the heavy truck traffic of the highway and had to be entirely removed and the space between slabs backfilled and surfaced with bituminous concrete. This terminal joint also was not equipped with a subslab. This had been a decision made by all interested parties previous to the building of the project.

Project 53 is not as old as Project 31, but was subjected to the severe temperatures encountered in the winter of 1960-1961. In all of the areas of this project which were reinforced with No. 5 bar mats, the performance has been very good. No detrimental cracks have been found and about the only place where many closely spaced cracks seem to occur is on the last poured side of construction joints. This is the usual performance of these areas. In the 2,000-ft area reinforced with welded wire fabric, the performance was not as satisfactory. Before the pavement was opened to traffic, four very wide cracks developed and several more have subsequently formed at the splices of the welded wire fabric sheets. In the use of this type of mat it was agreed that the splice would be in accordance with the recommendations of the proponents of this material. This recommendation was that the end transverse wire of one mat be placed directly over the end transverse wire of the adjoining mat. This procedure was carefully followed, the mats were tightly wired together, and an inspector was detailed to see that this condition prevailed before concrete was placed. As soon as the four wide cracks mentioned developed, exploratory cuts were made near one pavement edge of each crack. The steel was exposed and at two of the cracks despite the precautions taken, it was found that "creep" of the mats had occurred so that there was no effect of the transverse wires, and the only bonding present was that of the plain round wires. The proponents of this material have changed their recommendations so that at present a definite overlap of the end transverse wires occurs. The areas containing these wide cracks have not so far been repaired. They have been backfilled with bituminous material. It appeared that end movements of this particular section of continuously-reinforced pavement were being taken in these wide cracks rather than at the wide-flange terminal joint which is at the end of the section.

In an attempt to confirm this assumption, eight wide cracks in this section were

plugged in March 1962. It was necessary to place them at a fairly good distance from the cracks, and they were thus out of the range of the Whittemore gage. A reading to the nearest 1/64 in. was taken and considered as a zero reading. In September 1962 readings were again taken to the nearest 1/64 in., and all cracks showed significant movements. Closures had occurred at all of the eight cracks, ranging from a minimum of 4/64 in. to a maximum of 17/64 in.

ANNUAL END MOVEMENTS OF CONTINUOUSLY-REINFORCED SLABS

Terminal Joints

The program of observations of end movements of continuously-reinforced sections has been continued. All free ends of continuous sections on Project 31 are recorded (Table 5). However, the observations for Project 53 are limited. The north end of section 1 was selected as a free end with lugs; the north end of section 4-BM and the south end of section 4-WWF were selected as ordinary free ends but with different types of terminal joints—rubber and wide flange, respectively. The south end of section 2 is also an ordinary free end, equipped with a wide-flange terminal joint. It was selected as a duplicate to the south end of section 4-WWF, because the wide cracks in this section probably affect the end movements.

Maximum lengthening in September 1962 of any free end on Project 31 was about 1 1/8 in. at the south end of section 8. The average lengthening for the 14 free ends observed on Project 31 was about 5/8 in.

In connection with Project 53, the north end of section 1 showed a considerable lengthening in September 1962, even though it had been constructed with integrally cast lugs. This lengthening averaged about 1 1/8 in. At this same period the north end of section 4-BM had lengthened about 9/16 in. from the original, and the south end of section 2 had lengthened about 5/8 in. from February 1962. The south end of section 4-WWF showed close to 1-in. lengthening measured from original, but as previously noted the adjacent area is badly cracked, which may have some effect on this particular end movement.

In general the end movements of the continuously-reinforced pavement sections are not considered excessive.

Table 6 gives records of movements across terminal joints. For Project 31 the maximum movement measured from original position was about 2 3/16 in. closure. Two of the terminal joints were removed.

In Project 53, the rubber joints observed had not moved more than 1 in. from the original, according to September 1962 readings. In connection with the series of doweled joints, observations indicate that most of the movement takes place at the first joint, directly abutting the continuously-reinforced section. For wide-flange types of joints, movements have been recorded between the center of the steel section and plugs set in the continuously-reinforced pavement, and also set in the jointed pavement on the opposite side of the steel section. The nominal distance each side of the center line of steel section was 8 in. and most readings have been with a Whittemore-type hand gage. The fractional readings were out of range of this device; this comment also applies to readings across doweled joints. Movements at wide-flange types of joints have been very small.

End Anchorages

On Project 31 there was no attempt to provide end anchorages for any of the continuously-reinforced sections.

However, several ends of continuously-reinforced sections on Project 53 were provided with integrally cast lugs to determine if they had any effect on restraining movements at these points. These lugs were placed at the north end of section 6, at the north and south ends of section 5, and at the north end of section 1.

The lugs were 12 by 12 in., directly beneath the roadway slab, and cast integrally with it. The first lug is 10 ft from the end of the continuously-reinforced section, and there is a clear distance of 10 ft between lugs. Three lugs as described were provided for each anchorage, and they were reinforced with No. 5 stirrup-type bars.

It has already been mentioned that considerable end movement occurred at the north

TABLE 5

END MOVEMENTS, CONTINUOUSLY-REINFORCED SECTIONS

Project	Section	Location	Movement[a,b] (in. × 1/64) North End				South End			
			March 1961	Aug. 1961	Feb. 1962	Sept. 1962	March 1961	Aug. 1961	Feb. 1962	Sept. 1962
31	1	Shoulder	- 8	+39	+ 6	+52	-26	+31	-28	+27
		Median	- 9	+41	+ 5	+56	-32	+23	-30	+24
	2	Shoulder	-18	+32	- 6	+45	-14	+47	- 8	+46
		Median	-18	+31	0	+49	-14	+47	- 4	+49
	3	Shoulder	-17	+16	-25	+23	-18	+20	-12	+28
		Median	-17	+24	-25	+20	-20	+16	-15	+24
	4[c]	Shoulder	--	--	--	--	- 8	+36	0	+41
		Median	--	--	--	--	-11	+32	- 6	+39
	5[d]		--	--	--	--	--	--	--	--
	6	Shoulder	- 6	+32	-10	+35	--	--	--	--
		Median	- 5	+32	-10	+36	--	--	--	--
	7	Shoulder	-22	+22	-32	+16	- 8	+43	+14	+42
		Median	-22	+30	-24	+ 9	-11	+40	+10	+40
	8	Shoulder	- 7	+44	+ 6	+49	- 8	+69	+21	+76
		Median	0	+52	0	+45	- 1	+58	+ 6	+66
	9	Shoulder	0	+43	+ 5	+56	-17	+34	+ 1	+41
		Median	0	+47	+ 4	+57	-16	+44	+ 9	+53
53	1	Shoulder	- 8	+52	+36	+77	--	--	--	--
		Median	- 9	+52	+27	+68	--	--	--	--
	2[g]	Shoulder	--	--	--	--	--	--	--[h]	+34
		Median	--	--	--	--	--	--	--[h]	+42
	4-BM[j]	Shoulder	-28	+27	-14	+40	--	--	--	--
		Median	-28	+32	-16	+34	--	--	--	--
	4-WWF[k]	Shoulder	--	--	--	--	-65	+47	+24	+55
		Median	--	--	--	--	-87	+47	+24	+56

[a] From initial reading made at age of 1 or 2 weeks.
[b] + = lengthening; - = shortening.
[c] North end not free, continuous with section 5.
[d] Neither end free, continuous with sections 4 and 6.
[e] South end not free, continuous with section 5.
[f] No observations made for south end.
[g] No observations made for north end.
[h] Plugs to record end movements of south end not set until February 1962.
[j] South end not free, continuous with section 4-WWF.
[k] North end not free, continuous with section 4-BM.

end of section or site 1, which was monumented for end movement observations. It appears that for the type of soil and other conditions existing at this site, these lugs were ineffective. No unusual cracking has occurred at the several ends that were thus anchored.

General Conditions of Concrete Shoulder
Trucking Lanes vs Median Lanes

Neither project has attained any great age, Project 31 being only about 3 ½ years old, and Project 53 only slightly more than 2 years old.

Most of the badly cracked areas of Project 31 have been repaired and the remaining

TABLE 6

TOTAL MOVEMENT ACROSS TRANSVERSE TERMINAL JOINTS

PROJECT 31

ROADWAY LOCATION	DESCRIPTION OF PAVEMENT ABUTTING TERMINAL JOINTS	TYPE OF JOINT	EDGE	2/61	8/61	2/62	9/62
SOUTH END	TWO SECTIONS OF 9" JOINTED PAVEMENT AND EXISTING 9" PAVEMENT						
SOUTHBOUND ROADWAY	SECTION 1	RUBBER	SHOULDER	+30	-34	+12	-40
			MEDIAN	+29	-35	+9	-39
		FABRICATED STEEL	SHOULDER	+2	-58	-20	-75
			MEDIAN	+4	-56	-20	-74
	EXISTING 9" PAVEMENT & 2 SECTIONS OF 9" JOINTED PAVEMENT						
		BITUMINOUS	SHOULDER	+22	-47	+10	-45
			MEDIAN	+23	-48	+11	-48
	SECTION 2	RUBBER	SHOULDER	+32	-8	+28	-13
			MEDIAN	+30	-11	+26	-15
	STRUCTURE APPROACH						
	STRUCTURE APPROACH	BITUMINOUS	SHOULDER	+17	-22	+14	-27
			MEDIAN	+17	-22	+16	-26
	SECTION 3	RUBBER	SHOULDER	+4	-43	-3	-55
			MEDIAN	+9	-34	+2	-50
	CONTROL SECTION 9" JOINTED PAVEMENT						
	STRUCTURE APPROACH	FABRICATED STEEL	SHOULDER	+9	-36	-10	Joint removed & filled with bit. conc. (1962)
			MEDIAN	+9	-37	-6	
	SECTION 4						
	SECTION 6	RUBBER	SHOULDER	+11	-53	-7	-57
			MEDIAN	+17	-46	0	-54
NORTH END	400'± SECTION 9" JOINTED PAVEMENT						
NORTH END	400'± SECTION 9" JOINTED PAVEMENT						Joint removed & filled with bit. conc. (1962)
NORTHBOUND ROADWAY		BITUMINOUS	SHOULDER	+21	-48	+11	
			MEDIAN	+21	-48	+4	
	SECTION 7	RUBBER	SHOULDER	+8	-82	-39	-80
			MEDIAN	+11	-84	-40	-88
	CONTROL SECTION 9" JOINTED PAVEMENT						
		FABRICATED STEEL	SHOULDER	-41	-123	-83	-145
			MEDIAN	-36	-112	-70	-134
	SECTION 8	FABRICATED STEEL	SHOULDER	+6	-59	-11	-69
			MEDIAN	+3	-57	-10	-69
	STRUCTURE APPROACH						
	STRUCTURE APPROACH	BITUMINOUS	SHOULDER	+16	-30	+5	-39
			MEDIAN	+16	-29	+2	-39
	SECTION 9	FABRICATED STEEL	SHOULDER	+16	-46	-5	-67
			MEDIAN	+16	-47	-5	-69
SOUTH END	TWO SECTIONS OF 9" JOINTED PAVEMENT AND EXISTING 9" PAVEMENT						

PROJECT 53

ROADWAY LOCATION	DESCRIPTION OF PAVEMENT ABUTTING TERMINAL JOINTS	TYPE OF JOINT	EDGE	2/61	8/61	2/62	9/62
NORTH END	9" EXISTING JOINTED PAVEMENT & 1 SECTION 9" JOINTED PAVEMENT						
SOUTHBOUND ROADWAY		RUBBER	SHOULDER	+10	-40	-14	-58
			MEDIAN	+9	-43	-13	-61
	SECTION 1	RUBBER	SHOULDER	+13	-48	-7	-43
			MEDIAN	+11	-51	-11	-51
	CONTROL SECTION 9" JOINTED PAVEMENT						
		RUBBER	SHOULDER	+9	-55	-7	-55
			MEDIAN	+9	-51	-9	-55
	SECTION 2						
		WIDE FLANGE					
		N. Side Cont. Pvm.	SHOULDER	+.0559	-.0960	+15/64	-.0087
			MEDIAN	+.0546	-.0591	+21/64	+.0251
		S. Side Conv. Pvm.	SHOULDER	+.0607	+.0555	+12/64	+.2129
			MEDIAN	+.0511	+.0158	+3/64	+.1470
	STRUCTURE APPROACH						
	STRUCTURE APPROACH	RUBBER		NO READINGS			
	SECTION 3						
		WIDE FLANGE		NO READINGS			
	STRUCTURE APPROACH						
	STRUCTURE APPROACH	RUBBER	SHOULDER	+11	-32	+2	-30
			MEDIAN	+6	-33	-6	-32
	SECTION 4-BM						
	SECTION 4-WF						
		WIDE FLANGE					
		N. Side Cont. Pvm.	SHOULDER	+.0083	+.0198	+4/64	+.0698
			MEDIAN	+.0018	+.0024	+3/64	+.0309
		S. Side Conv. Pvm.	SHOULDER	+.0094	+.0047	+5/64	+.0199
			MEDIAN	+.0121	+.0063	+2/64	+.0225
	STRUCTURE APPROACH						
		SERIES OF DOWELLED EXPANSION JOINTS	#1 SHOULDER	+.1370	-26/64	+4/64	-21/64
			#1 MEDIAN	+.1715	-23/64	+8/64	-17/64
			#2 SHOULDER	+.0008	-8/64	+1/64	-7/64
			#2 MEDIAN	+.0043	-8/64	-2/64	-7/64
			#3 SHOULDER	+.0109	-.0635	-1/64	-.0237
			#3 MEDIAN	+.0022	-3/64	0	-3/64
			#4 SHOULDER	-.0003	-.0383	0	-.0084
			#4 MEDIAN	+.0011	-.0400	+1/64	-.0278
	SECTION 5						
		SERIES OF DOWELLED EXPANSION JOINTS	#1 SHOULDER	+.1239	-27/64	-3/64	-24/64
			#1 MEDIAN	+.1410	-27/64	0	-22/64
			#2 SHOULDER	+.0196	-8/64	+4/64	-6/64
			#2 MEDIAN	+.0020	-.1171	+1/64	-5/64
			#3 SHOULDER	+.0081	-.0170	+2/64	-.0355
			#3 MEDIAN	-.0004	-5/64	+3/64	+.0364
			#4 SHOULDER	+.0003	-.0529	0	-.0323
			#4 MEDIAN	+.0081	-.0233	+1/64	+.0066
	STRUCTURE APPROACH						
	NO READINGS OF JOINTS TAKEN SOUTH OF THIS JOINT.						

NOTE: + Indicates opening of joint.
- Indicates closing of joint.

[a] Movements in 1/64 in. from initial reading made at age of one to two weeks.
[b] Movements in 1/64 in. or as indicated from initial reading.

areas present a fairly good general appearance, especially in summer periods when transverse cracks are tightly closed. A few of the sections do not show up as well in the cold winter season when cracks are open. The conventional control section is in excellent condition.

As previously stated, the bar mat reinforced sections of Project 53 present a very good general appearance. The appearance of the 2,000-ft length of welded wire fabric reinforced pavement is poor due to the numerous wide cracks. The conventional control section for this project is in very good condition, but it contains many more transverse cracks than the control section for Project 31.

As previously noted, terminal joints for Project 31 were of the following three types: 9-cell Goodrich rubber joint, a bituminous fill placed between steel angle-armored slab ends, and fabricated steel plate type. Project 53 also used three types of terminal joints: the Goodrich rubber joint was again used, but of 6-cell construction; wide-flange steel section type of joint; and the multiple-doweled joint type. Up to the present the rubber joints and the steel wide-flange joints seem to have performed somewhat better than the others. The multiple-doweled joints would probably rank next in satisfactory performance; some spalling has occurred at these joints, but it is not necessarily associated with the type of joint. Precompressed, self-expanding filler material might improve these multiple-type joints. Weld failures have occurred in both the "bituminous" and fabricated plate joints, and some removal of both of these types has occurred. However, neither of these types of joints was provided with subslabs, this being agreed on as an experimental feature during the planning of the experiment. It is possible that subslabs could have improved their performance considerably.

Road roughness determinations were made along Project 31 in October 1959 and June 1962; they were made along Project 53 in June 1962. These measurements were made by this Commission's roughometer which is of the Bureau of Public Roads type. In all cases the roughometer was towed along the outer wheelpath of the lane being measured. Roughness data for the two projects are given in Table 7.

Table 7 pertaining to Project 31 gives a number of changes in roughness between the October 1959 and June 1962 readings. The changes are erratic, and a definite trend is not indicated so far. There are 11 sections, counting the two conventional pavement controls. In the shoulder lanes 5 sections showed increased roughness, 4 showed lower roughness readings, and 2 sections were the same. In the median lanes 10 of the sections decreased in roughness readings, and 1 remained the same. It is possible that the many patched areas had some effect on these roughness evaluations.

Only one determination of roughness has been made on Project 53, and a comparison between different dates is, of course, impossible.

This report has previously mentioned the considerable amount of heavy truck traffic which is using this expressway. Although it is usual for most of the trucks to use the shoulder lanes, observations indicate that the median lane gets a good share of truck traffic also.

A casual observation does not indicate that the shoulder lanes have so far been affected by traffic to a greater extent than the median lanes. After these projects have been in use for a significant period—perhaps 10 years—it is felt that a more definite indication should be available.

Performance and Cost of Continuously-Reinforced Pavement vs Conventional Pavement

The Baltimore-Harrisburg Expressway, Interstate I-83, is a concrete pavement project in its entirety in Maryland. Design and construction phases covered a long period, design having begun sometime in 1949; construction was completed in late 1960 when Project 53 was opened to traffic. Cost index factors could be applied to the very old jobs, and a comparison made with the continuously-reinforced projects.

However, Projects 31 and 53 and the two conventional paving projects between Project 31 and the Pennsylvania line were advertised between November 1957 and January 1960 and bid costs submitted by the contractor of each project are given in Table 8. Project 32 adjoins Project 31 directly to the north, includes both roadways of the divided

TABLE 7

AVERAGE ROUGHNESS UNITS PER MILE

Project	Section or Site	Avg. Roughness Units per Mile			
		Measurement Oct. 1959		Measurement June 1962	
		Shoulder Lane	Median Lane	Shoulder Lane	Median Lane
31	1	100	103	100	103
	2	92	94	91	85
	3	86	86	100	79
	Control southbound rdwy.	90	87	90	70
	4	106	120	121	111
	5	106	114	109	107
	6	100	107	90	100
	7	95	93	94	85
	Control northbound rdwy.	89	102	98	93
	8	111	116	107	89
	9	95	90	101	88
	Total:				
	Continuously-reinforced	99	103	101	94
	Conventional control	90	95	94	82
53[a]	1	--	--	88	95
	Control	--	--	101	105
	2	--	--	86	95
	3	--	--	92	88
	4-BM	--	--	85	100
	4-WWF	--	--	83	88
	5	--	--	87	85
	6	--	--	85	87
	Total:				
	Continuously-reinforced	--	--	87	91

[a]Southbound roadway only.

highway to a point north of Parkton, and is about 1.9 miles long. Between this contract and the Pennsylvania line is Project 35, about 4.4 miles long, and also including both roadways of the divided highway.

Although the contract bid prices for Project 31 showed identical unit prices for conventional and continuously-reinforced pavement, those for Project 53 indicated premiums of $0.66 per sq yd for bar mat reinforcing, and $0.76 per sq yd for welded wire fabric reinforcing. It must also be remembered that the terminal joints at the ends of continuously-reinforced sections are separate bid items, and when their cost is transformed to an equivalent square yard basis can add significantly to the continuously-reinforced pavement costs.

For Project 31 bid prices received were $800 for the bituminous joint, $1,200 for the fabricated steel plate joint, and $2,800 for the rubber type joint. Design changes in the fabricated steel plate joint after receipt of bids resulted in an increase of about $1,000 for each of these joints. Aggregate cost of the 14 terminal joints used on this project was $28,200, or about $0.37 per sq yd of continuously-reinforced concrete.

TABLE 8

BID COSTS FOR FOUR PROJECTS

Project	Date of Bid	Type of Construction	Bid Price of Pavement ($ per sq yd)[a]
32	11-57	Conventional	6.50
31	1-58	Continuously-reinforced	6.00
		Conventional (control)	6.00
35	3-58	Conventional	5.50
53		Continuously-reinforced (bar mat reinforcement)	5.69
	2-60	Continuously-reinforced (welded wire fabric reinf.)	5.79
		Conventional	5.03

[a]Bid price for conventional pavement includes reinforcing steel, longitudinal tie device, doweled joints, etc. Bid price for continuously-reinforced pavement includes reinforcing steel, tie devices, etc., but not terminal joints.

The rubber type of joint proved popular with Maintenance and District forces, and it was requested that this type of joint be used on Project 53. It was included in the bid proposal but resulted in a submitted contract price of $3,315. In an attempt to reduce the total price of terminal joints, and also to investigate this question of terminal jointing further, the three types previously described in this report were substituted, and prices for them were negotiated with the contractor. These negotiated prices were $400 for the series of doweled joints, $490 for the wide-flange joint, and $2,980 for the smaller 6-cell rubber joint. The total cost of the 12 terminal joints used north of the Shawan Road Bridge was $18,060 which is equivalent to an increase of $0.20 per sq yd for the continuous pavement in this same area.

It is not possible at this time to make a definite statement as to whether these premiums in cost are justified. The performance of the first continuously-reinforced pavement, Project 31, so far is not as good as either its own conventional control sections, or the adjacent conventional paving contracts. As indicated previously, the lack of full depth vibration, and the use of only one paver probably contributed to the lack of bonding and subsequent failures. The length of splice, and non-stagger of mats could also very well have contributed to the failures.

On the other hand, the bar mat reinforced sections of Project 53 have so far performed very well. Vibration, two pavers, staggered mats, and increased splice length were used on this project. But still, the increased cost does not yet appear justified, because the age of the pavement is still quite low.

It will be necessary to compile carefully pavement maintenance costs for all of the separate sections given in Table 8 over a rather long period before any reasonable conclusions can be drawn.

SUGGESTED IMPROVEMENTS

The experience in Maryland to date in connection with continuously-reinforced pavements is limited. Based on this limited experience, the following are suggested:

1. It is extremely important to vibrate both lifts of a continuously-reinforced pavement and to use two pavers when two lift construction procedure is followed.
2. Although it has not been used, preplacing the steel in very long lengths and completely randomizing splice locations would be a preferred type of construction. With this method of construction, the concrete would be placed in one lift and would be thoroughly vibrated for its entire depth.

Figure 7. Pavement construction showing internal vibration of concrete.

Figure 8. Pavement construction showing internal vibration of concrete, and staggered ends of bar mats.

Figure 9. Details of reinforcing steel cage in end restraint lugs.

Figure 10. Placing reinforcing steel and trimming subbase at end restraint lugs.

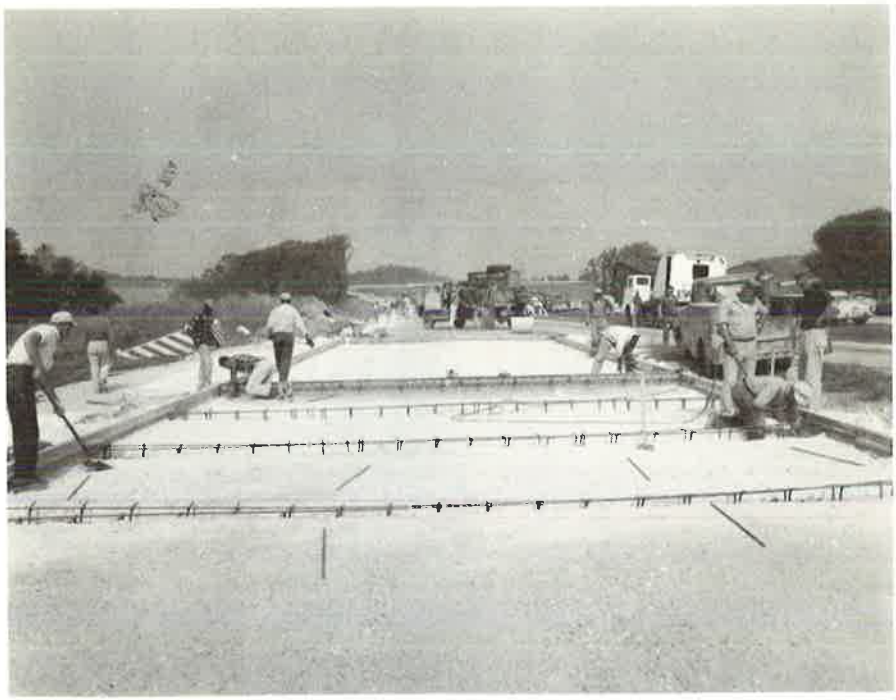

Figure 11. Trimming subbase at end restraint lugs.

Figure 12. Concrete pouring in vicinity of end restraint lug.

3. The 20-diameter lap which Maryland used on Project 31 seems to be too short. The 25-diameter lap used on Project 53 is better and although there is nothing definite to base it on, the authors would be inclined even to lengthen this amount of lap a little. The method of splicing the wire fabric on Project 53 was entirely too short and it would appear favorable to lengthen it considerably.

4. The simplest type of terminal joint should be used. The multiple-doweled joint and the wide-flange joint have performed satisfactorily so far.

5. If it is decided to use end anchorages they apparently must be quite massive to be effective.

Figures 7 through 12 show some of the construction details for Project 53.